Doctoral Dissertation (Shinshu University)

Research on development of biomedical nanocomposites in drug delivery system

薬物徐放システムにおけるバイオメディカルナノ複合材料の開発に関する研究

March　2019

MA　KE

CONTENTS

Abstract

Synthetic polymer materials and nature polymer materials are the two classes of conventional materials widely used in different fields such as as filters, wipes, drug delivery systems, biosensors and so on. Over recent decades, the nanocomposites have attracted more attention and versatile exploitations in various applications. In particular, synthesized polymers, such as polycaprolactone (PCL) and nature polymers, such as shellac and silk fibroin (SF), have been reported as efficient candidates for biomedical applications due to their prominent characteristics and performances compared with traditional materials. The nanocomposite applications have been exploited in drug delivery process owing to their large surface areas, high pore volume and stability against thermal and chemical agents [1]. Herein, I introduce a group of smart nanocomposites consisting of controllable drug release rates, and aim to combine good biocompatibility effects and high mechanical effects into one biomedical nanocomposite. The first nanocomposites-shellac nanofiber and nanoparticle are prepared for drug release in capsule, because the resultant application has very low mechanical properties. For improve the mechanical properties for wider application, synthetic polymers are added in. Four kinds of prepared nanocomposites, PCL/shellac/PCL sandwich structure nanofibers membrane, SF/PU/SF three layer nanofibrous tubes, PU/PCL nanofibrous tubes and PCL multi-layer nanofibrous tubes are succeed in obtaining good mechanical properties. Especially in the application of skin care system, compared with the

untreated PCL/shellac/PCL electrospun nanofiber membranes, the processed nanofiber membranes should about 8 times tensile strength increase and 38 times Young's modulus increase. For drug release in skin care system, PCL/shellac/PCL sandwich structure nanofiber membranes are fabricated for the transparence and high mechanical properties. The drug release process is controlled within 8 hours to fit the needs of skin care such as night face mask. For drug release in colon/stomach site system, shellac nanofibers and nanoparticles are studied to find the relationship of physical shapes and chemical properties of nanocomposites with the purpose of controlling the drug release speed. Besides, the strong potential in nano-targeting in drug delivery is revealed by characteristics of nanocomposites.

This dissertation is focus on biomedical nanocomposites which are applied to colon/stomach part capsules, skin care system and artificial blood vessels. For artificial blood vessels, the problem of thrombus has been discussed over decades. Our prepared drug release artificial blood vessels are considered to solve this problem. I also try to prepare three layers SF/PU/SF nanofibrous tubes in traditional steel mandrel method. This application combines good biocompatibilities and high mechanical properties. However, the traditional method cost at least 2 h to get each tube and the tubes are easily broken when they removed from the steel mandrel. The efficiency is low. To solve this problem, a smart method to fabricate nanofiber tubes is proposed and this method is more efficient and easier to control the diameter of nanofibrous tube which compare with traditional steel mandrel method. On the basis of nanofibrous tubes, antithrombotic drug was added into prepared multi-layer PCL nanofibrous tubes. Dual

drug release profiles can be obtained and the release rates can be controlled from 1.5 h to 62.5 days in one prepared tube. These two release profiles correspond to short-term thrombus and long-term thrombus respectively. It proves that the drug release rates of artificial blood vessels show the expected properties.

As a consequence, in this study, I designed release speed, mechanical strength, targeted delivery and even transparency against the needs of applications. This promising merits mainly profit from the characteristics of materials such as high mechanical properties of synthesized polymers (PCL) and good biocompatibility of nature polymers (SF). Besides the nanocomposites of nanofibers/nanoparticles, I studied single nanofiber membranes, sandwich structure and multi-layer structure, to obtain nanoparticle/nanofiber application, nanofiber membrane until nanofibrous tube applications of controllable release speed, good biocompatibility, mechanical strength and targeted delivery.

Chapter 1

General introduction

Chapter 1: General introduction

1.1. Drug release system

Over the past 20 years, the interactions of the fields of composite polymer and materials science with the pharmaceutical industry have resulted in the development of what are known as drug delivery systems (DDSs), or controlled-release systems [2-5]. The field of drug delivery focuses on the development of technologies to deliver macromolecule to the site of the disease so as to maximize therapeutic benefits, minimize side effects and enhance patient compliance [6]. When free drugs are suffered to various metabolic processes, they will form to distribution in non-target tissues. These processes not only reduce the drug concentration and descreace the drug efficacy at the active target site but also increase the possibility of unwanted side effects. Delivery systems for targeted drug delivery has been recently reviewed (Moghimi et al., 2001 [7]). The nanocomposite would be loaded with drugs and targeted to specific parts of the body where there is diseased, thereby avoiding effect with healthy tissue. The goal of a targeted drug delivery system is to prolong, localize, target and have a protected drug interaction with the diseased tissue [8]. The conventional drug delivery system is the absorption of the drug across a biological membrane, whereas the targeted release system releases the drug in a dosage form [9, 10].

Drug delivery systems can be classified according to the mechanism that controls the release of the drug [11], such as diffusion-controlled systems, dissolution controlled systems, osmotic-release systems and bioerodible-release systems [12-17].

(1) Diffusion-controlled systems

Diffusion can be defined as a process by which molecules transfer spontaneously from one region to another in such a way as to equalize chemical potential or thermodynamic activity. Although diffusion is a result of random molecular motion, with a wide spectrum of physicochemical properties occurring in various conditions and situations, the diffusion process can be abstracted to a simple system involving molecules of interest, a diffusional barrier, and a concentration gradient. The migrating molecules are termed diffusants (also called permeants or penetrants). The membrane or matrix in which the diffusant migrates is called the diffusional shelter[18]. The external phase is called the medium. The concentration gradient or profile of the diffusant within the diffusional barrier is the driving force for diffusion. The mathematics of diffusion are discussed briefly in this section, with emphasis on both diffusion across a barrier membrane and diffusional release from a preloaded matrix[19-22].

(2) Dissolution controlled systems

The dissolution process includes two steps, initial detachment of drug molecules from the surface of their solid structure to the adjacent liquid interface, followed by their diffusion from the interface into the bulk liquid medium. This process could be manipulated to design controlled release delivery systems with desired profiles and a

desired rate [23]. Acombination of both (coated matrix) is also possible[24]. The demarcation between a coated and a matrix-type pharmaceutical controlled release product is not always clear. Some of the materials used as coatings to control drug release also may be used for a similar function in matrix-type products[25].

(3) Osmotic-release systems

Osmosis can be defined as the spontaneous movement of a solvent from a solution of lower solute concentration to a solution of higher solute concentration through an ideal semipermeable membrane, which is permeable only to the solvent but impermeable to the solute [23]. The pressure applied to the higher-concentration side to prohibit solvent flow is called the osmotic pressure.

(4) Bioerodible-release systems

Bioerodible-release polymers may be synthetic or natural in origin. Natural biodegradable polymers include human serum albumin, low-density lipoproteins (LDLs), bovine serum albumin, gelatin, collagen, hemoglobin, polysaccharides, etc [23]. Use of the natural polymers is limited by cosmically manufacture and purification, and they are also known to cause immunogenic unfavorable reactions. With the advances in polymer science, extraordinary knowledge has been gained over the past 30 years on the synthesis manufacture process, handling, and degradation mechanism of many biodegradable polymers. Today, many kinds of synthetic biodegradable polymers are being stated successfully for drug delivery applications. Irrespective of their source and chemistry, all biodegradable polymers possess some common characteristics, such as (1)

stability and compatibility with the drug molecule, (2) biocompatible and biodegradable, (3) ease of manufacture on a larger scale, (4) amenability to sterilization, and (5) flexibility to yield multiple release profiles [23].

1.2. Materials in drug release system

Because the historical breakthroughs of parcelling-up and delivery of drugs, numerous new application domains have been applied to materials-based systems for the past few decades. The advancing improvement of materials — for example, biocompatible nanoparticles that encapsulate drugs and respond to environmental stimuli, biodegradable hydrogels with adjustable drug-release profiles has been active by our enhanced knowledge of sickness and the biomedical methods concerned [25]. The complexity of materials of various sizes, shapes, compositions, designs and physicochemical properties decided the functions of clinic applications. As a result, some of clinically available materials-based drug delivery applications have been substantiated, and the side effects for patients is beginning to become obvious.

1.2.1. Synthesized polymer materials in drug release system

Polymer is one kind of the most commonly used materials for designing drug delivery carriers [26]. The carrier materials need to be compatible with the drug to ensure stability during synthesis, storage, and administration. A number of different strategies have been employed to control the release profiles of polymeric drug delivery

systems. Synthetic polymers, which includes the large group known as plastics, came into prominence in the early twentieth century [27]. Chemists' abilities to engineer them to yield a desired set of properties (strength, stiffness, density, heat resistance, electrical conductivity) have greatly expanded the many roles they play in the modern industrial economy [28].

PCL (polycaprolactone) as a base polymer has been chosen owing to its vast applicability and characteristics suitable for biomedical applications. The material is a semi-crystalline aliphatic polyester with melting point (Tm) 60°C possessing broader in vivo and in vitro bio-compatibility. It has been reported to be biocompatible and bio-resorbable material for both soft and hard tissues[29,30]. The U.S. Food and Drug Administration has approved PCL for substantial number of drug delivery and other biomedical applications[31].

The Polyurethane (PU) material is studied by most of the researchers as PU is a kind of block copolymers which are consisted by different of hard and soft segments. PU materials have properties of good biocompatibility and hemocompatibility and it can choose resolve resolution and different monomers through molecular structure design in order to control the physical and chemical properties [32]. PU artificial blood vessels have the similar elastic modulus with human arteries and the anastomotic PU materials can avoid platelet activation which is caused by blood vortex. Anastomotic PU can be used in the large-scale artificial blood vessels because of these influences[33]. However, the conventional PU materials are probably carcinogenic during degradation process.

1.2.2. Nature polymer materials in drug release system

The nature polymer materials appoint locations in the human body using materials-based systems has been approaching the perspective of biomedical research in drug release system for the past few decades [25]. The concepts have arisen from our advancing knowledge of materials — for example, biocompatible nanocomposite that encapsulate drugs and respond to environmental stimuli, biodegradable hydrogels with tunable drug-release profiles, and implanted depots that control the spatiotemporal presentation of a therapeutic — and has been enabled by our increased understanding of disease and the biochemical pathways involved. The complexity of clinical settings have been tackled with the elegant engineering of nature polymer materials of various sizes, shapes, compositions and physicochemical properties [25].

Silk fibroin (SF) is a kind of natural high molecular fiber protein which extracted from silk and contents about 70%-80% of silk. SF has excellent biocompatibility and good physicochemical properties. The contents of Gly, Ala and Ser occupy highest amount of silk fibroin. Silk fibroin is composed of crystalline and non-crystalline regions. The crystalline regions are composed of Gly, Ala and Ser residues with smaller side chains. This structure has more non-polar groups. The two - stage conformations are mainly composed by β- lamellar structure with peptide chain clearnucleus. The peptide chains are combined by hydrogen bonds and intermolecular forces which have Strong binding force. This phenomenon endows a strong stretch ability and great of SF

and great breaking strength to resistance forces. The Phe, Tyr and Trp which mainly exist in non-crystalline regions. This structure with more polar groups and weaker intermolecular binding force. The peptide chains arrangement which is more loose with molecule bending and tangles make silk fibroin has better fracture extension length and elastic recovery rate [34].

Silk fibroin is soluble in some neutral salt solution. The regenerated silk fibroin solution can be obtained after dialysis for desalination. Fibroin solution can be easily solidified to be prepared into fibers, powder, membrane, gels, and other forms of materials. A lot of research work shows that silk fibroin can support adhesion and proliferation to many kinds of cells as its good cytocompatibility. Silk fibroin has excellent physicochemical properties which can be improved and modified by blending, grafting, crosslinking and other methods [35, 36]. In biomedical field, silk fibroin has been carried out multifarious applied researches in artificial cornea [37], ligament [38], cartilage repair [39], blood vessels [40], connective tissue [41], nerve tissue [42]and other similar areas.

Shellac, also referred to as lac, is a kind of resin secreted by the female lac bug on trees in the forests of India and Thailand. Refined shellac can be made by rinsing and filtration of crude shellac which is directly secreted by lac bug. Shellac has been widely used in food, medicine, military, coating, dyes and other industries fields due to its excellent properties of film-forming, waterproof, fixability and biocompatibility. In the pharmaceutical industry, shellac was originally used in the coating of the enteric drug.

However, due to the emergence of various synthetic materials since the 1950s gradually, shellac faded out of their original role in various fields.

However, with the development of biomedical science, increasing attention has been paid to the limitations of synthetic materials, such as irritation, carcinogenicity, etc. The application of shellac has been extended to DDS, since it is the only animal-secreted resin that can be used in pharmaceutical applications.

1.3. Biomedical nanocomposites

Biomedical nanocomposites are the composites containing biomedical fillers with at least one dimension in nanoscale. Over recent years, diomedical nanocomposites have become a hot topic very fast by the reason of the quick development of nanocomposites (nanoparticles, nanotubes, nanowhiskers, nanofibers, nanolayers, nanosheets and hydrogels) as well as the excellent material performances resulted from the great specific surface area, high surface energy, quantum benefit, small size effect, and macroscopic quantum tunneling. The materials for biomedical nanocomposties are usually be synthetic polymer, natural polymer materials, metal, silica and so on. For example, the drugs based on metal nanocomposites can overcome various diseases such as cancer and bacterial pathogens [43]. Also, silver nanoparticles were extensively applied as an antibacterial media in healthful and preventive health care, even before the arrival of synthetically manufactured medicines such as penicillin [44].

For polymers, many kinds of polymer can be applied for biomedical applications

such as natural polymers including polysaccharides or proteins (soy, collagen, fibrin gels) and synthetic polymers such as poly(lactic acid) (PLA), poly(ε-caprolactone) (PCL), poly(glycolic acid) (PGA) and poly(hydroxyl butyrate) (PHB) [45-49]. They are biocompatible and degradable into non-toxic components with a certain controllable degradation rate [50].

There is also a concern for safety risks of biomedical nanocomposites. Consequently, the studies of toxicological on nano-systems are increasing for improved characterization and reliable toxicity appraisals. In vitro methods are usually used for toxicity assessment of nanocomposites because it has even more challenge in vivo environment. The discrepancies in experimental conditions are disorienting and there is a serious necessity to a standard of toxicity measurement to investigate in vivo fate of nanocomposites. The nanocomposites may not be filtered by the body's defense system, due to the small size which suggests that they may cause inflammatory and other toxic responses [51]. Additionally, the physical, the size and surface chemistry and chemical characterizations of nanocomposites are also important for cytotoxicity examines [50]. Generally, smaller size nanocomposites (especially nanoparticles) show greater toxicity, because smaller size nanocomposites are more uptaken into the cell or even near the nucleus of cells. In order to venture the possible toxicity of nanocomposites in vivo applications, some items should be examined [51].

In fact, the present work expresses the biomedical nanocomposites of the above

materials in the current time and their potential usages in the future efforts. The nature polymers (collagen, fibroin) and the different factors of metal nanoparticles result in various technical applications for polymer/metal nanocomposites. The nanocomposites also can be differ by different shapes and sizes, such as nanoparticles, nanotubes, nanowhiskers, nanofibers, nanolayers, nanosheets, etc. Therefore, various properties and applications can be combinated by assembly of chemical natures otherness, physical properties otherness and morphologies otherness.

1.4. Progress of artificial blood vessel

The materials which used in current clinical graft are mostly synthetic polymer materials, such as Dacron, Polytetrafluoroethylene (Teflon), Polyurethane(PU) etc. But the above synthetic polymer materials have poor histocompatibility and easy to cause thrombus. Because of this, these materials can't be used in small-diameter artificial blood vessels (diameter<6mm). Silk fibroin is a natural polymer material which has good biocompatibility. It has a wide range of application prospects in the medical field. Based on the current research status of small-diameter artificial blood vessels， the researchers found that fibroin can develop its characters as SF has both good biocompatibility and good mechanical properties. In chapter 5, a kind of three-layer structure bionic small-diameter artificial vascular has been studied. This bionic tubular scaffold which is made from nanofiber has intima, middle membrane, and adventitia. The three-layer structure offers both biocompatibility and mechanical properties to

simulate the natural vessels. And intima SF nanofiber layer is designed to carry drug to improve blood clotting properties for antithrombotic.

1.4.1. Thrombosis mechanism

Thrombosis is a formation of blood clots inside of blood vessels, which prevents the blood flow rate through the circulatory system. When a blood vessel (a vein or an artery) is injured, the body uses platelets (thrombocytes) and fibrin to from blood clots to prevent blood loss. Even the blood vessel is not injured, blood clots may still form under certain conditions. A clot, or a piece of the clot, which breaks free and begins to travel around the body is known as an embolus.[52, 53]

1.4.2. Antithrombus materials

Several species of materials have been used for artificial blood vessels such as polyurethane, polysulfone, polyacrylate, polyether sulfone, polytetrafluoroethylene[54], and so on. Thus these materials have good mechanical properties, flexibility and a certain biocompatibility. However, their anticoagulant performance is not satisfactory. The researchers used a variety of methods to modify these materials in order to improve their anticoagulant.

In 1984, Lin et al. proposed a hypothesis to maintain normal conformation[55]. This hypothesis has important significance for improving the biocompatibility of the materials, the immobilization of biological macromolecules and so on. At the same time,

the surface grafting reaction of polyurethanes, polysiloxanes and polyolefins are also be developed. A varieties of new good materials with excellent surface anticoagulant had been synthesis through this hypothesis.

In 1988, Nakajima et al. [56] proposed the anti-coagulation mechanism of micro-phase separation structure material for the first time using the pro / hydrophobic difference of different kinds of plasma proteins. When micro-phase separation materials contacted with blood， different plasma proteins would selective to adsorb on different domains. This particular protein adsorption layer structure will not activate the platelet surface glycoprotein, therefore the material will not appear the coagulation phenomenon. The anticoagulant biomaterial can be studied according to this mechanism.

1.4.3. Advances of artificial blood vessels

The ideal graft should have the follow properties: Firstly, no toxicity for biology. It should not cause foreign body reaction or rejection, and also should have good compatibility for tissue and blood; No adverse effects on cell growth, teratogenicity and mutagenic effects; It also should not cause thrombosis and arterial aneurysm after grafting in order to maintain a long-term patency; Own body vessels have been proved to go well enough with the alternative vessels and have a certain anti-infective ability. Secondly, on the aspect of mechanical properties, the grafts should have similar mechanical properties with the nature ones and not easy to occur degenerative deformation; It is also important to withstand the vessel pressure and stable elastic

recovery in order to fit with surgery needs. It is also necessary that the grafts should easy stitch and hard to tear; Thirdly, three-dimensional porous structure is needed for exterior to grow the tissue cells, exchange of nutrients and metabolic discharge; The inner surface should have a certain roughness for endothelial cells adhere, proliferation and endothelialization.

In order to fit these requirements, two categories of biomaterials were used at present: Natural materials and synthetic polymer materials. Natural materials include natural polymer and natural inorganics, such as: collagen, gelatin, chitin, silk fibroin and so on. Synthetic materials are mostly synthetic polymers, which are divided into biodegradable materials and non-degradable materials. Biodegradable materials include polylactic acid, polyglycolic acid and so on. Non-degradable materials include polyester material, polyurethane and polytetrafluoroethylene, etc.

Synthetic polymer material grafts are widely used in clinical at present. Such as polyester (polyethylene terephthalate) artificial blood vessels, expended polytetrafluoroethylene (e-PTFE) artificial blood vessels and so on. The polyester artificial blood vessels are one of the first to became commercialization. They are manufactured by knitting and woven method. This kind of artificial blood vessels have good mechanical properties and able to match well with surrounding tissue. They are the best choice for big diameter artificial blood vessels because they can also keep a certain strength after a long-time transplant [57]. But the hemocompatibility of these products are poor and easy to cause thrombosis after graft survey. As a result, the

patients have to use antithrombotic drugs for a long-term. However, the polyester grafts can't fit the requirement of small-diameter (within 6 mm) artificial blood vessels[58]. After artificial blood vessels transplant survey, the polymer artificial materials will occur self-degradation along with the growth and tissue repair. At last the artificial vessels will become one part of own vascular function tissue. Polylactic acid (PLA), polyglycolic acid (PGA), polylactic acid hydroxy acid (PLGA), polycaprolactone (PCL), polyhydroxybutyrate (PHB) and other polymer materials had been extensive researched in this case [59-63].

Above all, natural materials have more excellent cell compatibility than synthetic polymer materials in artificial blood vessels field. Natural materials are also more conducive to the formation of endothelial layer. However, the tubular scaffolds prepared by electrospinning process or freeze-drying method always have poor mechanical properties.

1.4.4. Traditional method of preparating nanofiber tubes

Nanotechnology has revolutionized the scientific world owing to the very small size and greater surface area of the unique nanoscopic materials. Because the historical breakthroughs of nanotechnology and developments, a numerous of new application domains have been applied such as lters, wipes, drug delivery systems, battery and capacitor electrodes, regenerative scaffolds, biosensors and catalysts. Electrospinning has received greater recognition due to the simplicity, versatility and diversity. The

electrospun polymer nanofibers and their composites have received greater attention and versatile exploitations in various applications.

When a sufficiently high voltage is applied to a liquid droplet, the shape of the liquid will be charged. This point of eruption is known as Taylor cone. If the molecular cohesion of the liquid is sufficiently high, stream breakup will not occur (if it occurs, droplets are electrosprayed) and a charged liquid jet is formed.

As the jet dries in flight, the mode of current flow changes from ohmic to convective as the charge migrates to the surface of fibers. The jet is then elongated by a whipping process caused by electrostatic repulsion initiated at small bends in the fiber, until it is finally deposited on the grounded collector. The elongation and thinning of the fiber resulting from this bending instability leads to the formation of uniform fibers with nanometer-scale diameters [64].

The traditional method of preparation nanofiber tubes is using a rotated stainless steel to collect nanofibers. Electrospun nanofibers were deposited continuously over stainless steel mandrel for several hours. The mandrel was rotated at about 1000 rpm and reciprocated for uniform deposition. However, this method is low efficiency and the tubes are easily broken when they are removed from the mandrel.

1.5. Purpose of this research

This research aims to develop new kinds of biomedical nanocomposites combining the drug release effect, biocompatibilities and higher mechanical properties by

compounding diverse function of materials and treatment. In this study synthesized polymer (PCL, PU) and natural polymer (fibroin, shellac) are used to fabricate nanocomposites for artificial blood vessels, biomedical applications for skin care and target drug delivery capsules. As what I discussed above, not every nanocomposites would acquire expected properties because a number of confusing factors have effect on the final material performances. The combination of nanocomposites such as, nanofiber-nanoparticle composities, nanofiber mat sandwich structure and multi-layer nanofibrous tube are discussed in this study.

The study of drug release shellac nanocomposites capsules prove the theory that various properties can be combinated by assembly of chemical natures otherness, physical properties otherness and morphologies otherness in order to obtain the needs. This application is combined by shellac/sodium shellac nanofiber and nanoparticles. The results revealed that the release speed rates are totally different of shellac nanoparticles, sodium shellac nanoparticles, shellac nanofibers and sodium shellac nanofibers. Therefore, the results show that controlled drug release rate can be achieved by tuning chemical composition or changing physical shapes. Meanwhile, compare with the physical shapes, chemical compositions of nanocomposites effect more in this study. However, this application has very low mechanical properties. Because of this reason the application can only be used inside of capsule. Synthetic material (PCL) is added to obtain nanofiber membrane to get better mechanical properties and wider application.

The PCL/shellac transparent nanofiber films for skin care system is also

combined by natural polymer (shellac) nanofiber and synthesized polymer (PCL). The combination reaches unexpected effect of transparence, and great improvement of mechanical property. The regular transmittance at 555 nm of the membranes is about 35%. The composite treated nanofiber film exhibites tensile strength that which is 5 times higher and 38 times higher of Young's modulus than the PCL/shellac nanofiber film before treatment. The biomedical nanofiber membrane for skin care are designed and discussed in this study.

Further more, nanofibrous tube applications are considered to manufacture. The chapter 5 to 7 mainly discussed combination of nanofiber tube. The SF/PU/SF nanofiber tubes through traditional method are aim to have both biocompatibility from SF and high mechanical properties from PU. As what I discussed, various properties of applications can be combinated by assembly of chemical natures otherness, physical properties otherness and morphology otherness to obtain the needs. However, this method is low efficiency. So we improve the manufacture method-thermal method to obtain new nanofibrous tubes. The method of the PCL/PU nanofibrous tubes manufacture is more easily and greatly improved efficiency than the traditional methods. The method of multi-layer PCL nanofibrous tube manufacture is similar with the PCL/PU ones, while anti-thrombus drug was added inside of this application. As a result, the prepared multi-layer PCL nanofibrous tube the can carry two drug release profile of drug, the rapid drug release rate can be fast within 2 hours and the slowly rate can keep release effect about 62.5 days. These two release rates correspond to short-term

thrombus and long-term thrombus but still need further test in vivo.

In this dissertation, nanofiber applications which from nanoparticle/nanofiber, nanofiber membrane until nanofibrous tube are designed and discussed. A qualitative improvement of mechanical properties can be observed from nanofiber and nanoparticle application to nanofiber membrane. Meanwhile, wider application and higher efficiency method are searched through this study.

Reference

1. Ke M, Wahab J A, Hyunsik B, et al, Allantoin-loaded porous silica nanoparticles/polycaprolactone nanofiber composites: fabrication, characterization, and drug release properties, *RSC Advances*, 2016, 6(6): 4593-4600.

2. Kim Y C, Park J H, Prausnitz M R, Microneedles for drug and vaccine delivery, *Advanced drug delivery reviews*, 2012, 64(14): 1547-1568.

3. Park J H, Saravanakumar G, Kim K, et al, Targeted delivery of low molecular drugs using chitosan and its derivatives, *Advanced drug delivery reviews*, 2010, 62(1): 28-41.

4. Zhang Y, Chan H F, Leong K W, Advanced materials and processing for drug delivery: the past and the future, *Advanced drug delivery reviews*, 2013, 65(1): 104-120.

5. Wokovich A M, Prodduturi S, Doub W H, et al, Transdermal drug delivery system (TDDS) adhesion as a critical safety, efficacy and quality attribute, *European Journal of Pharmaceutics and Biopharmaceutics*, 2006, 64(1): 1-8.

6. Mitragotri S, Lahann J, Materials for drug delivery: innovative solutions to address

complex biological hurdles, *Advanced Materials*, 2012, 24(28): 3717-3723.

7. Moghimi S M, Hunter A C, Murray J C, Long-circulating and target-specific nanoparticles: theory to practice, *Pharmacological reviews*, 2001, 53(2): 283-318.

8. Rani K, Paliwal S, A review on targeted drug delivery: Its entire focus on advanced therapeutics and diagnostics, *Sch. J. App. Med. Sci*, 2014, 2(1C): 328-331.

9. Muller RH, Keck CM, Challenges and solutions for the delivery of biotech drugs-a review of drug nanocrystal technology and lipid nanoparticles, *Journal of Biotechnology*, 2004, 113 (1–3): 151-170.

10. Allen TM, Cullis PR, Drug Delivery Systems: Entering the Mainstream, *Science*, 2004,303 (5665): 1818-1822.

11. Siepmann J, Peppas N A, Higuchi equation: derivation, applications, use and misuse, *International journal of pharmaceutics*, 2011, 418(1): 6-12.

12. De Gaetano F, Ambrosio L, Raucci M G, et al, Sol-gel processing of drug delivery materials and release kinetics, *Journal of Materials Science: Materials in Medicine*, 2005, 16(3): 261-265.

13. Siepmann J, Peppas N A, Higuchi equation: derivation, applications, use and misuse, *International journal of pharmaceutics,* 2011, 418(1): 6-12.

14. Immich A P S, Arias M L, Carreras N, et al, Drug delivery systems using sandwich configurations of electrospun poly (lactic acid) nanofiber membranes and ibuprofen, *Materials Science and Engineering: C*, 2013, 33(7): 4002-4008.

15. Langer R, Cima L G, Tamada J A, et al, Future directions in biomaterials,

Biomaterials, 1990, 11(9): 738-745.

16. Ponchel G, Irache J M, Specific and non-specific bioadhesive particulate systems for oral delivery to the gastrointestinal tract, *Advanced drug delivery reviews*, 1998, 34(2-3): 191-219.

17. Raiche A T, Puleo D A, Modulated release of bioactive protein from multilayered blended PLGA coatings, *International journal of pharmaceutics*, 2006, 311(1-2): 40-49.

18. Allen L, Ansel H C, Ansel's pharmaceutical dosage forms and drug delivery systems, *Lippincott Williams & Wilkins*, 2013.

19. Morf W E, Lindner E, Simon W, Theoretical treatment of the dynamic response of ion-selective membrane electrodes, *Analytical Chemistry*, 1975, 47(9): 1596-1601.

20. Woodside W, Messmer J H, Thermal conductivity of porous media. I. Unconsolidated sands, *Journal of applied physics*, 1961, 32(9): 1688-1699.

21. Meter D M, Bird R B, Tube flow of non-Newtonian polymer solutions: PART I. Laminar flow and rheological models, *AIChE Journal*, 1964, 10(6): 878-881.

22. Flynn G L, Yalkowsky S H, Roseman T J, Mass transport phenomena and models: theoretical concepts, *Journal of Pharmaceutical Sciences*, 1974, 63(4): 479-510.

23. Shen S I, Jasti B R, Li X, Design of controlled release drug delivery systems, *Standard Handbook of Biomedical Engineering & Design*, 2003, 5.1-5.14.

24. CDER 1999 Report to the Nation, Improving Public Health Through Human Drugs. US Department of Human Services, Food and Drug Administration and Center for Drug Evaluation and Research.

25. Chien Y W, Oral drug delivery and delivery systems, 1992.

26. Kim P, Kim D H, Kim B, et al, Fabrication of nanostructures of polyethylene glycol for applications to protein adsorption and cell adhesion, *Nanotechnology*, 2005, 16(10): 2420.

27. Saunders K J, Organic polymer chemistry: an introduction to the organic chemistry of adhesives, fibres, paints, plastics and rubbers, *Springer Science & Business Media,* 2012.

28. Osborn J D, Rubber and plastic bonding: *U.S. Patent* 5, 604, 277[P]. 1997-2-18.

29. Hutmacher D W, Schantz T, Zein I, et al, Mechanical properties and cell cultural response of polycaprolactone scaffolds designed and fabricated via fused deposition modeling, Journal of Biomedical Materials Research: *An Official Journal of The Society for Biomaterials, The Japanese Society for Biomaterials, and The Australian Society for Biomaterials and the Korean Society for Biomaterials,* 2001, 55(2): 203-216.

30. Pitt C G, Chasalow F I, Hibionada Y M, et al, Aliphatic polyesters. I. The degradation of poly (ϵ-caprolactone) in vivo, *Journal of Applied Polymer Science*, 1981, 26(11): 3779-3787.

31. Kost J, Wiseman D, Domb A J, Handbook of biodegradable polymers, *CRC press*, 1998.

32. Ge J, Wu R, Deng B, et al, Studies on the biodegradable polyurethane materials based on bagasse (I) the liquefaction of bagasse and preparation of polyether e ster polyol, *Polymeric Materials Science & Engineering*, 2003, 2: 049.

33. Kakisis J D, Liapis C D, Breuer C, et al, Artificial blood vessel: the Holy Grail of peripheral vascular surgery, *Journal of vascular surgery*, 2005, 41(2): 349-354.

34. Tan H, Lao L, Wu J, et al, Biomimetic modification of chitosan with covalently grafted lactose and blended heparin for improvement of in vitro cellular interaction, *Polymers for Advanced Technologies*, 2008, 19(1): 15-23.

35. Wang S G, Chen C F, Li Z F, et al, Mixed polyether-polyester multiblock copolymer and its blood compatibility, *Journal of Macromolecular Science—Chemistry,* 1989, 26(2-3): 505-518.

36. Santerre J P, Ten Hove P, VanderKamp N H, et al, Effect of sulfonation of segmented polyurethanes on the transient adsorption of fibrinogen from plasma: possible correlation with anticoagulant behavior, *Journal of biomedical materials research*, 1992, 26(1): 39-57.

37. Miyairi S, Sugiura M, Fukui S, Immobilization of β-glucosidase in fibroin membrane, *Agricultural and Biological Chemistry*, 1978, 42:1661-1667.

38. Demura M, Asakura T, Immobilization of glucose oxidase with Bombyx mori silk fibroin by only stretching treatment and its application to glucose sensor, *Biotechnology and Bioengineering*, 1989, 33:598-603.

39. Minoura N, Aiba S, Higuchi M, et al, Attachment and growth of fibroblast cells on silk fibroin, *Biochemical and Biophysical Research Communications*, 1995, 208:511-516.

40. Gotoh Y, Tsukada M, Minoura N,et al, Synthesis of poly(ethylene glycol)–silk

fibroin conjugates and surface interaction between L-929 cells and the conjugates, *Biomaterials*, 1997, 18:267-271.

41. Inouye K, Kurokawa M, Nishikawa S, et al, Use Bombyx mori silk fibroin as a substratum for cultivation of animal cells, *Journal of Biochemical and Biophysical Methods*, 1998, 37:159-164.

42. Higuchi A, Yoshida M, Ohno T, et al, Production of interferon-β in a culture of fibroblast cells on some polymeric films, *Cytotechnology*, 1998, 34:165-173.

43. Goddard J M, Hotchkiss J H, Polymer surface modification for the attachment of bioactive compounds, *Progress in polymer science*, 2007, 32(7): 698-725.

44. Avci-Adali M., Paul A., Ziemer G., Indel H. P, New strategies for in vivo tissue engineering by mimicry of homing factors for self-endothelialisation of blood contacting materials, *Biomaterials*, 2008, 29(29): 3936-3945.

45. Wu H. C., Wang T. W., Kang P. L., Tsuang Y. H., Sun J. S., Lin, F. H, Coculture of endothelial and smooth muscle cells on a collagen membrane in the development of a small-diameter vascular graft, *Biomaterials*, 2007, 7(28):1385-1392.

46. Lee, Po-Han, et al, A prototype tissue engineered blood vessel using amniotic membrane as scaffold, *Acta biomaterialia,* 2012, 8(9) : 3342-3348.

47. Dong S, Jiang G, Jin H, et al, Research of hyaluronic acid and hydroxyethyl starch in the prevention of postoperative peritoneal adhesion in rats, *Shandong Medical Journal*, 2012, 29: 013.

48. Boland E. D., Matthews J.A., Pawlowski K. J., Simpson D. G., Wnek G. E., Bowlin

G. L, Electrospinning collagen and elastin: preliminary vascular tissue engineering, *Frontiers in bioscience: a journal and virtual library*, 2004(9): 1422-1432.

49. Boland, Eugene D., et al, Electrospinning collagen and elastin: preliminary vascular tissue engineering, *Front Biosci,* 2004(9), 1422 : e32.

50. Mc Clendon M. T., Stupp S. I, Tubular hydrogels of circumferentially aligned nanofibers to encapsulate and orient vascular cells, *Biomaterials*, 2012, 23(32): 5713-5722.

51. Mocan T, Hemolysis as expression of nanoparticles-induced cytotoxicity in red blood cells, *BMBN*, 2013, 1(1): 7-12.

52. Li, D.; Xia, Y, Electrospinning of Nanofibers: Reinventing the Wheel, *Advanced Materials*, 2004,16 (14): 1151.

53. Shukla M K, Singh R P, Reddy C R K, et al, Synthesis and characterization of agar-based silver nanoparticles and nanocomposite film with antibacterial applications, *Bioresource technology*, 2012, 107: 295-300.

54. Williams D H, Bardsley B, The vancomycin group of antibiotics and the fight against resistant bacteria,. *Angewandte Chemie International Edition*, 1999, 38(9): 1172-1193.

55. Seyedjafari E, Soleimani M, Ghaemi N, et al, Nanohydroxyapatite-coated electrospun poly (l-lactide) nanofibers enhance osteogenic differentiation of stem cells and induce ectopic bone formation, *Biomacromolecules*, 2010, 11(11): 3118-3125.

56. Shabani I, Haddadi-Asl V, Seyedjafari E, et al, Cellular infiltration on nanofibrous

scaffolds using a modified electrospinning technique, *Biochemical and biophysical research communications*, 2012, 423(1): 50-54.

57. Shabani I, Haddadi-Asl V, Soleimani M, et al, Ion-exchange polymer nanofibers for enhanced osteogenic differentiation of stem cells and ectopic bone formation, *ACS applied materials & interfaces*, 2013, 6(1): 72-82.

58. Shabani I, Hasani-Sadrabadi M M, Haddadi-Asl V, et al, Nanofiber-based polyelectrolytes as novel membranes for fuel cell applications, *Journal of membrane science*, 2011, 368(1-2): 233-240.

59. Shabani I, Haddadi-Asl V, Soleimani M, et al, Enhanced infiltration and biomineralization of stem cells on collagen-grafted three-dimensional nanofibers, *Tissue Engineering Part A,* 2011, 17(9-10): 1209-1218.

60. Zare Y, Shabani I, Polymer/metal nanocomposites for biomedical applications, *Materials Science and Engineering: C*, 2016, 60: 195-203.

61. Choi J, Wang N S, Nanoparticles in biomedical applications and their safety concerns, Biomedical Engineering-From Theory to Applications, *InTech*, 2011.

62. Furie B, Furie B C, Mechanisms of thrombus formation, *New England Journal of Medicine*, 2008, 359(9): 938-949.

63. Handin R I, Bleeding and thrombosis, *Harrison's principles of internal medicine,* 2005.

64. Wheatley DJ, Raco L, Bernacca GM, et al, Polyurethane: material for the next generation of heart valve prostheses? *European Journal Cardio-Thoracic Surgery*，2000,

17: 440-447.

Chapter 2

Drug release on colon/ stomach site with shellac nanocomposites (nanofiber and nanoparticle)

Chapter 2: Drug release on colon/ stomach site with shellac nanocomposites (nanofiber and nanoparticle)

2.1. Introduction

The development of biocompatible nanocomposites for biomedical applications such as drug release has attracted increasing attention in recent years. Shellac/sodium shellac nanofibers and nanoparticles were produced for drug delivery applications. Ketoprofen was loaded on the drug delivery system (DDS), and three schemes based on shellac/sodium shellac were chosen. The biocompatibility and nontoxicity of shellac and the promising results of the nanofibers and nanoparticles highlighted their challenging potential for controlled drug delivery applications. A significant increase of drug release rate can be observed at the gastric site. The prepared drug-loaded nanofibers and nanoparticles were characterized by scanning electron microscopy (SEM), Fourier transform infrared spectroscopy (FTIR) and X-ray diffraction (XRD). The results show that the above-mentioned drug delivery system is able to support high-efficiency encapsulation. A new drug delivery system was designed and studied through shellac and sodium shellac. The application scope of shellac to DDSs is extended.

Nanotechnology drug delivery system (DDS) research has attracted the attention of pharmaceutical, biotechnology, and healthcare industries during the recent decades[1–5].

As the nanotechnology has been developed during the decades with several historical breakthroughs [6–11], numerous new applications have been applied to DDSs [12–14]. Nanoparticles and nanofibers have been widely used in DDSs due to their popular and simple production methods. Drug delivery system characteristics are improved with the incorporation of biodegradable polymer carriers which sustain the release of encapsulated drugs and reduce the side effects. For a viable DDS, a drug carrier needs to overcome several major problems such as loading capacity for large amounts of drugs, controlled release profile of therapeutics at the targeted location, non-toxicity, biodegradability and cost effectiveness. Nano DDS technology, such as nano-formulated drugs, drug eluting stents, drug coatings and devices, involves improved efficacy, targeted drug delivery, reduced active drug ingredients and reduced drug side effects. This technology is able to enhance the efficacy and sustain drug release. It can also promote the business value of the health-care applications. The main aim of the nano-formulations is to adjust the normal metabolic profile of proven established drug molecules by significantly improving the drug efficacy, sustaining release and reducing side effects simultaneously[15]. Nanotechnology applications based on DDSs include nanoemulsions, nanoparticles, liposomes and nanofibers. Nanoproduct drug delivery systems (DDSs) have the advantages of lower cost, scalability, targeted delivery, reduced side effects, biodegradability, biocompatibility, sustainability in release of encapsulated drug and improved efficacy[16]. In this work, nanofibers and nanoparticles were prepared to fine-tune the release speed by their

different drug effects. Shellac is always used in colon DDS due to the very poor drug effect in gastric environment. A simple method was employed to improve the shellac drug release effect in gastric environment to expand the scope of shellac carrier in vivo environment DDS. Less drug wastage was observed in this new DDS than the formerly ones.

The major difference between electrospinning and electrospray lies in their working medium. The electrospray process adopts a low viscosity solution while the electrospinning process adopts a high viscosity solution. Electrospray is the most common molding method to obtain monodisperse particles[17,18]. Electrospinning is a nanoscale fiber production method employing the electric force to draw charged threads of polymer solutions, which results in surface deformation of the charged liquid[19–22].

The elongation of the liquid resulting from this bending instability leads to the formation of uniform nanofibers[23]. Electrospinning processes characteristics of both electrospray and dry spinning of fibers[24]. The in-depth study of electrospinning involves electrostatic, electrohydrodynamics, rheology, aerodynamics and other fields[25–27]. Shellac has a chemical structure which shown in Figure 2-1. The application of shellac has been extended to DDS, since it is the only animal-secreted resin that can be used in pharmaceutically applications[28,29]. In this study, shellac carrying drug effect was improved by alkalization method adopting sodium shellac through in gastric environment. Shellac's acid groups are not easy to dissociate because of its high acid dissociation constant (pKa). This results in a poor drug effect of shellac

in acid fluid environment (pH 2) and there is a limitation of release rate at only about 10%. In this study, a one-step chemical modification of the shellac is carried out by weak alkaline sodium carbonate solution.

By adopting this one-step chemical modification, better degradation performance was observed in simulating gastric fiuid environment. The drug effect of shellac in intestinal fiuid was also improved. Although extensive study has been done on shellac nanofiber in colon DDS, little literature is available on the synthesis of sodium shellac and its composite with shellac as drug carrier in gastric environment. Therefore, this study on nanofiber and nanoparticle mats composed of shellac/sodium shellac loaded with ketoprofen (Figure 2-1) as a guest drug is carried out. For optimization, three ratios of shellac/sodium shellac mixing schemes were used. The results obtained from scanning electron microscope (SEM), Fourier transform infrared spectroscopy (FTIR) and X-ray diffraction (XRD) and drug release analysis confirmed the nanocomposite mat to be suitable for the controlled release of ketoprofen for biomedical applications with a tunable release profile. Thanks to excellent biocompatibility and nontoxicity of shellac and sodium shellac, the corresponding nanocomposite can be considered as a viable drug carrier medium. And hence, it can be applied in drug delivery systems, tissue engineering and other biomedical applications. Further study on shellac/ sodium shellac nanocomposites can be carried out to extend its application to biomedical use.

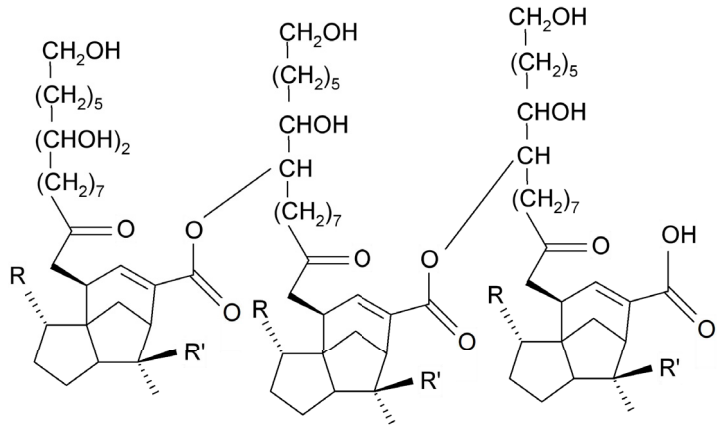

(1)

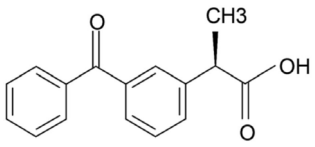

(2)

Figure 2-1. Chemical structure of shellac (1) and ketoprofen (2).

2.2. Materials and methods

2.2.1 Shellac and modified shellac nanocomposite

The wax free shellac used in this study was provided by Kigata, Japan. Ketoprofen 5 g (Mw =254.28), phosphate buffered saline (PBS, 1/15 mol L^{-1} with pH 6.8), hydrochloric acid (HCl), sodium carbonate and ethanol were purchased from SigmaAldrich (Japan) or Wako Pure Chemicals (Japan). All chemicals were used without further purification. Water was doubledistilled just before use.

Sodium shellac (shellac – COONa) was obtained by neutralization reaction of shellac and sodium carbonate solution. 5 g shellac was added every half hour into 50

mL, 0.1 mol L^{-1} sodium carbonate solution during magnetic stirring until it was no longer dissolved, the temperature was kept at 40 °C to speed up the reaction. No gas was observed during the neutralization process. And there was no weight lost after the neutralization process. Then the sodium shellac was obtained after drying 48 hours under room temperature.

A mixed solution composed of 65% (w/v) of shellac and 5% (w/v) ketoprofen in ethanol were mixed with solvent formulation for an optimal electrospinning solution to make NF1. 40% (w/v) shellac and 5% (w/v) ketoprofen for electrospray fluid to obtain NP1. 32.5% (w/v) of shellac, 32.5% (w/v) of sodium shellac and 5% (w/v) ketoprofen in ethanol to prepare NF2. 20% (w/v) of shellac, 20% (w/v) of sodium shellac and 5% (w/v) ketoprofen in ethanol to prepare NP2. 65% (w/v) of sodium shellac and 5% (w/v) ketoprofen in ethanol to prepare NF3. 65% (w/v) of sodium shellac and 5% (w/v) ketoprofen in ethanol to prepare NP3. These six parameters were investigated in three types of nanoparticles and three types of nanofibers. The resultant nanofibers and nanoparticles were collected on a metal collector wrapped with aluminum foil at affixed distance of 15/20 cm from the needle tip of the spinning/spray head. Their average sizes were determined by measuring the diameters of more than 100 particles in SEM images using the Image J software (National Institutes of Health, USA). Details of the parameters for electrospinning, electrospray process and the resultant products are listed in Table 1.

Table 2-1. Parameters used for electrospinning and electrospray process[e,f]

Number	Solution ingredient	Distance (cm)	Diameter (nano-meter)
NF[a]1	S[c] 100%	20	512 ± 250
NF2	S : SS[d] 50% : 50%	20	448 ± 250
NF3	SS 100%	20	351 ± 250
NP[b]1	S[c] 100%	15	699 ± 750
NP2	S : SS 50% : 50%	15	526 ± 600
NP3	SS 100%	15	345 ± 600

[a] NF: nanofiber. [b] NP: nanoparticle m. [c] Shellac. [d] Sodium shellac. [e] All tips with inner diameter of 0.6 mm. [f] The shell fluid consisted of 5% (w/v) ketoprofen in ethanol solution.

For electrospinning and electrospray process, an electrospinning apparatus manufactured by Kato Tech Co. Ltd. (Kyoto, Japan) was used. The applied voltage for both electrospinning and electrospray process was 15 kV. The distance from needle tip to collector was 20 cm for electrospinning process and for electrospray process was 15 cm.

2.2.2. Characteristics

After the Na_2CO_3 solution treatment, it can be observed that the colour of sodium shellac changed from yellow to brown as shown in Figure 2-2. No gas release was observed during the reaction process and no weight were lost during the process.

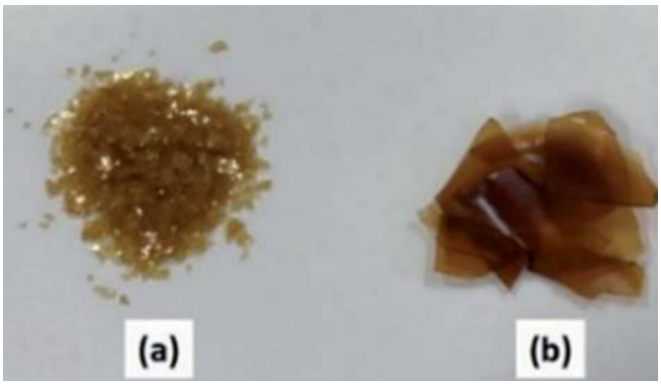

Figure 2-2. Photo of shellac (a) and sodium shellac (b).

The FTIR of sodium and shellac sodium, ATR-FTIR were conducted to investigate the compatibility between the shellac and the shellac sodium salt. It can be observed from Figure 2-3 that the basic trends of sodium shellac and shellac are similar, indicating that the change in the general structure is not very significant of shellac sodium salt relative to the shellac. But the shellac sodium has a characteristic at 1560 cm^{-1}. The appearance of this characteristic peak shows the difference between the sodium shellac and shellac, it also proves the presence sodium shellac meanwhile. The characteristic peak at 1560 cm^{-1} is because after the formation of the carboxylic acid salt, the carboxylic acid anion occurred resonance effect and produced coupling effect. I also analyse the FTIR spectrum of drug filled shellac nanofiber composite with sodium shellac with 0% (NF1), 50% (NF2) and 100% (NF3) in Figure 2-4(a) and FTIR spectrum of drug filled shellac nanofiber composite with sodium shellac with 0% (NP1), 50% (NP2) and 100% (NP3) in Figure 2-4(b). The results show that no chemical difference between NF and NP.

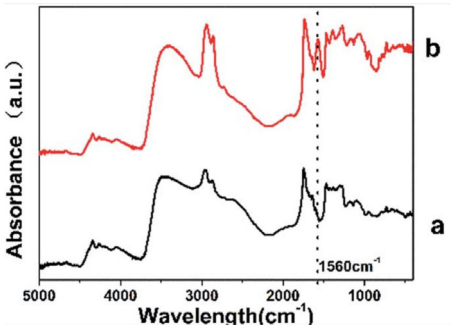

Figure 2-3. FTIR spectra of shellac (a) and sodium shellac (b).

By XRD analysis, no distinct peaks in the spectrum of shellac sodium and shellac evidently indicated in Figure 2-4 that the molecular orientation and arrangement of the polymers were disordered, i.e., an amorphous state. Similarly, there were no discrete peaks in the spectrum of nanofiber and nanoparticle from curve a and b which implied that the crystalline structure cannot be changed no matter it is in the nanofiber or in the nanoparticle part. And there were no discrete peaks in the spectrum of shellac and sodium shellac nanofibers and nanoparticles too. It indicates that in the nanomaterials, shellac and sodium shellac salt existed as the amorphous state in the both nanofiber and nanoparticle forms. The FTIR spectra of shellac and sodium shellac nanofibers and nanoparticles are illustrated in Figure 2-5 a and b respectively. For all samples, the characteristic peaks of shellac can be observed at 1710 cm^{-1} , 2860 cm^{-1} and 2930 cm^{-1} . In addition, sodium shellac characteristic peak can be observed at 1560 cm^{-1} as shown in NF 3 and NP3. The rate of sodium shellac content shows a proportional relationship in the curve which prove the exit of sodium shellac. In the case of shellac/ketoprofen-sodium shellac, the characteristic peaks of ketoprofen overlapped completely with the absorption bands of shellac and sodium shellac so that these bands

are unavailable for differentiation. The FTIR results show that there is no difference in chemical structure between nanofiber and nanoparticle.

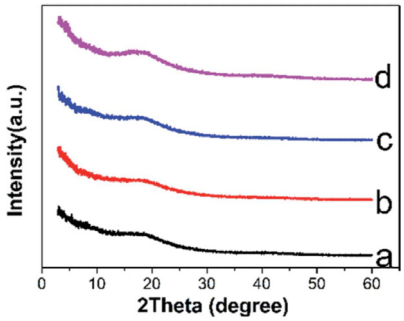

Figure 2-4. XRD spectra of shellac nanofiber (a), shellac nanoparticle (b), sodium shellac nanofiber (c), sodium shellac nanoparticle (d).

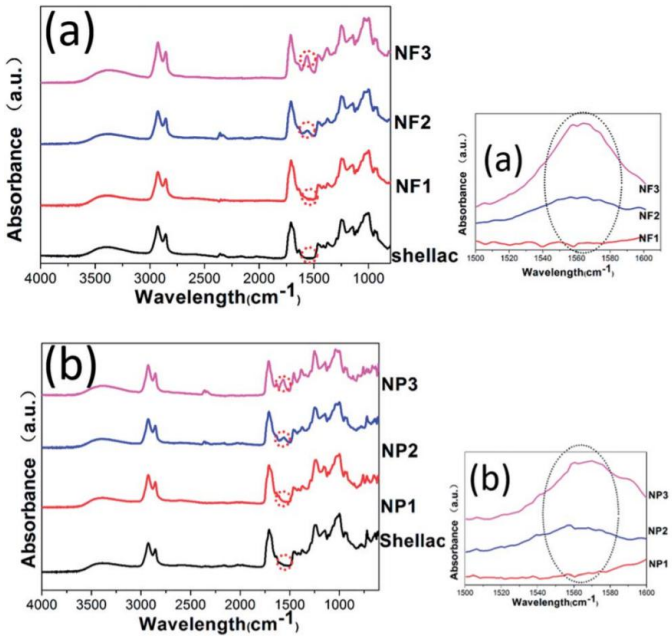

Figure 2-5. (a) FTIR spectrum of drug filled shellac nanofiber composite with sodium shellac with 0% (NF1), 50% (NF2) and 100% (NF3). (b) FTIR spectrum

of drug filled shellac nanofiber composite with sodium shellac with 0% (NP1), 50% (NP2) and 100% (NP3).

2.2.3. Microscopic morphology

Three kinds of shellac/sodium shellac/ketoprofen nanofibers and three kinds of nanoparticles have been observed respectively in Figure 2-5 a and b. Different sizes of extreme distribution nanoparticles can be observed. It is because the droplets tend into ellipsoid or irregular spherical in the role of gravity deformation. Larger charge density occurs in distribution on the sphere surface is heterogeneity. There is larger charge density in regions with larger curvatures. This caused the droplets affected by different directions and uneven forces. Different sizes of extreme distribution nanoparticles were generated during the division process of droplets. This phenomenon has more significant effect when the molecular mass is greater. The diameter distribution in NP1 is the most uneven one for this reason. Table 2-1 lists the details of shellac and sodium shellac resulted in nanofibers in which NF1, 2, 3 were obtained by electrospinning whilst NP1, 2, 3 were obtained by electrospray method (Figure 2-6 b). It can be found that the average diameters of both nanofiber and nanoparticle will be finer if more sodium shellac was added as shown in Figure 2-6 a and d.

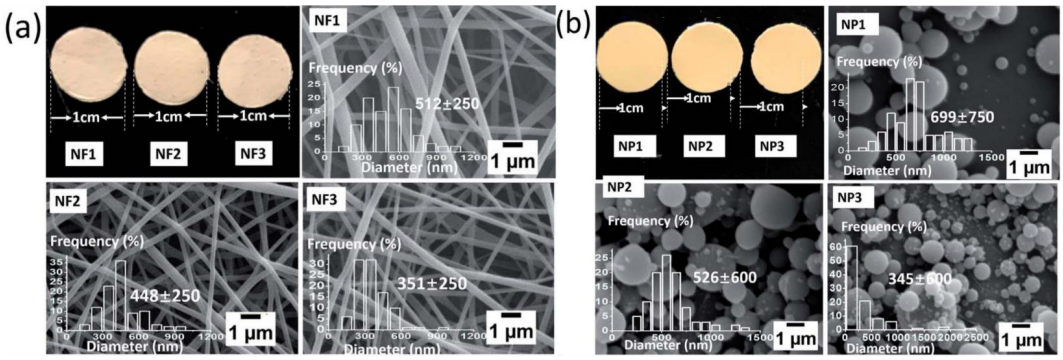

Figure 2-6. (a) Photographs, SEM images and diameter distribution of shellac/sodium shellac nanofiber composite sodium shellac with 0% (NF1), 50% (NF2) and 100% (NF3). (b) Photographs, SEM images and diameter distribution of shellac/sodium shellac nanofiber composite sodium shellac with 0% (NP1), 50% (NP2) and 100% (NP3).

The photographs of nanofibers and nanoparticles mats that evaluated in Figure 2-6 a and b are obtained after 15 min of electrospinning/electrospray process to detect the macroscopic difference. A light yellow appears on nanofibers at room temperature while darker yellow can be observed on nanoparticles. As all of the nanofibers and nanoparticles have bigger than 100 nm (bigger than the wavelength of the light). This phenomenon may because nanoparticle mats have a bigger density than nanofiber.

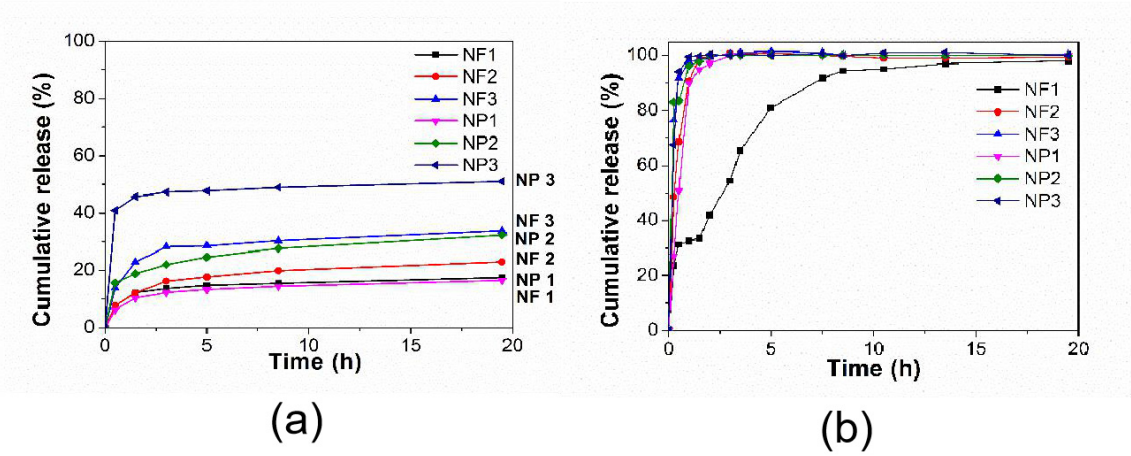

Figure 2-7. (a) Cumulative release from shellac nanofiber/nanoparticle composite with sodium shellac with 0 % (NF1, NP1), 50% (NF2, NP2) and 100 % (NF3, NP3) in pH 2. (b) Cumulative release from shellac nanofiber/nanoparticle composite with sodium shellac with 0 % (NF1, NP1), 50% (NF2, NP2) and 100 % (NF3, NP3) in pH 6.8.

2.2.4. Functional performance and controlled-release mechanism

The drug releases characteristics of the prepared samples were investigated by immersing all nano-composites into 50 mL 0.01 N HCl (pH 2) for 24 hours and PBS (pH 6.8) respectively and thermostatically shaken (100 rpm) for 24 hours at 36 °C. To determine the drug concentration, 4 mL of the test solution was taken at particular time intervals; 4 mL of new test solution was then added for capacity adjustment. A UV visible spectro photometer (V-530, JASCO, Japan) was used to determine the concentration of the ketoprofen released from collected test solution. To determine the concentration of ketoprofen, a calibration curve from the ultraviolet-visible absorption

spectrum of ketoprofen was prepared in advance.

In the vitro drug release profiles of the three kinds nanofibers and nanoparticles are given in Figure 2-7 a and b. In the acidic conditions of pH 2 (Figure 2-7 a), the release amount of the shellac/shellac sodium nanoscale application cannot reach to 100% as that in pH 6.8 dissolution medium. Agglomeration of the carrier can be observed in the bottom of the bottle. This is mainly because, at low pH conditions, the acid ions in the shellac combine with high concentrations of oxygen ions. The drug release behaviors are also studied in colon situation (pH 6.8) to keep the integrity of drug release in vitro. The sodium shellac has larger drug effect than pure shellac. The nanoparticles NP1 release entirely instantly when they were put into the pH 6.8 medium. The drug release effect of the sodium shellac is larger and drug release rate is quicker than pure shellac, whereas the drug release effect of nanoparticle is larger and drug release rate is higher than nanofiber. It is because the specific surface area of nanoparticle is obviously bigger than nanofiber. In addition, sodium shellac nanoscale applications (NF3, NP3) can be proved with good biodegradability because they can be observed almost totally dissolved after drug release process in pH 6.8 PBS solution. In the same condition, NF1/NP1 can not be observed dissolved obviously and NF2/NP2 can be observed part dissolved.

2.3. Results and discussion

2.3.1.Drug release curve in colon and stomach environment

The drug release effect of the sodium shellac is improved mainly through the principle of neutralization reaction. The functional groups at extremity of shellac molecule are not easy to dissociate. In sodium shellac, they changed to carboxylate radical which are easier ionized in water. The aforementioned reasons make sodium shellac can be dissolved easier at low pH conditions. In the same simulated environment with the pH value of the intestinal juice, the drugloaded film of the sodium salt of the shellac should a good release effect. Some studies carried out by other researchers are further discussed below. Wang et al.[29] synthesizedd shellac nanofiber for colon-targeted drug delivery. The researchers claimed a very small percentage of drug release at pH 2.0. They claimed the preparation of shellac nanofiber a release rate 8.2% and 9.3% during the first two hours at pH 2.0 PBS. And around 40% drug was released after 30 min immersion in pH 6.8 PBS. This result provided very similar sustained release profiles with our study for shellac nanofiber. The study did not report a further study for the suitability of the shellac nanoparticles and sodium shellac for drug delivery. Comparing the study of Wang et al.[29] and Cui et al., [30] pure shellac nanofibers and shellac nanoparticles were respectively analyzed for drug delivery in vitro. Both of their whole in vitro dug release processes (pH 2 and pH 6.8) were only last for about 10 hours. They claimed the preparation of shellac nanofiber/nanoparticle a release rate under 10% during the first two hours at pH 2.0 environment. And the drug release in gastric environment almost stop within 2 hours. While in our study, the release rate effect improved to 50% and lasting 20 hours in gastric environment. In another study,

Luo et al.[31] successfully developed sodium shellac particles for wrapping disperse multiscale emulsion. Sodium shellac has been reported as a novel wrapping material that can aggregate and wrap emulsion micelles driven by different forces. However, due to the high solid content of the nanoscale emulsion particles, they are difficult to wrap by the spray-drying method. Electrospray may be used as an easier way to produce shellac nanoparticles.

2.4. Conclusions

This study reported a novel method of shellac synthesis in the suitable utilization of a natural animal secreted resin. A potential to develop capsule form applications which can remain in the stomach for a long time. The sodium shellac which proved a larger and quicker drug effect in gastric environment. The sodium shellac was mixed in three concentrations with shellac (0%, 50% and 100%) and then electrospinning/electrospray into a composite mat. Nanofibers and nanoparticles loaded with ketoprofen were prepared successfully for sustained drug release. The results revealed that the release speed increased with the further addition of sodium shellac. And nanoparticle shows better drug effect than nano- fiber. Therefore, the results show that controlled drug release profile can be achieved by tuning sodium shellac in nanofiber/ nanoparticle composite. Thus, it is confirmed that the sodiumshellac/shellac composite as a sustained drug delivery nanofiber/nanoparticle mat.

However, the prepared nanofiber/nanoparticle mat has very low mechanical

properties. They are too low to install the samples on the testing machine because it is even hard to keep the shape of the samples. To solve this problem, synthetic material-PCL is added inside of nanocomposites to prepare nanofiber membrane to slove the problem.

Reference

1. Zhu Y, Ding J, Fu Y, et al, Fabrication and characterization of vapor grown carbon nanofiber/epoxy magnetic nanocomposites, *Polymer Composites*, 2016, 37(6): 1728-1734.

2. Yu X, Trase I, Ren M, et al, Design of nanoparticle-based carriers for targeted drug delivery, *Journal of nanomaterials*, 2016, 2016.

3. Wang Y, Zhu Y, Fu X, et al, Effect of TW-ZnO/SiO2-compounded shear thickening fluid on the sound insulation property of glass fiber fabric, *Textile Research Journal*, 2015, 85(9): 980-986.

4. Ni Q Q, Zhu Y F, Yu L J, et al, One-dimensional carbon nanotube@ barium titanate@ polyaniline multiheterostructures for microwave absorbing application, *Nanoscale research letters*, 2015, 10(1): 174.

5. Zhu Y F, Ni Q Q, Fu Y Q, One-dimensional barium titanate coated multi-walled carbon nanotube heterostructures: synthesis and electromagnetic absorption properties, *Rsc Advances*, 2015, 5(5): 3748-3756.

6. Dong Y, Ni Q Q, Li L, et al, Novel vapor-grown carbon nanofiber/epoxy shape memory nanocomposites prepared via latex technology, *Materials Letters*, 2014, 132: 206-209.

7. Ding J, Zhu Y, Fu Y, Preparation and properties of silanized vapor-grown carbon nanofibers/epoxy shape memory nanocomposites, *Polymer Composites*, 2014, 35(2): 412-417.

8. Fu X, Wang J, Ding J, et al, Quantitative evaluation of carbon nanotube dispersion through scanning electron microscopy images, *Composites Science and Technology*, 2013, 87: 170-173.

9. Dong Y, Ding J, Wang J, et al, Synthesis and properties of the vapour-grown carbon nanofiber/epoxy shape memory and conductive foams prepared via latex technology, *Composites Science and Technology*, 2013, 76: 8-13.

10. Dong Y, Wang R, Li S, et al, Use of TX100-dangled epoxy as a reactive noncovalent dispersant of vapor-grown carbon nanofibers in an aqueous solution, *Journal of colloid and interface science*, 2013, 391: 8-15.

11. Jin X, Ni Q Q, Fu Y, et al, Electrospun nanocomposite polyacrylonitrile fibers containing carbon nanotubes and cobalt ferrite, *Polymer Composites*, 2012, 33(3): 317-323.

12. Vasir J K, Tambwekar K, Garg S. Bioadhesive microspheres as a controlled drug delivery system, *International journal of pharmaceutics*, 2003, 255(1-2): 13-32.

13. Kenawy E R, Abdel-Hay F I, El-Newehy M H, et al, Processing of polymer

nanofibers through electrospinning as drug delivery systems[M]//Nanomaterials: Risks and Benefits, *Springer, Dordrecht*, 2009: 247-263.

14. Ke M, Wahab J A, Hyunsik B, et al, Allantoin-loaded porous silica nanoparticles/polycaprolactone nanofiber composites: fabrication, characterization, and drug release properties, *RSC Advances*, 2016, 6(6): 4593-4600.

15. Sridhar R, Ramakrishna S, Electrosprayed nanoparticles for drug delivery and pharmaceutical applications, *Biomatter*, 2013, 3(3): e24281.

16. Siebers M C, Walboomers X F, Leeuwenburgh S C G, et al, Electrostatic spray deposition (ESD) of calcium phosphate coatings, an in vitro study with osteoblast-like cells, *Biomaterials*, 2004, 25(11): 2019-2027.

17. Ma K, Qiu Y, Fu Y, et al, Improved shellac mediated nanoscale application drug release effect in a gastric-site drug delivery system, *RSC Advances*, 2017, 7(84): 53401-53406.

18. Bitz C, Doelker E, Influence of the preparation method on residual solvents in biodegradable microspheres, *International Journal of Pharmaceutics*, 1996, 131(2): 171-181.

19. Falk R, Randolph T W, Meyer J D, et al, Controlled release of ionic compounds from poly (L-lactide) microspheres produced by precipitation with a compressed antisolvent, *Journal of controlled release*, 1997, 44(1): 77-85.

20. Genta I, Costantini M, Asti A, et al, Influence of glutaraldehyde on drug release and mucoadhesive properties of chitosan microspheres, *Carbohydrate polymers*, 1998,

36(2-3): 81-88.

21. Berkland C, Kim K K, Pack D W, Fabrication of PLG microspheres with precisely controlled and monodisperse size distributions, *Journal of controlled release*, 2001, 73(1): 59-74.

22. Berkland C, Pack D W, Kim K K, Controlling surface nano-structure using flow-limited field-injection electrostatic spraying (FFESS) of poly (d, l-lactide-co-glycolide), *Biomaterials*, 2004, 25(25): 5649-5658.

23. Zeleny J, The electrical discharge from liquid points, and a hydrostatic method of measuring the electric intensity at their surfaces, *Physical Review*, 1914, 3(2): 69.

24. Fenn J B, Mann M, Meng C K, et al, Electrospray ionization for mass spectrometry of large biomolecules, *Science*, 1989, 246(4926): 64-71.

25. Nagy Z K, Balogh A, Drávavölgyi G, et al, Solvent-free melt electrospinning for preparation of fast dissolving drug delivery system and comparison with solvent-based electrospun and melt extruded systems, *Journal of pharmaceutical sciences*, 2013, 102(2): 508-517.

26. Li W, Yu D G, Chen K, et al, Smooth preparation of ibuprofen/zein microcomposites using an epoxy-coated electrospraying head, *Materials Letters*, 2013, 93: 125-128.

27. Nagy Z K, Wagner I, Suhajda Á, et al, Nanofibrous solid dosage form of living bacteria prepared by electrospinning, *Express Polymer Letters*, 2014, 8(5).

28. Limmatvapirat S, Panchapornpon D, Limmatvapirat C, et al, Formation of shellac

succinate having improved enteric film properties through dry media reaction, *European Journal of Pharmaceutics and Biopharmaceutics,* 2008, 70(1): 335-344.

29. Wang X, Yu D G, Li X Y, et al. Electrospun medicated shellac nanofibers for colon-targeted drug delivery, *International journal of pharmaceutics*, 2015, 490(1-2): 384-390.

30. Cui L, Liu Z P, Yu D G, et al, Electrosprayed core-shell nanoparticles of PVP and shellac for furnishing biphasic controlled release of ferulic acid, *Colloid and Polymer Science*, 2014, 292(9): 2089-2096.

31. Luo Q, Li K, Xu J, et al, Novel Biobased Sodium Shellac for Wrapping Disperse Multiscale Emulsion Particlesm, *Journal of agricultural and food chemistry*, 2016, 64(49): 9374-9380.

Chapter 3

Drug release on skin care with PCL/shellac transparent nanofiber membranes

Chapter 3: Drug release on skin care with PCL/shellac transparent nanofiber membranes

3.1. Introduction

In the last chapter, shellac nanoparticle/nanofiber composities are studied and discussed as a drug release application which are restricted inside of capsule because of the very low mechanical properties. For solving this problem, in this chapter, synthetic material - PCL is added and prepare nanofiber membrane together with nature material shellac. Since nanoscale drug delivery systems (DDSs) have attracted the attention of pharmaceutical, biotechnology, and health-care industries during the past 20 years [1-5], and numerous new DDSs have been developed [6-11]. As nanotechnology has evolved with several historical breakthroughs [12-14], nanofibers have become widely used in DDSs because of their simple production methods and high specific surface area. DDSs need to meet several major requirements such as controlled drug release at the target location, high drug loading capacity, biodegradability, non-toxicity, and cost-effectiveness. DDS technology such as drug-eluting stents, nanoformulated drugs, devices to improve efficacy, and drug coatings have allowed targeted drug delivery with decreased drug side effects. One of the most promising biodegradable polymers for use in DDSs is polycaprolactone (PCL), the chemical structure of which is shown in Figure.

3-1a, because its mechanical and biological properties make it suitable for biomedical applications. PCL is a semicrystalline aliphatic polyester with a low glass transition temperature (- 60°C) that possesses broad in vivo and in vitro biocompatibility [15, 16]. The US Food and Drug Administration has approved PCL for use in a substantial number of DDSs and other biomedical applications [17].

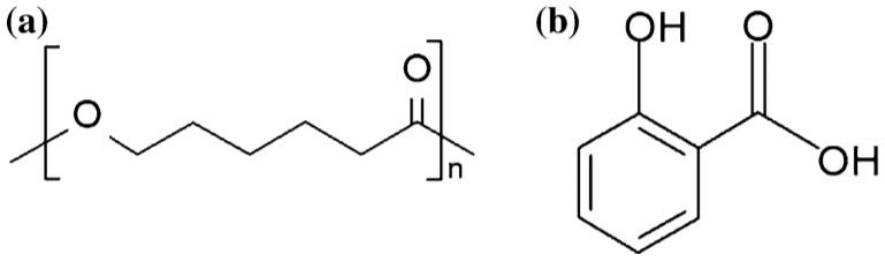

Figure 3-1. Chemical structure of PCL (a) and salicylic acid (b).

Shellac is a kind of resin secreted by the female lac bug on trees in the forests of India and Thailand and has a chemical structure as shown in Figure 3-2. Refined shellac can be obtained by purification of crude shellac directly secreted by the lac bug. Shellac has been widely used in medicine, food, coatings, military, dyes, and other fields because of its excellent waterproofing, film-forming, and fixing abilities as well as biocompatibility. Shellac was originally used as a drug coating in the pharmaceutical industry in the 1950s. With the development of biomedical science, increasing attention has been paid to the limitations of synthetic materials, such as their irritant and carcinogenic effects. The products of shellac have been extended to DDSs because it is the only natural animal-secreted resin that can be used in pharmaceutical applications

[18, 19]. In this study, shellac is used to improve the performance of a DDS. Higher mechanical strength, flexibility, and transparency are obtained after shellac treatment of the DDS. Immich et al. [20] fabricated sandwich-structured polylactic acid (PLA)/ibuprofen/PLA membranes for ultrafiltration by simply putting ibuprofen between two pieces of PLA nanofiber membrane without any further treatment. Thus, their membranes cannot display higher mechanical strength than that of PLA. Chen et al. [21] fabricated a sandwich-structured biodegradable nanofibrous membrane that released large amounts of vancomycin, gentamicin, and lidocaine in vivo. However, the tensile strength and elongation of the prepared membrane at break were just 1.13 MPa and 116%, respectively. In addition, the transparency of the prepared samples was not considered. Although DDSs have been sufficiently studied, very little literature is available on the synthesis of ethanol vapor-treated PCL/shellac/PCL sandwichstructured membranes as a drug carrier. Therefore, here I report our study on electrospun PCL/shellac/PCL sandwich-structured nanofiber mats loaded with salicylic acid (Figure. 3-1b) as a guest drug. The objective of this study is to evaluate the sustained release of salicylic acid from treated electrospun PCL/shellac/PCL nanofiber membranes designed for use in medical applications. The prepared sandwich-structured nanofiber membranes are transparent, mechanically strong, and obviously slow the release of salicylic acid. Therefore, this new system can be directly used in skin care applications for patients who want to dilute pigment spots, shrink pores, remove fine wrinkles and decrease sun-induced aging. The transparency of the prepared nanofiber membrane increases its

aesthetics.

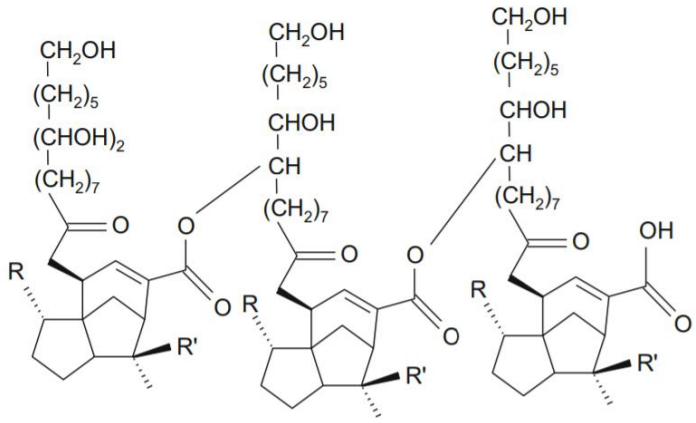

Figure 3-2. Chemical structure of shellac.

3.2 Materials and methods

3.2.1. Preparation of Shellac/PCL nanofiber membrane

PCL (Mn: 70 000 – 90 000) and the wax-free shellac were provided by Kigata, Japan. Salicylic acid (FW = 138.12), phosphate-buffered saline (PBS; 1/15 mol/L, pH 7.2), ethanol, dichloromethane (DCM), and dimethylformamide (DMF) were purchased from Sigma-Aldrich (Japan) or Wako Pure Chemicals (Japan). All chemicals were used without further purification. Water was double-distilled just before use. Preparation of PCL solution DCM/DMF (6:4 w/w) was used as the solvent for PCL. The optimal electrospinning solution contained 10 wt % PCL in DCM/DMF, as reported previously [22]. Salicylic acid/PCL (1:20) were mixed before making the PCL solution to obtain a homogeneous solution faster.

For preparation of shellac solution. Three concentrations of shellac solution in ethanol (55, 65, and 75 wv%) were mixed to determine the optimal electrospinning

solution. The results (Figure 3-3) should that the 65 wv% shellac solution produced smooth, regular shellac nanofibers without beads in the structure along with a small mean diameter. A smaller nanofiber diameter allows higher permeability [23] for liquids along with increased specific surface area, which enhances the adhesion between fibers. For the other shellac formulations, undesirable results (beads, shellac surface, and structural irregularities) were observed. Therefore, a shellac concentration of 65 wv% was used in further experiments. Salicylic acid was added to the shellac solution to give an acid/shellac ratio of 1:20. As above, the salicylic acid was added to shellac before the solvent to obtain a homogeneous solution faster.

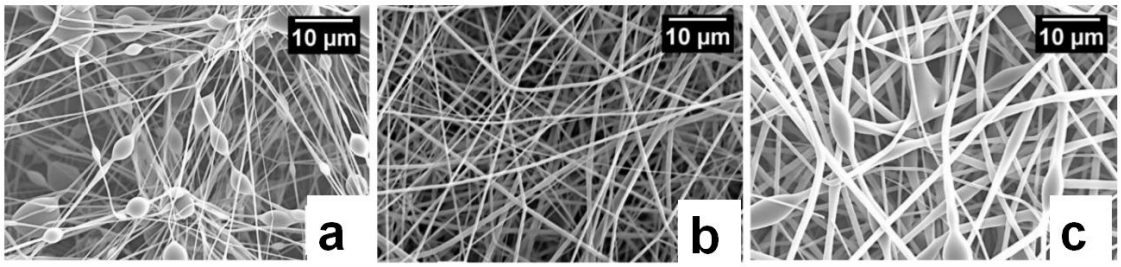

Figure 3-3. SEM image of 55, 65, and 75wv% shellac nanofiber.

For preparation of PCL/shellac/PCL sandwich structured nanofiber membranes. An electrospinning apparatus manufactured by Kato Tech Co. Ltd. (Kyoto, Japan) was used. The PCL solution was placed into a 10-mL syringe (SS-10T; Terumo, Tokyo, Japan) with a stainless steel needle (NN-2138 N; Terumo) connected to a high voltage power supply. For the PCL solution, the applied voltage was 12 kV and the distance from the

needle tip to the substrate was 15 cm. For the shellac solution, the applied voltage was 15 kV and the distance from the needle tip to the substrate was 20 cm. The PCL solution flow rate was 0.3 mm/min, and the shellac solution flow rate was 0.5 mm/min. Ethanol vapor-treated samples were prepared by placing rectangular ceramics fixed with the nanofibers in a desiccator saturated with ethanol vapor at 25 C for 4 h and then drying under vacuum at room temperature for 24 h. Fabrication of PCL/shellac/PCL sandwichstructured membranes Shellac nanofibers were contained between two adjacent layers of the PCL nanofiber membranes as follows. After the first layer of the electrospun PCL membrane was dried and solidified, shellac nanofibers were collected on the membrane surface. After placing the shellac nanofiber on the PCL membrane surface, the second PCL membrane layer was electrospun on top. The sandwich-structured membrane configuration is illustrated in Figure 3-4.

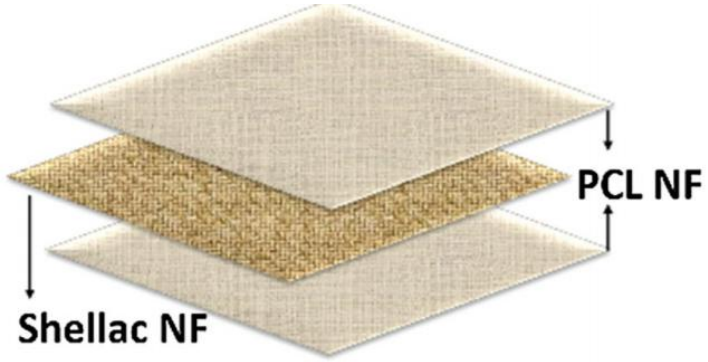

Figure 3-4. Schematic illustration of a PCL/shellac/PCL sandwich structured membrane.

3.2.2. Microscopic morphology

To compare the drug release behavior of the PCL/shellac/PCL nanofiber membranes before and after treatment, membrane thickness (δ) was recorded. All the δ data mentioned in this study are the thickness of prepared membranes before the drug release process. The δ values do not reflect the real sample thicknesses during the drug release process, when the membrane is swollen and wet. The results for d determination before and after treatment are presented in Figure 3-5.

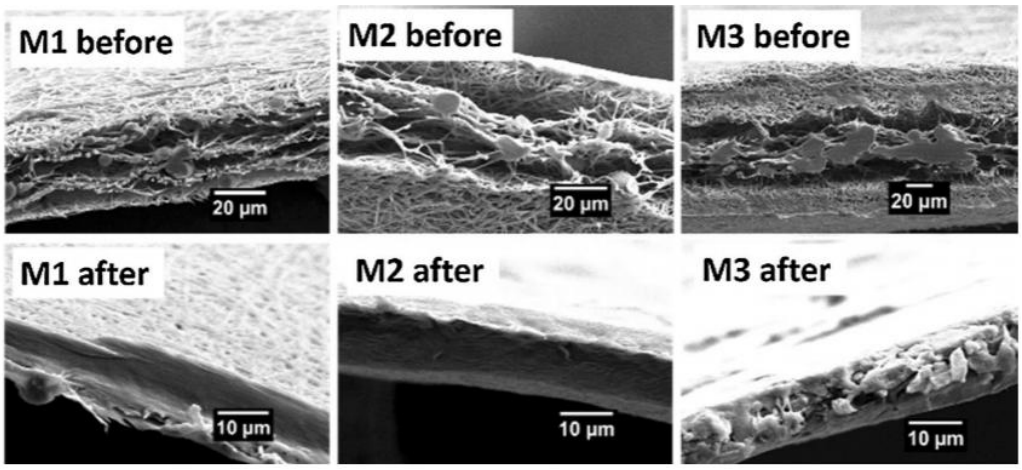

Figure 3-5. Cross-sectional SEM images before and after treatment

Table 3-1. Thickness of PCL/shellac/PCL membranes before and after treatment

Number	Amount ratios of PCL/shellac/PCL	Before treatment	After treatment
M1	1mL/2mL/1mL	0.031mm	0.009mm
M2	2mL/2mL/2mL	0.047mm	0.012mm
M3	4mL/2mL/4mL	0.095mm	0.0125mm

The determined δ values for the PCL/shellac/PCL membranes were 1/2/1, 2/2/2, and 4/2/4 mL (mL is milliliter) during electrospinning process. These three different ratios were obtained using various PCL/shellac/PCL solution ratios for the electrospinning process. The results are presented in Table 3-1.

In Figure 3-5, the differences between membranes before and after treatment are noticeable. The crosssectional image of the membrane before treatment clearly shows empty spaces between the PCL and shellac nanofibers. After treatment, the nanofibers are tightly bound together. The shellac nanofibers melt during ethanol vapor treatment, as illustrated in Figure 3-6a and b. In contrast, the morphology of the PCL nanofibers does not change during treatment. During the treatment process, shellac nanofibers melted and slowly penetrated through the small gaps between PCL nanofibers to fill the gaps until a uniform coating formed on the membrane surface. This process can explain the thickness decrease observed after treatment.

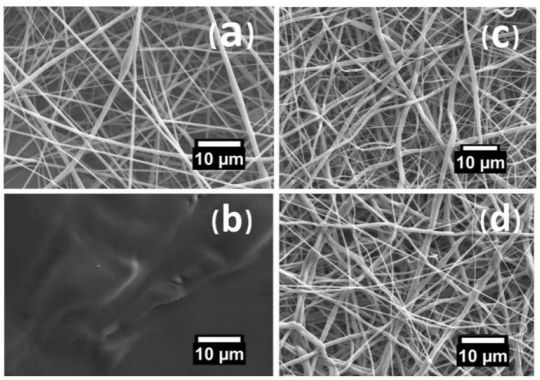

Figure 3-6. SEM images of a shellac nanofibers before treatment, b shellac nanofibers after treatment, c PCL nanofibers before treatment, and d PCL nanofibers after treatment.

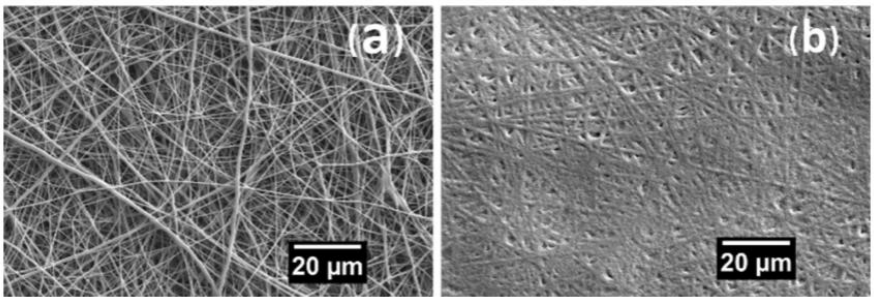

Figure 3-7. SEM images of PCL/shellac/PCL membranes a before and b after treatment.

The morphologies of the PCL and shellac nanofibers before and after treatment are illustrated in Figure 3-6. The surface morphologies of the PCL/shellac/PCL nanofiber membranes before and after treatment are presented in Figure 3-7.

3.2.3. Chemical Characteristics

The morphology of the electrospun mats was investigated by scanning electron microscopy (SEM; 3000H, Hitachi, Japan). Fourier transform infrared (FTIR) analysis (IR Prestige 21, Shimadzu, Japan) was carried out to study the chemical structure of the surface of the prepared nanofiber membranes. X-ray diffraction (XRD) was performed on a D/Max-BR diffractometer (Rigaku, Tokyo, Japan) over the 2h range of $5-80^\circ$ using CuKa radiation at 40 mV and 30 mA. Mechanical properties of the prepared nanofiber membranes were determined by a universal testing machine (Tensilon RTC1250A, A&D Company Ltd., Japan) at a crosshead speed of 20 mm/min. Transparency was measured on a UV– Vis spectrophotometer (V-530, JASCO, Japan).

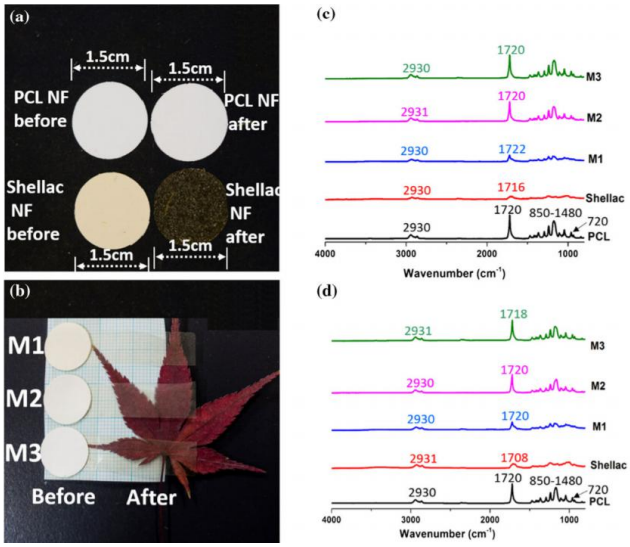

Figure 3-8. Photographs of a PCL nanofibers and shellac nanofibers before treatment and b PCL/shellac/PCL membranes before and after treatment. FTIR spectra of samples c before and d after treatment.

Figure 3-8a shows that the shellac nanofibers form a light yellow membrane, which ethanol vapor treatment changes to a yellow translucent film. The photograph of the prepared membranes (M1, M2, M3) in Figure 3-8b reveals that their transparency increases considerably after ethanol vapor treatment. FTIR spectroscopy was conducted to analyze the chemical composition of the prepared nanofiber membranes before and after treatment. Comparing the spectra of membranes before and after treatment revealed that there were almost no changes in the spectra. The characteristic peak from the carbonyl groups (C=O stretching vibration) at 1708 cm^{-1} in spectrum of the shellac nanofibers before treatment shifted to 1716 cm^{-1} after treatment [23]. The FTIR spectra of PCL and PCL/shellac/PCL membranes are presented in Figure 3-8. For all samples,

characteristic peaks from PCL [24] are observed at 720, 850 – 1480, and 1720 cm^{-1} . For the PCL/shellac/PCL membranes, the characteristic peaks from shellac and salicylic acid overlapped completely with the absorption bands of PCL, so these bands were unavailable for differentiation. The intensity of the numerous peaks in the finger region of PCL for all three nanofiber membranes (M1, M2, M3) increased after treatment. The lack of distinct peaks in the XRD patterns of shellac indicated that shellac was amorphous (Figure 3-9 (a)). There were no discrete peaks in the XRD patterns of the membranes before and after treatment, which implies that the crystalline structure is not changed by ethanol vapor treatment even though the shellac nanofibers melt in ethanol vapor. Only the result for M1 has been shown because the flat peak from shellac and distinct peaks from PCL can both be observed easily for this sample. The XRD results show that ethanol vapor treatment did not induce any large changes in the crystallinity of the membranes. The XRD patterns of the pure PCL nanofibers before and after treatment were the same (Figure 3-9 (b)), which is similar to the result for M1. Figure 3-10 shows the XRD patterns of M1, M2, and M3 before and after treatment. The PCL peaks indicate that PCL does not change during treatment.

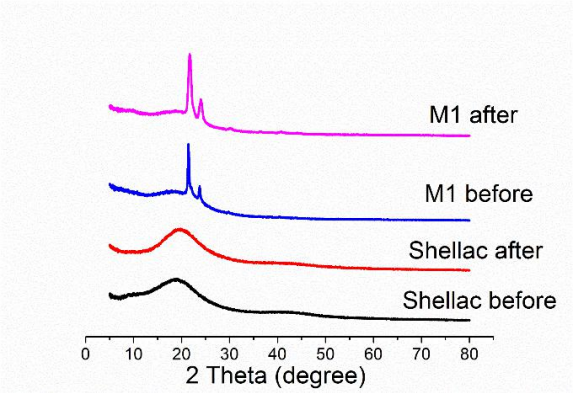

(a)

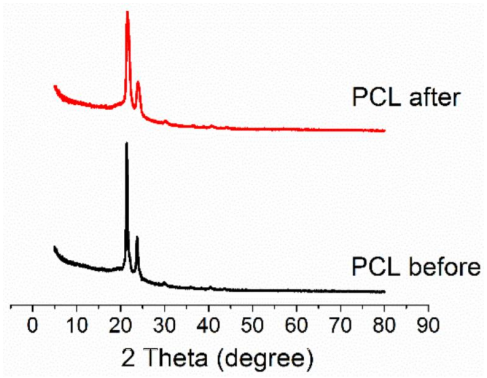

(b)

Figure 3-9. XRD patterns of shellac and M1 samples (a) and PCL nanofibers (b) before and after treatment.

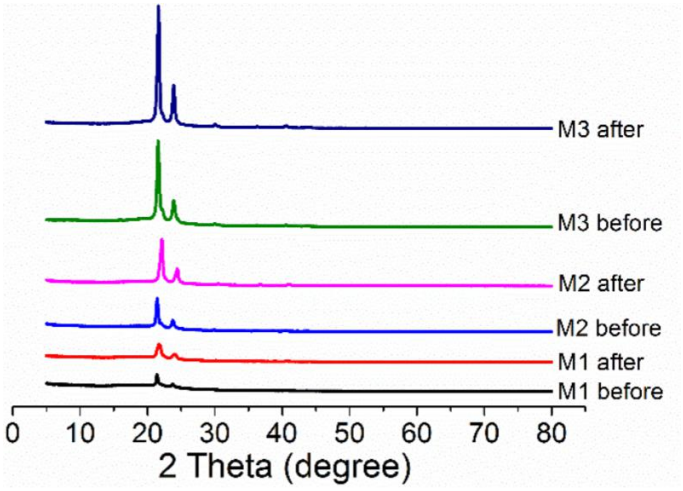

Figure 3-10. XRD patterns of samples before and after treatment.

3.2.4 Tensile test

Figure 3-11 shows typical stress-strain curves of the M1, M2, and M3 membranes before and after ethanol vapor treatment. The mechanical properties, tensile strength, elongation, and Young's modulus of M1, M2, and M3 after treatment were markedly improved compared with the corresponding values before treatment. The tensile strengths of treated M1, M2, and M3 were 7.27, 12.05, and 21.56 MPa, respectively.

(a)

The elongation percentages of M1, M2, and M3 were 8.21, 12.05, and 5.83%, respectively. Meanwhile, the Young's moduli calculated at 0.8% strain were 194.85, 275.88, and 778.05 MPa for treated M1, M2, and M3, respectively. The increases in tensile strength and Young's modulus could be attributed to shellac melting and adhering to the PCL nanofibers increasing the fiber interactions to form a film. The lower elongation percentages before and after treatment could be attributed to this reason as well. After treatment, M1 exhibited tensile strength that was 5.02 times higher and Young's modulus that was 7.8 times higher than the corresponding values before treatment. The tensile strength of M2 was 4.59 times higher after treatment, and its Young's modulus was 13.81 times higher. Meanwhile, M3 exhibited tensile strength 8.44 times higher and a Young's modulus 37.99 times higher after treatment. The increased density of PCL nanofibers following treatment contributed to the rises of tensile strength and Young's modulus.

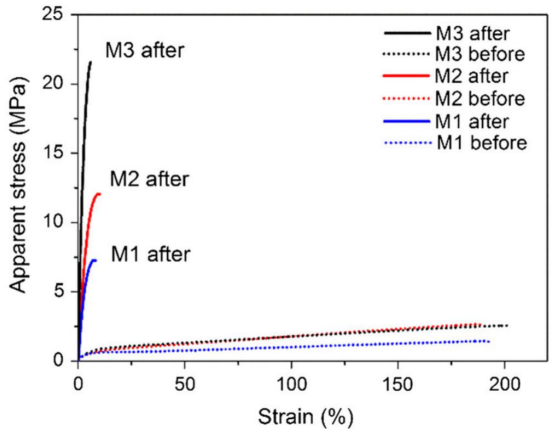

Figure 3-11. Stress–strain curves of the prepared membranes before and after treatment.

3.2.5 Transparent mechanism

The photograph in Figure 3-8b reveals that the membranes were clearly transparent after treatment. Figure 3-12 depicts the regular light transmittance spectra of the treated membranes along with those of the membranes before treatment. The regular transmittances of the membranes are similar in the visible wavelength range, especially at 555 nm, to which the naked human eye is most sensitive [25]. The regular transmittance at 555 nm of the membranes is high (about 35%), which is suitable to make them invisible, which is an attractive feature for skin care applications. The regular transmittance of the membranes can also be observed as a small peak in the UV region (280-360 nm); the intensity of this peak increases after treatment for M1. The treated membranes are smoother than the untreated ones because shellac nanofibers melted and filled the pores of the PCL nanofibers. For this reason, light scattering is decreased and the transparency of the membranes is increased following ethanol vapor treatment.

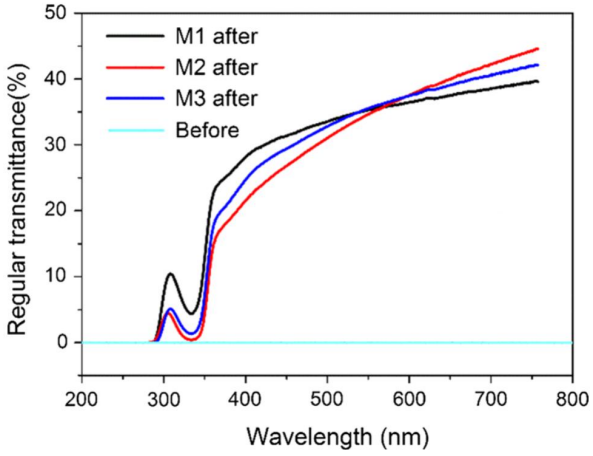

Figure 3-12. Transmittance curves of the prepared membranes before and after treatment.

3.2.6 Drug release curve

The release of salicylic acid from the pure PCL nanofibers and pure shellac nanofibers is shown in Figure 3-13. For the pure PCL nanofibers, slower salicylic acid release was observed over the whole release process compared with that by the shellac nanofibers, which rapidly released all the drug after 60 h. For both shellac and PCL nanofibers, salicylic acid was adsorbed on the surface of the nanofibers. Salicylic acid is a polar molecule and has high affinity for ethanol/DMF, whereas shellac and ethanol and PCL and DMF have low affinities for each other. As a result, during the electrospinning process, the dissolved salicylic acid concentration of the working solution changed on volatilization and salicylic acid moved to the surface of nanofibers.

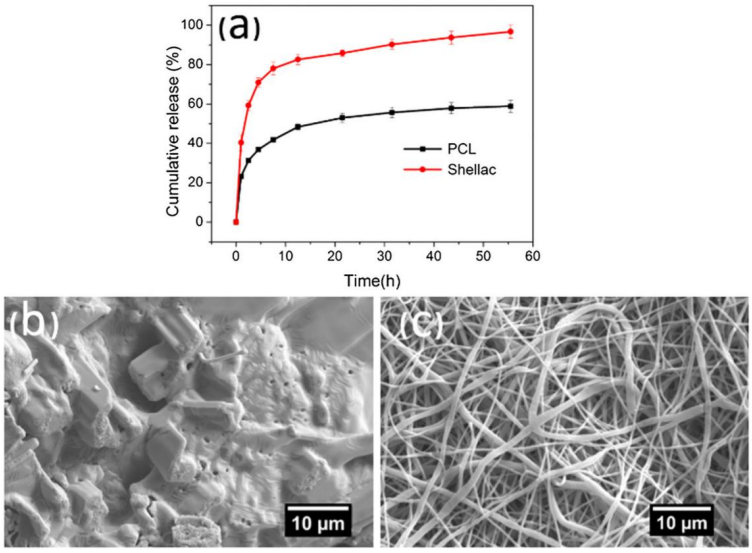

Figure 3-13. In vitro dissolution tests. a Salicylic acid release profiles from PCL and shellac nanofiber. b SEM images of shellac nanofibers after the release process and c SEM images of PCL nanofibers after the release process.

Therefore, the rapid release of salicylic acid was observed at the beginning for both shellac and PCL nanofibers.

The comparatively higher release rate of shellac nanofibers than PC nanofibers is because the shellac nanofibers broke during the drug release process in neutral PBS solution, as can be observed in Figure 3-13b. The shellac nanofibers seem to erode as dissolution progresses [26]. This is believed to be a result of the changes in the shellac molecular conformations as the salicylic acid molecules are released into solution. When the nanofibers are transferred into the dissolution media, shellac molecules can absorb water, which causes the nanofibers to swell, break, melt, and then gradually expand, unfold, and dissolve. The melting of shellac nanofibers and concomitant unfolding of shellac molecules releases the salicylic acid. The PCL nanofibers did not change obviously after the drug release process, as illustrated in Figure 3-13c, consistent with the release behavior of a non-erodible system. Although the PCL nanofibers are biodegradable and erodible, in this study, these phenomena were negligible because the release process finished before the biodegradation of the PCL nanofibers. Therefore, the PCL membrane was considered to be a non-erodible system. The influence of the shellac/PCL ratio on the release kinetics of salicylic acid by the membrane was studied; the results are presented in Figure 3-14. The cumulative salicylic acid release from nanofiber membranes reached equilibrium within about 10 h (Figure 3-14). After treatment, the membranes presented increased kinetics initially (Figure 3-14b), whereas the untreated membranes displayed higher release of

approximately 75-90% of their salicylic acid during the drug release process (Figure 3-14a). This initial rapid release of the treated membranes occurred because in the treated samples, the shellac nanofiber membranes melted and covered the PCL nanofiber surface. Figure 3-14 d reveals that the shellac coating broke during the drug release process and parts of the PCL nanofibers were naked on the membrane surface so they could directly contact the neutral PBS solution. After treatment, the membranes displayed a smaller cumulative release amount compared with that of the untreated membranes.

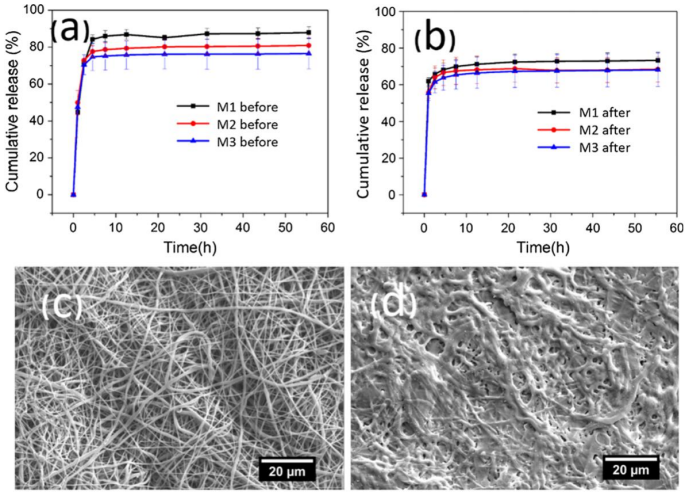

Figure 3-14. In vitro dissolution tests. Salicylic acid release profiles from membranes a before and b after treatment. SEM images of the PCL/ shellac/PCL membranes c before treatment after the release process and d treated PCL/shellac/PCL membranes after release process.

This may be because the PCL nanofibers were covered, and this did not have enough space to unfold. In the case of the untreated membranes, the salicylic acid in the shellac nanofibers could permeate through the external PCL nanofibers. As a result, the PCL nanofibers were uncovered and had enough space to unfold, resulting in a larger cumulative release amount during the drug release process.

3.3. Conclusions

Our experimental results should that ethanol vaportreated sandwich-structured PCL/shellac/PCL-salicylic acid membranes possessed good mechanical properties and mensurable transparency. The membrane tensile strength increased with the PCL ratio of the samples. Conversely, PCL ratio had little influence on transparency and the drug release process. About 70% cumulative release of salicylic acid by the ethanol vapor-treated membranes was obtained, and the release process was almost finished after about 10 h (although most of the drug was released within 8 h). These characteristics satisfy the demands for use of the membranes in skin care applications on the face. A drug release process which takes 8 h is commensurate with overnight application.

The mechanical properties are substantial improvement and wider application with special character (such as transparence) are obtained for certain needs, but the application is limited in nanofiber membrane. A nanofibrous tube application is considered to manufacture. Before that, a simple tensile test of nanofiber mat and nanofiber tube is done to prepare the mechanical properties between the two shape of

applications.

Reference

1. Formalas A US patent 1, 1934, 975, 504.

2. Doshi J, Reneker DH, Electrospinning process and applications of electrospun fibers, *J Electrostat,* 1995, 35(2–3): 151–160.

3. Shin YM, Hohman MM, Brenner MP, Rutledge GC, Electrospinning: a whipping fluid jet generates submicron polymer fibers, *Appl Phys Lett,* 2001, 78(8):1149–1151.

4. Reneker DH, Yarin AL, Fong H, Koombhongse S, Bending instability of electrically charged liquid jets of polymer solutions in electrospinning, J Appl Phys, 2000, 87(9):4531–4547.

5. Fridrikh SV, Jian HY, Brenner MP, Rutledge GC, Controlling the fiber diameter during electrospinning, *Phys Rev Lett,* 2003, 90(14):144502-1–144502-4.

6. Davidson A, Al-Qallaf B, Das DB, Transdermal drug delivery by coated microneedles: geometry effects on effective skin thickness and drug permeability, *Chem Eng Res Des,* 2008, 86(11):1196–1206

7. Langer R, Cima LG, Tamada JA, Wintermantel E, Future directions in biomaterials, *Biomaterials,* 1990, 11(9): 738–745.

8. Ponchel G, Irache JM, Specific and non-specific bioadhesive particulate systems for oral delivery to the gastrointestinal tract, *Adv Drug Deliv Rev,* 1998, 34(2–3):191–219.

9. Raiche AT, Puleo DA, Modulated release of bioactive protein from multilayered

blended PLGA coatings, *Int J Pharm,* 2006, 311(1–2):40–49.

10. Gupta B, Revagade N, Hilborn J, Poly (lactic acid) fiber: an overview, *Prog Polym Sci*, 2007, 32(4):455–482.

11. Auras, Rafael A., et al., eds. Poly (lactic acid): synthesis, structures, properties, processing, and applications, *John Wiley & Sons,* 2011, Vol. 10.

12. Yoshimoto H, Shin YM, Terai H, Vacanti JP, A biodegradable nanofiber scaffold by electrospinning and its potential for bone tissue engineering, *Biomaterials,* 2003, 24(12): 2077–2082.

13. Kim G, Kim W, Highly porous 3D nanofiber scaffold using an electrospinning technique, *J Biomed Mater Res B Appl Biomater,* 2007, 81(1):104–110.

14. Baker SE, Tse KY, Lee CS, Hamers RJ, Fabrication and characterization of vertically aligned carbon nanofiber electrodes for biosensing applications, *Diam Relat Mater*, 2006, 15, (2–3):433–439.

15. Hutmacher DW, Schantz T, Zein I, Ng KW, Teoh SH, Tan KC, Mechanical properties and cell cultural response of polycaprolactone scaffolds designed and fabricated via fused deposition modeling, *J Biomed Mater Res Part A,* 2001, 55(2):203–216.

16. Pitt CG, Chasalow FI, Hibionada YM, Klimas DM, Schindler A, Aliphatic polyesters. I. The degradation of poly (e-caprolactone) in vivo, *J Appl Polym Sci,* 1981, 26(11):3779–3787.

17. Domb AJ, Kost J, Wiseman D (eds), *Handbook of biodegradable polymers*, 1998,

vol 7. CRC Press, Boca Raton.

18. Limmatvapirat S, Panchapornpon D, Limmatvapirat C, Nunthanid J, Luangtana-Anan M, Puttipipatkhachorn S, Formation of shellac succinate having improved enteric film properties through dry media reaction, *Eur J Pharm Biopharm,* 2008, 70(1):335–344.

19. Wang X, Yu DG, Li XY, Bligh SA, Williams GR, Electrospun medicated shellac nanofibers for colon-targeted drug delivery, *Int J Pharm*, 2015, 490(1–2):384–390.

20. Immich APS, Arias ML, Carreras N, Boemo RL, Tornero JA, Drug delivery systems using sandwich configurations of electrospun poly (lactic acid) nanofiber membranes and ibuprofen, *Mater Sci Eng C,* 2013, 33(7):4002–4008.

21. Chen DWC, Liao JY, Liu SJ, Chan EC, Novel biodegradable sandwich-structured nanofibrous drug-eluting membranes for repair of infected wounds: an in vitro and in vivo study, *Int J Nanomed*, 2012, 7:763–771.

22. Ke M, Wahab JA, Hyunsik B, Song KH, Lee JS, Gopiraman M, Kim IS, Allantoin-loaded porous silica nanoparticles/polycaprolactone nanofiber composites: fabrication, characterization, and drug release properties, *RSC Adv,* 2016, 6(6):4593–4600.

23. Ahn J, Chung WJ, Pinnau I, Guiver MD, Polysulfone/ silica nanoparticle mixed-matrix membranes for gas separation, J Membr Sci, 2008, 314(1–2):123–133.

24. Wu C-S, Physical properties and biodegradability of maleated-polycaprolactone/starch composite, *Polym Degrad Stab*, 2003, 80:127–134.

25. Barten PG, Contrast sensitivity of the human eye and its effects on image quality, Spie Optical Engineering Press, *Bellingham*, 1999, vol 19.

26. Wang X, Yu DG, Li XY, Bligh SA, Williams GR, Electrospun medicated shellac nanofibers for colon-targeted drug delivery. *Int J Pharm,* 2015, 490(1–2):384–390.

Chapter 4

Mechanical property of nanofibrous tube and nanofiber membrane

Chapter 4: Mechanical property of nanofibrous tube and nanofiber membrane

4.1. Introduction

The high mechanical property is always considered of one of the main purposes to develop nanocomposite materials. Nanofibers from electrospinning process have attracted great attention owing to their unique features such as high specific surface areas, high porosity, and interconnected pore structure. Nanofibrous tubes produced via electrospinning represent a new class of promising scaffolds to instead artificial blood vessel because the electrospinning represents an attractive approach to fabricate nanofibers continuously for artificial blood vessel application [1]. One challenge of the nanofibrous tube is mechanical property. Traditional methods of preparing nanofibrous tudes are abundantly reported by using a rotated stainless steel to collect. Electrospun nanofibers were deposited continuously over stainless steel mandrel for several hours. The mandrel was rotated and reciprocated for uniform deposition. However, this method need long time and the nanofibrous tubes are easily broken when they are removed from the mandrel.

Clendon et al. [2] synthesizedd a nanofiber-tube scaffold which nanofiber distribution in the circumferential direction through polylactic acid hydrogel. Hydrogel materials

contain more than 99% moisture which offer adequate growing space for cells. The oriented nanofiber structures made coated smooth muscle cells can grow along nanofibers direction. This method can easy to get artificial blood vessels with a similar structure to the natural ones without other irritants. Herein, I report a much more efficiency way to prepare nanofibrous tube, and compare mechanical property of nanofiber mat and nanofiber tudes. PCL is used in this application as its low melting point and good spinnability.

Polymer nanofibers attract much attention because of their fundamental importance in a broad range of applications [3], such as filters [4], wipes [5], drug delivery systems [6,7], battery and capacitor electrodes[8,9], regenerative scaffolds [10,11], biosensors [12] and catalysts[13]. Meanwhile, nanofibrous tube can be designed to numerous applications. Reduction of nanofibrous diameter into the <6mm range gives rise to a set of favorable properties including an increase in surface-to-volume ratio, supportive ability and the special shape, variations in artificial blood vessel [14], nerve-regenerative guide [15]. Mechanical property of nanofiber mat and nanofibrous tube is still a challenge to studied.

4.2. Materials and methods

4.2.1. Preparation of PCL nanofiber tubes

A smooth stainless-steel mandrel with a diameter of 4 mm was used to roll up the prepared nanofiber membranes to produce tubes with diameters of 2.5 cm (two layers).

The length of all tubes was 2.5 cm. The diameter and scaffold wall were controllable during this procedure. The prepared nanofiber tubes were then thermally treated in hot water at 50°C for 5 min.

4.2.2. Tensile experiments

For the tensile testing of nanofiber mat, a dumbbell specimens made according to the standard of JIS K-6251-7 (Figure 4-1) were stretched at the speed of 10 mm/min at the room temperature by a tensile testing machine (RTC1250A, A&D Co., Ltd, Japan). Cardboard were used to cover the tested dumbbell specimen for protection. The blue part of Figure 4-1 is cardboard. The PCL nanofiber mat was warmed 5 min under 50°C for uniform condition.

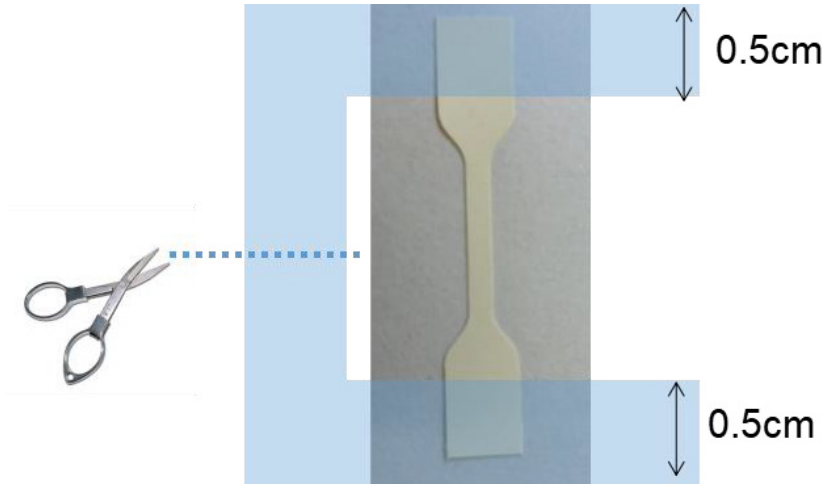

Figure 4-1. A dumbbell specimen for tensile testing (JIS K-6251-7)

The tensile testing of tubes was conducted using the custom specimen configuration shown in Figure 4-2. Plastic junctions were used to connect each PCL nanofiber tube to screws to form each specimen. Photosensitive resin (Bondic, Japan)

was used to fix the connections. Figure 4-2 shows that the radian of the plastic junctions can resist unnatural fracture. Consequently, the tubes could be stretched smoothly and their tensile strength was accurately measured.

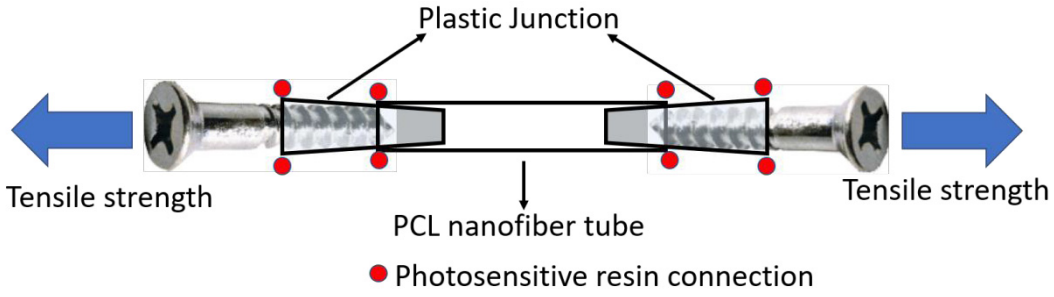

Figure 4-2. Schematic of a nanofiber tube specimen used for tensile testing

4.3. Optimization of drug release performance

This PCL multi-layer nanofiber tubes can be analyzed as dual drug-release systems. The interlayer of each tube was loaded with 1 mg of drug by dissolved in ethanol and then coating the solution evenly on the nanofiber membrane. The PCL-based nanofibers were loaded with 1% drug with respect to the weight of PCL. The drug-loaded nanofiber membrane was then rolled into a nanofiber tube following the steps described in Section 6.1. The tubes were covered with aluminum foil during the heat-treatment process to protect them from water. In addition, electrospun membranes containing 1wt% drug were prepared. The PCL drug loaded solution was stirred for 12 h to obtain a homogeneous solution before electrospinning. Then dual drug release profiles can be get. The rapid release profile is from inter-layer, and the slow one should from inside of nanofibers.

4.4. Advance of mechanical property

Figure 4-3 shows typical stress – strain curves of the prepared PCL multi-layer nanofiber tubes and nanofiber mat. The tensile strengths, Young’ s moduli calculated at 1% strain. The Young’s moduli and the elongations were obviously affected of the tube. However, the curve of nanofibrous tube is not as smooth as the nanofiber mat’s one.

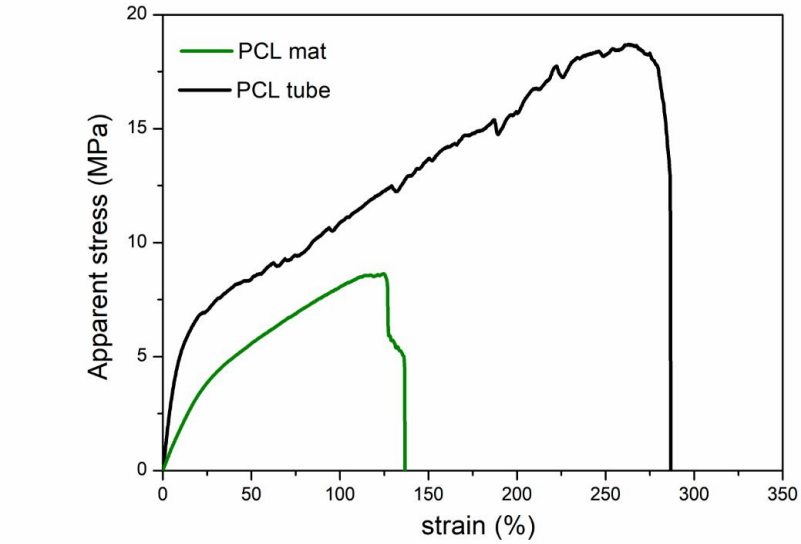

Figure 4-3. Stress–strain curves of polycaprolactone nanofiber tube with two layers and polycaprolactone nanofiber mat by thermal treatment.

4.5. Conclusions

Compare the tensile strength cure of nanofibers and nanofirous tube. The nanofiber tube show higher Young’s moduli and the elongations. It prove that this smart method prepare a solid nanofibrous tube. The inter-layer connection may make the tube have

higher Young's moduli and the elongations. However, the curve of nanofibrous tube are not smooth. This proved that the wall of the tube sustained uneven force, because the tubes were damaged uneven.

Reference

1. Hasan A, Memic A, Annabi N, et al, Electrospun scaffolds for tissue engineering of vascular grafts, *Acta biomaterialia*, 2014, 10(1): 11-25.

2. Mc Clendon M. T., Stupp S. I, Tubular hydrogels of circumferentially aligned nanofibers to encapsulate and orient vascular cells, *Biomaterials*, 2012, 23(32): 5713-5722.

3. Arinstein A, Zussman E, Electrospun polymer nanofibers: mechanical and thermodynamic perspectives, *Journal of Polymer Science Part B: Polymer Physics*, 2011, 49(10): 691-707.

4. Qin X H, Wang S Y, Filtration properties of electrospinning nanofibers, *Journal of applied polymer science*, 2006, 102(2): 1285-1290.

5. Sudo T, Yamabe T, Kim I S, et al, Frictional properties of electrospun polyurethane nanofiber web, *Tribology Online*, 2010, 5(6): 262-265.

6. Yoo H S, Kim T G, Park T G, Surface-functionalized electrospun nanofibers for tissue engineering and drug delivery, *Advanced drug delivery reviews*, 2009, 61(12): 1033-1042.

7. Kenawy E R, Abdel-Hay F I, El-NeIhy M H, et al, Processing of polymer nanofibers

through electrospinning as drug delivery systems[M]//Nanomaterials: Risks and Benefits, *Springer, Dordrecht,* 2009: 247-263.

8. Kim B H, Yang K S, Woo H G, Thin, bendable electrodes consisting of porous carbon nanofibers via the electrospinning of polyacrylonitrile containing tetraethoxy orthosilicate for supercapacitor, *Electrochemistry Communications*, 2011, 13(10): 1042-1046.

9. Kim C, Yang K S, Kojima M, et al, Fabrication of electrospinning-derived carbon nanofiber webs for the anode material of lithium-ion secondary batteries, *Advanced functional materials*, 2006, 16(18): 2393-2397.

10. Yoshimoto H, Shin Y M, Terai H, et al, A biodegradable nanofiber scaffold by electrospinning and its potential for bone tissue engineering, *Biomaterials*, 2003, 24(12): 2077-2082.

11. Kim G H, Kim W D, Highly porous 3D nanofiber scaffold using an electrospinning technique, *Journal of Biomedical Materials Research Part B: Applied Biomaterials: An Official Journal of The Society for Biomaterials, The Japanese Society for Biomaterials, and The Australian Society for Biomaterials and the Korean Society for Biomaterials,* 2007, 81(1): 104-110.

12. Baker S E, Tse K Y, Lee C S, et al, Fabrication and characterization of vertically aligned carbon nanofiber electrodes for biosensing applications, *Diamond and related materials*, 2006, 15(2-3): 433-439.

13. Zhao T J, Sun W Z, Gu X Y, et al, Rational design of the carbon nanofiber catalysts

for oxidative dehydrogenation of ethylbenzene, *Applied Catalysis A: General,* 2007, 323: 135-146.

14. Ma Z, Kotaki M, Yong T, et al, Surface engineering of electrospun polyethylene terephthalate (PET) nanofibers towards development of a new material for blood vessel engineering, *Biomaterials*, 2005, 26(15): 2527-2536.

15. Panseri S, Cunha C, Lowery J, et al, Electrospun micro-and nanofiber tubes for functional nervous regeneration in sciatic nerve transections, *BMC biotechnology*, 2008, 8(1): 39.

Chapter 5

Preparation of SF/PU three-layer nanofibrous tube

Chapter 5: Preparation of SF/PU three-layer nanofibrous tube

5.1. Introduction

In this chapter a kind of three layer nnaofiber tube is prepared through traditional method. The study of small-diameter artificial blood vessels (Inner diameter⩽6mm) is difficult as low blood flow in artificial endovascular, and low pressure may cause thrombus [1-3]. The synthetic materials have poor histocompatibility and tend to cause thrombus and rejection reaction [4-5]. Silk fibroin (SF) is a natural polymer material which has good biocompatibility, biosafety, and biocompatibility [6, 7]. The polyurethane (PU) materials can probably release carcinogenic degradation, regretful these influence the large-scale application of PU artificial blood vessels [8-9]. Oligomeric Proanthocyanidins (OPC) are a class of polyphenols found in a variety of plants. Chemically, they are oligomeric flavonoids which abundantly exist in grape seeds and have been suggested to inhibit the pathogenesis of several systemic diseases as the antioxidant and anti-inflammatory properties [10-12]. SF is selected to carry OPC in inter-layer to resist thrombosis in this study.

In this study, a bionic three-layer structure is designed to offer biocompatibility, antithrombotic property and mechanical properties to simulate the natural blood vessels (Figure 5-1a). In inter-layer SF carrying OPC improve blood clotting properties for antithrombotic and an inert structure by linking with fibrous tissue [13-17].

Polyurethane (PU) for mid-layer which has good mechanical property remain a certain strength after a long-time transplant but has a carcinogenic degradation. SF nanofiber was also used as outer-layer to avoid PU immediate contact to human tissue.

5.2. Materials and methods

Sodium carbonate (Na_2CO_3), ethanol (CH_3CH_2OH), calcium chloride ($CaCl_2$), dimethylformamide (DMF), Methyl Ethyl Ketone (MEK), formic acid (HCOOH, 98 %), Trypsin/EDTA, Trypan bule, Eagle MEM with 10% Fetal Bovine Serum and PBS (phosphate buffered salime) were purchased from Wako Pure Chemicals or Sigma-Aldrich (Japan). Cellulose dialysis membranes (molecular weight cutoff, MWCO: 12000-14000) were purchased from Viskase, USA. Polyurethane (Nippon Miractran, Japan), Oligomeric Proanthocyanidins (Kangmei, China). All chemicals were used without further purification. The cocoons were collected from Aichi Prefecture of Japan and processed before use.

5.2.1. Bionics mechanism of three-layer artificial tube

All arteries and veins contain three layers. The innermost layer is called the tunica intima, the muscular middle layer is called the tunica media, and the outermost layer is called the tunica adventitia. Because capillaries are only one cell layer thick, they only have a tunica intima. Our design reports a bionic three-layer microtube which successful

synthesis of drug carried SF & Oligomeric Proanthocyanidins (OPC) nanofiber for inner-layer, PU nanofiber for mid-layer and SF nanofiber again for outer-layer. The results suggest that the three-layer tubes are attractive biomaterials for vascular grafts. Synthetic materials have poor histocompatibility and tend to cause thrombi and rejection reactions. However, the bionic three-layer structure offers favorable biocompatibility, antithrombotic, and mechanical properties and is designed to simulate natural blood vessels.

5.2.2. Preparation of SF/PU three-layer nanofiber tube

100g cocoons were cut into 1cm^2 pieces and treated with 1000mL 0.5 wt.% sodium carbonate solution for 30 min at 100°C followed by washing with distilled water and then drying at 60°C for 24 h in oven. A mixture of three solvents was prepared from $CaCl_2$: CH_3CH_2O : H_2O (1:2:8 molar ratio) and was stirred at 70°C for 7h. Then, the suspension was dialyzed with distilled water for 72 h at 25°C. The SF was dried in oven at 60°C for 24 h. SF film was finally gained.

Three kinds of solution were prepared for the three-layer nanofiber tube. For inter-layer, 15wt% SF and 1wt% OPC by dissolving in formic acid was used. For mid-layer, MEK, DMF and PU at molar ratio 5 : 2.5 : 1 was used. PU was put into solution slowly to prevent condensation. For outer-layer, 15wt% SF by dissolving in formic acid was used.

An electrospinning apparatus was used. A 10-mL syringe with a stainless-steel needle were connected to a high-voltage power supply. The voltage was fixed at 9 kV

for all electrospinning solutions. The distance between the capillary tip and the collector was fixed at 12 cm for SF solution and 22 cm for PU solution, the flow rate was 0.3 mm/min and the plastic syringe was placed at an angle of 30° from the horizontal plane. Electrospun nanofibers were deposited continuously over stainless steel mandrel (diameter of 0.8 mm) for 45-30-45 min (inter-mid-outer). The mandrel was rotated at 200 rpm and reciprocated for uniform deposition.

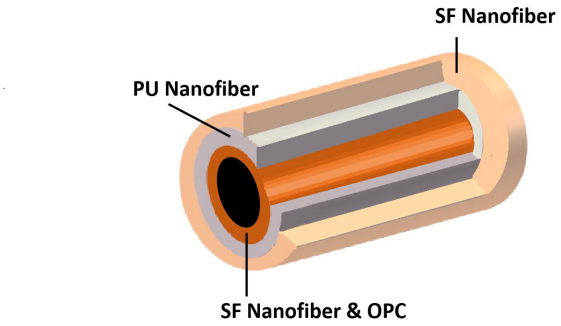

Figure 5-1. Schematic illustration of a three-layer nanofibrous tube

5.2.3. Microscopic morphology

Figure 5-2 shows that the prepared nanofiber tube had an inner diameter of 800 μm. The SF/PU/SF nanofibers had relatively good cohesiveness in nanofibers that led the scaffold compact with cross section close to a circular shape (i), while the SF nanofiber had a smaller diameter (iii) than PU nanofiber (ii). The nanofibers demonstrated smooth, regular morphologies with no beads that were produced via continuous electrospinning.

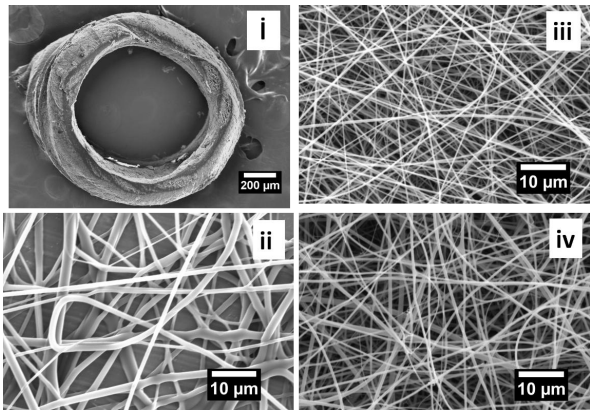

Figure 5-2. SEM images of (i) nanofiber tube (ii) PU nanofibr (iii) SF nanofibers (iv) SF & OPC nanofibers.

5.2.4. Tensile test

Figure 5-3 shows typical stress-strain curves of the PU and SF nanofibrous membranes. It can be found that PU exhibits much higher strength and better ductility, with a tensile strength of 11.15 MPa and an elongation ratio of 420%. In contrast, SF is much more brittle, which breaks at only 2.3 MPa at elongation ratio only 3.5%.

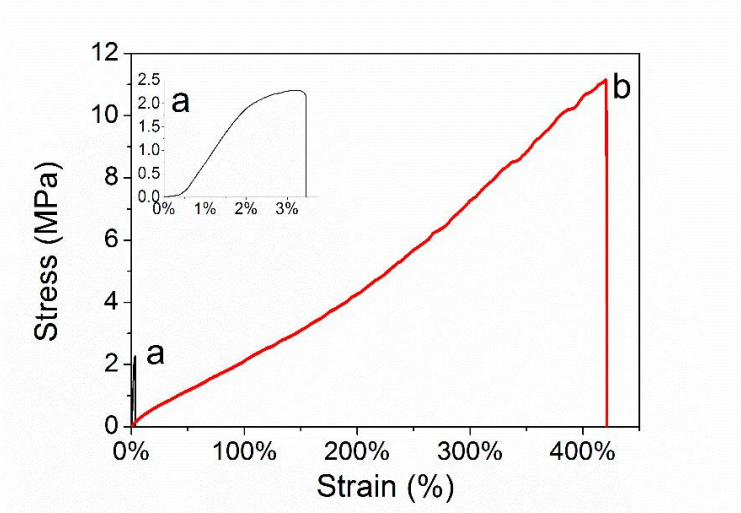

Figure 5-3. Stress–strain curves of the prepared (a) SF nanofiber, (b) PU nanofiber.

5.2.5. Characteristics of the preparation three-layer nanofibtors tube

The morphologies of prepared nanofibers after mineralization were examined by scanning electron microscopy (SEM, JSM-6010LA, JEOL, Japan). The molecular structure was examined by Fourier transform infrared spectroscopy (FT-IR, IR Prestige-21, Shimadzu Co., Japan). X-ray diffraction (XRD) was performed on a D/Max-BR diffractometer (RigaKu, Tokyo, Japan) over the 2θ range of 5°−80° using CuKα radiation at 40 mV and 30 mA. Mechanical properties of the prepared nanofiber membranes were determined by a universal testing machine (Tensilon RTC1250A, A&D Company Ltd., Japan) at a crosshead speed of 10 mm/min.

The FTIR spectra of SF nanofiber, SF & OPC nanofiber, and OPC powder are shown in Figure 5-4. The spectrum of pure OPC shows characteristic bands of carbonyl stretching (C=O) at around 1720 cm^{-1}, C-N at 1170 cm^{-1}, and C-O at 1016 cm^{-1}. The FT-IR spectra of SF show typical amide absorption band of C=O stretching (1651 cm^{-1}, amide I), NH deformation and C-N stretching (1520 cm^{-1}, amide II) and C-N stretching and N-H deformation (1236 cm^{-1}, amide III). The SF nanofiber diffraction spectra have only a wide dispersion peak at 20.5° (Figure 5-5), the lack of distinct peaks in the XRD patterns indicated that it was amorphous. Similarly, there were no distinct peaks in the spectrum of OPC and SF & OPC evidently indicating that the molecular orientation and arrangement of them were disordered, i.e., an amorphous state.

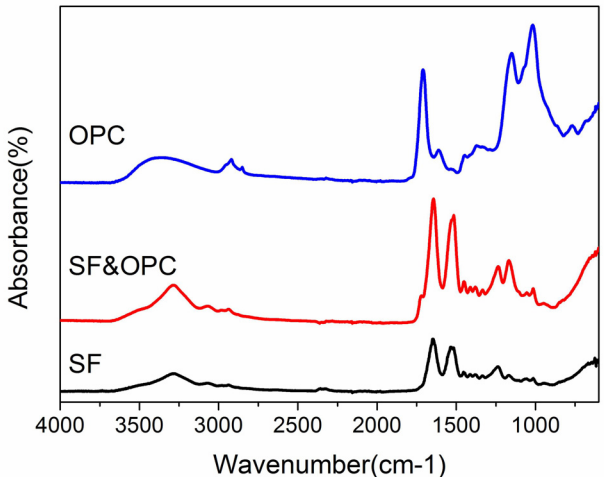

Figure 5-4. FTIR spectra of OPC powder, SF nanofiber and SF &OPC nanofibers.

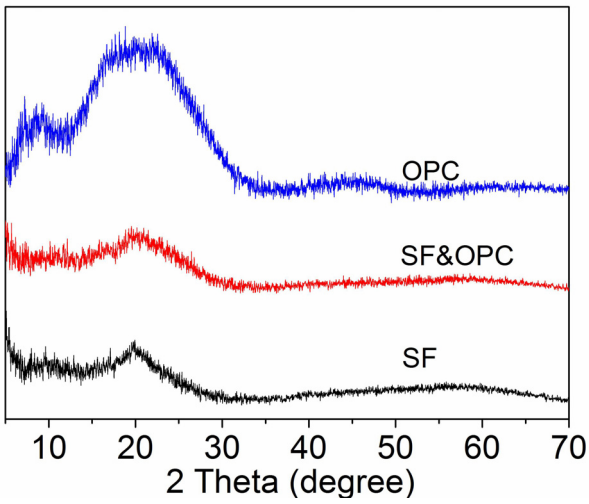

Figure 5-5. XRD spectra of OPC powder, SF nanofiber and SF &OPC nanofibers

5.2.6. Evaluation of biocompatibility in vitro

NIH3T3 cells were cultured in MEM at 37°C in a humidified atmosphere (5%

CO_2). Cells were seeded on the three kinds of nanofibers and cultured for 7 days. At 1, 3, 5, and 7 days of cell-seeding, lactate dehydrogenase release (LDH) assay was conducted for cellular cytotoxicity and cytolysis.

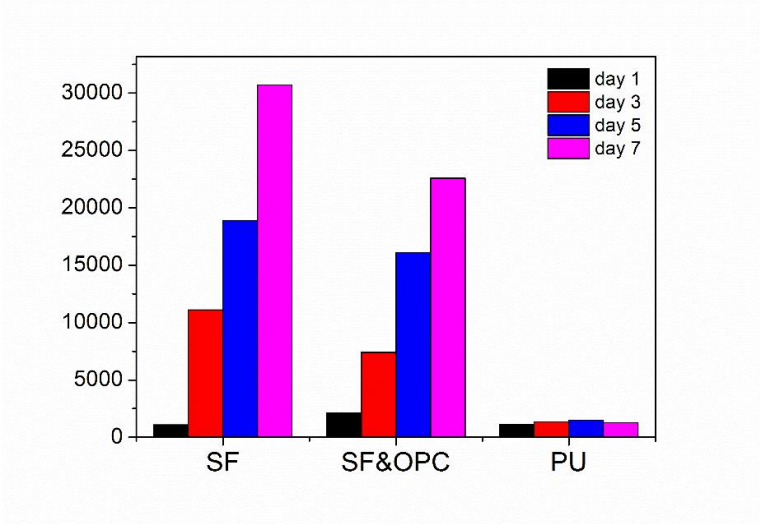

Figure 5-6. LDH assay result of SF nanofiber, SF & OPC nanofiber and PU nanofiber.

5.3. Results and discussion

I succeeded to prepare the three-layer nanofiber tube for artificial vessel by electrospinning method. The PU nanofibers should a higher tensile strength and better elasticity. SF nanofiber should a better biocompatibility. It was confirmed that this three-layer nanofiber tube can promote the development of graft vessel engineer.

5.4. Conclusions

SF/PU/SF composites drug carried three layers nanofiber tube present good shape support performances and the addition of PU nanofiber layer give rise to the significant increase of tensile strength. SF nanofiber shows good biocompetibilty. These results are

actually strong evidences to demonstrate the applicability of SF / PU /SF three layer nanofiber tube. Furthermore, I aim to understand the tensile behaviors of tube deeply. The molecular mechanism of PU is established upon the molecular mechanism. However, it costs about 2 hours at least to prepare each tube and it is easily to broken the tube when the tube be removed from the stick. The low efficiency is a problem to solve. In order to solve this problem, a smart thermal method is studied and discussed in the next chapter.

Reference

1. L'heureux N, McAllister TN, de la Fuente LM, Tissue-engineered blood vessel for adult arterial revascularization, *New England Journal of Medicine*, 2007, 357:1451-3.

2. Losi P, Lombardi S, Briganti E, Soldani G, Luminal surface microgeometry affects platelet adhesion in small-diameter synthetic grafts, *Biomaterials*, 2004, 25:4447-55.

3. Frost-Arner L, Bergqvist D, Effect of isovolemic hemodilution with dextran and albumin on thrombus formation in artificial vessel grafts inserted into the abdominal aorta of the rabbit, *Microsurgery*, 1995, 16:357-61.

4. Frohlich M, Grayson WL, Wan LQ, Marolt D, Drobnic M, Vunjak-Novakovic G , Tissue engineered bone grafts: biological requirements, tissue culture and clinical relevance, *Current stem cell research & therapy,* 2008, 3:254-64.

5. Stefanini GG, Byrne RA, Serruys PW, de Waha A, Meier B, Massberg S, Biodegradable polymer drug-eluting stents reduce the risk of stent thrombosis at 4 years in patients undergoing percutaneous coronary intervention: a pooled analysis of individual patient data from the ISAR-TEST 3, ISAR-TEST 4, and LEADERS randomized trials, *European heart journal,* 2012, 33:1214-22.

6. Miyairi S, Sugiura M, Fukui S, Immobilization of β-glucosidase in fibroin membrane, *Agricultural and Biological Chemistry,* 1978, 42:1661-7.

7. Min BM, Jeong L, Lee KY, Park WH, Regenerated silk fibroin nanofibers: Water vapor-induced structural changes and their effects on the behavior of normal human cells, *Macromolecular Bioscience,*2006, 6:285-92.

8. Yao J, Bastiaansen CW, Peijs T, High strength and high modulus electrospun nanofibers, *Fibers,*2014, 2:158-86.

9. Ting L, CHEN Z-l, SHEN Y-f, Lu G, Li C, LV Z-z, Monitoring bioaccumulation and toxic effects of hexachlorobenzene using the polyurethane foam unit method in the microbial communities of the Fuhe River, Wuhan, *Journal of Environmental Sciences*, 2007, 19:738-44.

10. Fine AM, Oligomeric proanthocyanidin complexes: history, structure, and phytopharmaceutical applications, *Alternative medicine review: a journal of clinical therapeutic,*2000, 5:144-51.

11. Zhang Y, Shi H, Wang W, Ke Z, Xu P, Zhong Z, et al, Antithrombotic effect of grape seed proanthocyanidins extract in a rat model of deep vein thrombosis, *Journal of vascular surgery,* 2011, 53:743-53.

12. Arslan R, Bor Z, Bektas N, Meriçli AH, Ozturk Y, Antithrombotic effects of ethanol extract of Crataegus orientalis in the carrageenan-induced mice tail thrombosis model, *Thrombosis Research,* 2011, 127:210-3.

13. Zhang Y, Venugopal J, Huang Z-M, Lim C, Ramakrishna S, Characterization of the surface biocompatibility of the electrospun PCL-collagen nanofibers using fibroblasts, *Biomacromolecules,* 2005, 6:2583-9.

14.Venugopal J, Ramakrishna S, Biocompatible nanofiber matrices for the engineering

of a dermal substitute for skin regeneration, *Tissue engineering,* 2005, 11:847-54.

15. Hao C, Ding L, Zhang X, Ju H, Biocompatible conductive architecture of carbon nanofiber-doped chitosan prepared with controllable electrodeposition for cytosensing, *Analytical chemistry*, 2007, 79:4442-7.

16. Mo X, Xu C, Kotaki M, Ramakrishna S, Electrospun P (LLA-CL) nanofiber: a biomimetic extracellular matrix for smooth muscle cell and endothelial cell proliferation, *Biomaterials,* 2004, 25:1883-90.

17. Jo JH, Lee EJ, Shin DS, Kim HE, Kim HW, Koh YH, et al, In vitro/in vivo biocompatibility and mechanical properties of bioactive glass nanofiber and poly (ε-caprolactone) composite materials, *Journal of Biomedical Materials Research Part B: Applied Biomaterials*, 2009, 91:213-20.

Chapter 6

Preparation of PCL/PU nanofiber tube

Chapter 6: Preparation of PCL/PU nanofiber tube

6.1. Introduction

A traditional method to prepare nanofibrous tube is studied and discussed in the last chapter. However, it costs about 2 hours at least to prepare each tube and it is easily to broken the tube when the tube be removed from the stick. The low efficiency is a problem to solve. In this chapter, a smart thermal method is designed to prepare nanofibrous tube to solve the efficiency problem.

The demand for tubular constructs in tissue engineering is high because of the increasing interest in small-diameter vascular grafts (≤6 mm) [1-4]. The small gap can be filled by implanting an extra nerve conduit (blood vessel) [5]. However, the study of small-caliber artificial blood vessels is difficult because of low blood flow in the artificial endovascular thrombus from incompatible blood components and interfacial interactions as well as luminal stenosis caused by intimal hyperplasia on new grafts [6]. Synthetic polymers are potential materials to replace large arteries, and there have been reports of satisfactory outcomes [7]. However, preparing allogeneic blood vessels is challenging because it is difficult to avoid rejection by the immune system, especially in patients with degenerative diseases and aneurysms. To address the above issues, bioengineered grafts have been developed from synthetic polymeric materials with

tailored properties and dimensions [8]. Nanofiber tubes are a new class of promising scaffolds to support tissue regeneration application [9-11].

Polycaprolactone (PCL) has good mechanical stability, high biocompatibility, and slow biodegradation. Polyurethane (PU) has high elasticity. The chemical structure of PCL is shown in Figure 6-1. Because of its mechanical and biological properties, PCL has been previously suggested as a suitable material for small-diameter vascular graft applications [12]. PCL is a semicrystalline aliphatic polyester with a low glass transition temperature (−60 °C) and high biocompatibility [13, 14]. The US Food and Drug Administration has approved PCL for use in grafts and a substantial number of other biomedical applications [15]. PU is a block copolymer that is widely used in biomedical applications such as artificial organs, medical devices, and disposable clinical apparatus because it is highly versatile for use in the fabrication of devices and has excellent mechanical properties and a high blood biocompatibility [16-19]. PU consists of hard and soft segments and its chemical structure is shown in Figure 6 -2[20].

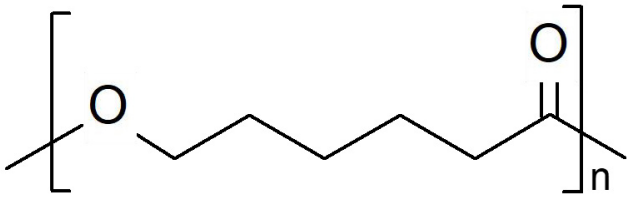

Figure 6-1. Chemical structure of polycaprolactone.

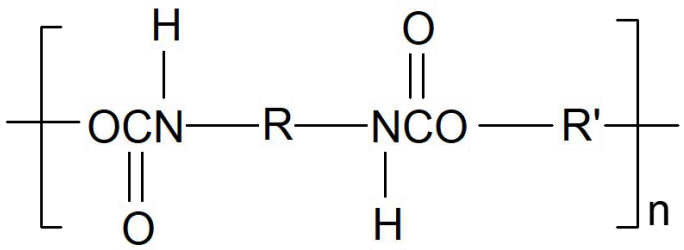

Figure 6-2. Chemical structure of polyurethane.

The advantage of mixing polymers is to create a new composite with complementary properties from each polymer. For example, PCL can provide high biocompatibility, biodegradability, and physical and mechanical stability, and PU can enhance the elasticity. I aim to prepare blends of PCL–PU nanofiber tubes using thermal treatment as a new method to apply electrospun nanofibers as vascular grafts. The porosity can be controlled by the temperature of the thermal treatment. This study presents the preliminary analysis and a future study will evaluate nanofiber tubes for in vivo and in vitro applications. Khatri et al. have reported a method of continuously electrospinning nanofibers over a stainless-steel mandrel to prepare nanofiber tubes [11]. They prepared nanofiber tubes with a uniform structure. However, their process took 120–150 min to fabricate one tube, which was easily broken when the tube was being removed from the steel mandrel.

6.2. Materials and methods

6.2.1. Synthesis of PCL/PU nanofiber tube

Poly-caprolactone (Mw 80000) was purchased from Sigma–Aldrich, Japan. A

solution of 10 % (w/w) PCL was dissolved in 4:3 w/w dichloromethane (DCM) :dimethylformamide (DMF). Thermoplastic PU (TPU E990) was purchased from Miractran. A 23% (w/w) PU solution was prepared by dissolving in 2:1 w/w methyl ethyl ketone (MEK) :dimethylformamide (DMF). Three different blend ratios of PCL and PU were prepared as 3:1, 2:1, and 1:1 (w/w). For comparison, solutions containing only PCL or PU were also prepared. Each blended polymer solution was stirred for 24 h before electrospinning. dichloromethane (DCM), and dimethylformamide (DMF) and methyl ethyl ketone (MEK) were purchased from Wako Pure Chemicals (Japan). All chemicals were used without further purification.

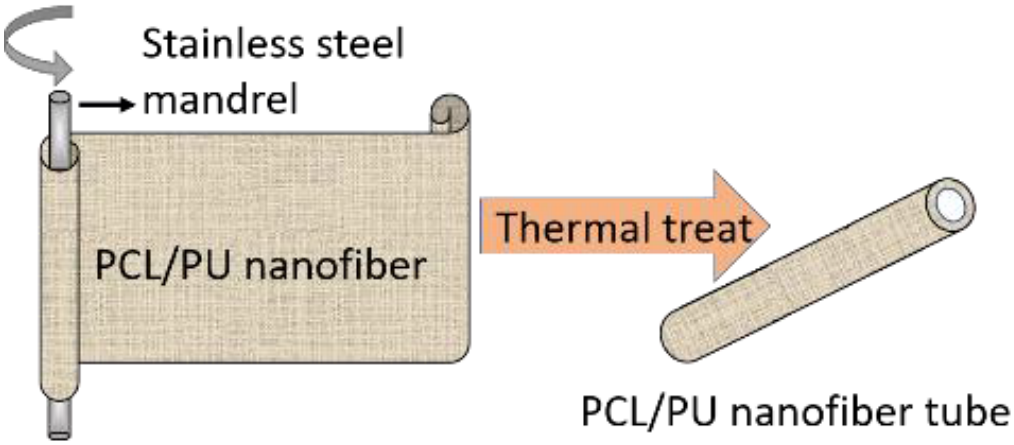

Figure 6-3. Polycaprolactone–polyurethane (PCL–PU) nanofiber tube preparation.

The nanofiber tube preparation is illustrated in Figure 6-3. A smooth stainless steel mandrel (diameter of 0.8 mm) was used to roll up 10 layers of the prepared nanofiber mats with a length of 2.5 cm. The diameter and scaffold wall can be controlled at this

step of the method. The prepared nanofiber tubes were thermally treated at 50 or 60 °C in a hot water bath for 5 min.

6.2.2. Microscopic morphology

In this study, the nanofibers produced from electrospinning were bead-free and uniformly shaped. Figure 6-4 shows the decrease in nanofiber uniformity with increasing PU ratio in the blends, and the PU nanofibers should the largest distribution of fiber diameters. Table 6-1 shows that the average diameter of electrospun nanofibers increases with increasing PU ratio in the blends.

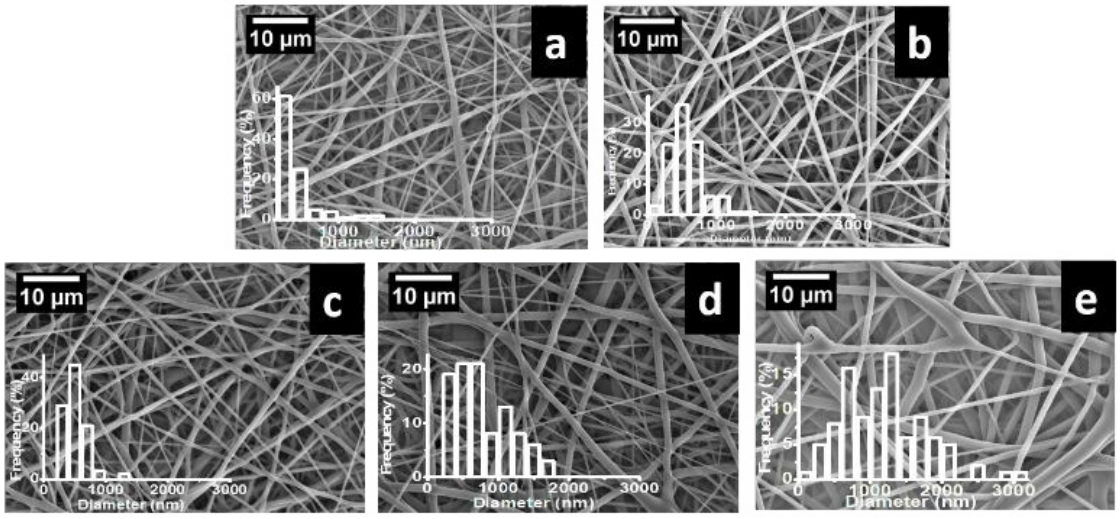

Figure 6-4. Scanning electron microscopy images and diameter measurements of polycaprolactone–polyurethane (PCL–PU) nanofibers. a, PCL, b, PCL–PU 3:1, c, PCL–PU 2:1, d, PCL–PU 1:1, and e, pure PU.

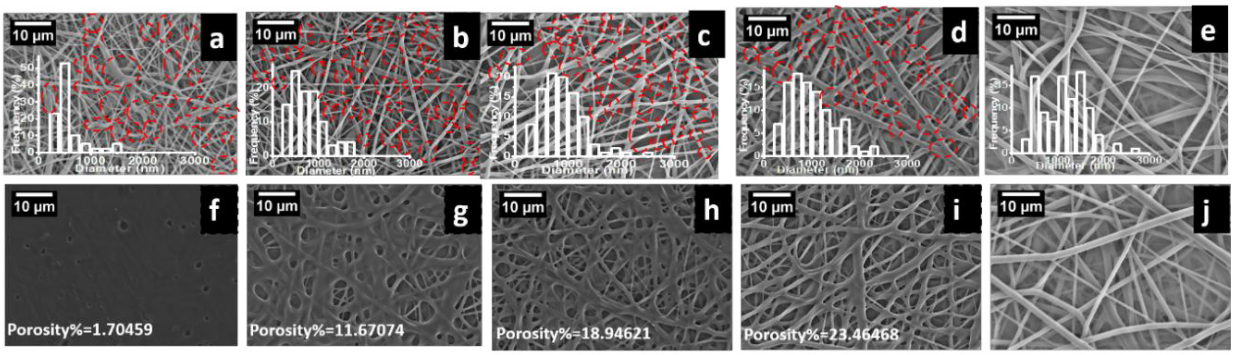

Figure 6-5. Scanning electron microscopy images and diameter measurements of polycaprolactone–polyurethane (PCL–PU) nanofibers after thermal treatment at a–e, 50 °C or f–j, 60 °C. a and f, PCL, b and g PCL–PU 3:1, c and h PCL–PU 2:1, d and i PCL–PU 1:1, and e and j, PU

Table 6- 1. Nanofiber diameter and tube wall thickness

PCL : PU	Average diameter of nanofibers (nm)/ Porosity %			Tube wall thickness (µm)	
(blend ratio)	Unheated	50°C	60°C	50°C	60°C
1:0	461.8	556	Porosity 1.7%	_____	_____
3:1	511.6	772	Porosity 11.7%	46.45909	45.90422
2:1	580.6	894.3	Porosity 18.9%	65.61446	60.64442
1:1	779.7	992.4	Porosity 23.5%	76.24431	73.19172
0:1	1195.7	1146.7	1230.6	_____	_____

The results of the morphological study of PCL–PU nanofibers after rolling into a tube and thermal treatment at 50 or 60 °C are shown in Figure 6-5. Table 6-1 shows that the average diameter of thermally treated electrospun nanofibers increased compared with those before thermal treatment, except for the PU nanofiber. For PCL–PU nanofibers,

the thermal treatment temperature of 50 °C was close to the melting temperature (Tm) of PCL (60 °C) [23], and the morphology shows some fusing and bonding between nanofibers at several places (Figure 6-5 a–d). Figure. 6-5a shows conglutination in the PCL-only nanofiber. Figure 6-5j indicates no change in morphology of the PU nanofibers after thermal treatment compared with PU before thermal treatment, shown in Figure 6-5e. The Vicat Softening Point of PU is 115°C (supplier's information), which is much higher than the treatment temperature. The PU nanofibers displayed no glass transition (Tg), crystallizing (Tc), or melting temperature (Tm) between 30 to 250 °C.

The PCL–PU samples after heating to 60 °C, which is the melting temperature of PCL, should more conglutination than those treated at 50 °C. As shown in Figure 6-5 f–i, the nanofibers containing PCL melted, and fusing and bonding between the nanofibers occurred. The PCL nanofibers were nearly completely melted and should an appearance similar to that of a porous film. Figure 6-5 f–i shows the increase in porosity with increasing PU ratio in the blends. The PU nanofibers treated at 60 °C should no change in morphology compared with the PU samples in Figure 6-4e and 6-5e.

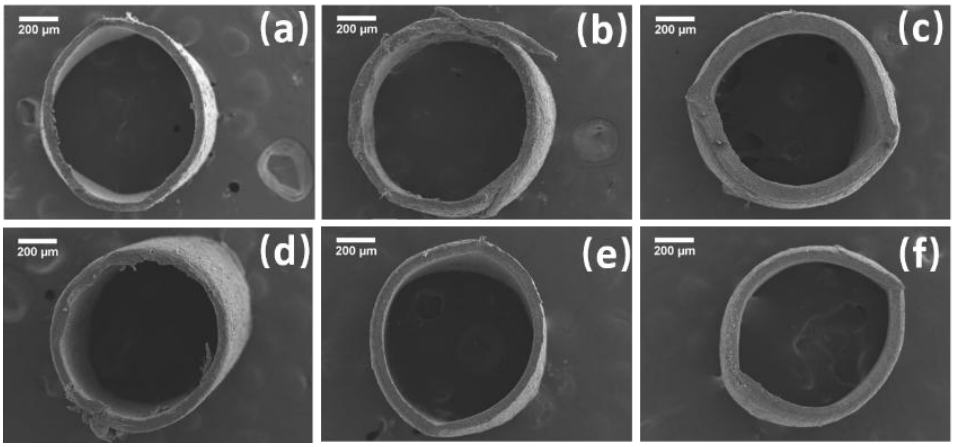

Figure 6-6. Scanning electron microscopy images of polycaprolactone–polyurethane (PCL–PU) nanofiber tubes prepared by thermal treatment at a–c, 50 °C or d–f 60 °C. a and d, PCL–PU 3:1, b and e, PCL–PU 2:1, and c and f, PCL–PU 1:1.

Table 6-1 shows the diameter distribution of electrospun nanofibers and wall thickness of scaffold obtained for all blends. The tube wall thickness increases with increasing PU ratio in the blends. The morphologies of nanofibers before and after thermal treatment are shown in Figure 6-5 a–j. All the nanofibers that were produced via continuous electrospinning demonstrated smooth morphologies with no beads.

Figure 6-6 shows SEM images for the nanofiber tubes, which have an inner diameter of approximately 800 µm because that is the diameter of the steel mandrel used in their preparation. The PCL–PU nanofiber should good cohesiveness, and a compact scaffold with an approximately circular cross section. Figure 6-6 shows that increased PU in the ratio improves the shape of the cross section because of improvements in physical and structural stabilities. The increasing PU ratio in the PCL–PU blends increased the thickness of the tube wall because the solute in the electrospinning solution increases

when the PU ratio increases and the increase in fiber diameter also causing a larger fiber matrix after layering on the mandrel.

6.2.3 Characteristics of the preparation PCL/PU nanofiber tube

DSC was used to investigate the thermodynamic compatibility of PCL–PU nanofiber blends (Figure 6-7). The Tm of PCL nanofibers was 60.3 °C. The PU nanofibers displayed neither glass transition (T_g), crystallizing (T_c), nor melting temperature (T_m) between 30 and 150°C. PCL–PU nanofiber blends exhibited melting temperature peaks at 57.7, 58.8, and 56.2 °C for ratios PCL:PU 1:1, 1:2, and 1:3 respectively. However, these melting temperatures were slightly lower than that of the PCL nanofibers. This result suggests the alignment and orientation of chains in PCL–PU blends.

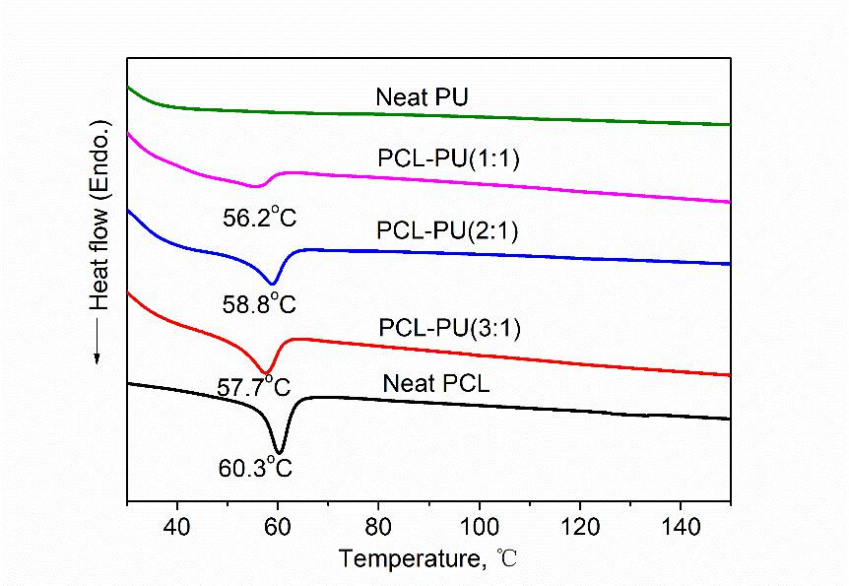

Figure 6-7. Differential scanning calorimetry thermograms of polycaprolactone (PCL), polyurethane (PU) nanofibers, and their blends.

Figure 6-8 presents the XRD peaks of the PCL, PU, and PCL–PU nanofibers. The PCL nanofibers should two main peaks at Bragg angles 2θ = 21.4° and 23.8°. These peaks were observed in the PCL–PU nanofibers blends, because they correspond to the diffraction of PCL crystals [11]. The peaks of PCL–PU nanofibers were slightly lower than that of the PCL nanofibers, and decreased in relative height with decreasing PCL ratio. No peaks were present in the XRD pattern of PU, indicating that PU is amorphous.

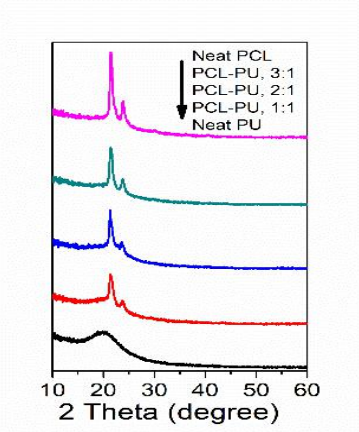

Figure 6-8. X-ray diffraction patterns of nanofiber mats fabricated from polycaprolactone (PCL), polyurethane (PU), and their blends (PCL–PU)

FTIR spectroscopy was conducted to analyze the chemical composition of the PCL–PU nanofibers (Figure 6-9). Comparing the spectra, there were almost no changes among samples. The characteristic peak from the carbonyl groups (C=O stretching vibration) at 1725 cm^{-1} in spectrum of the PU nanofibers shifted to 1520 and 1590 cm^{-1} in the PCL-PU blends [24]. The characteristic peaks from PCL [25] were observed at

850–1480 and 1725 cm^{-1}. The spectra of the PCL–PU nanofiber blends show characteristic peaks from PCL and PU with varying degrees of intensities corresponding to the ratio of PCL and PU. This result indicates that the polymer blending was homogeneous. There was no new peak observed other than the characteristic peaks of PCL and PU nanofibers, which confirms that the PCL–PU nanofibers retained their corresponding chemical structures.

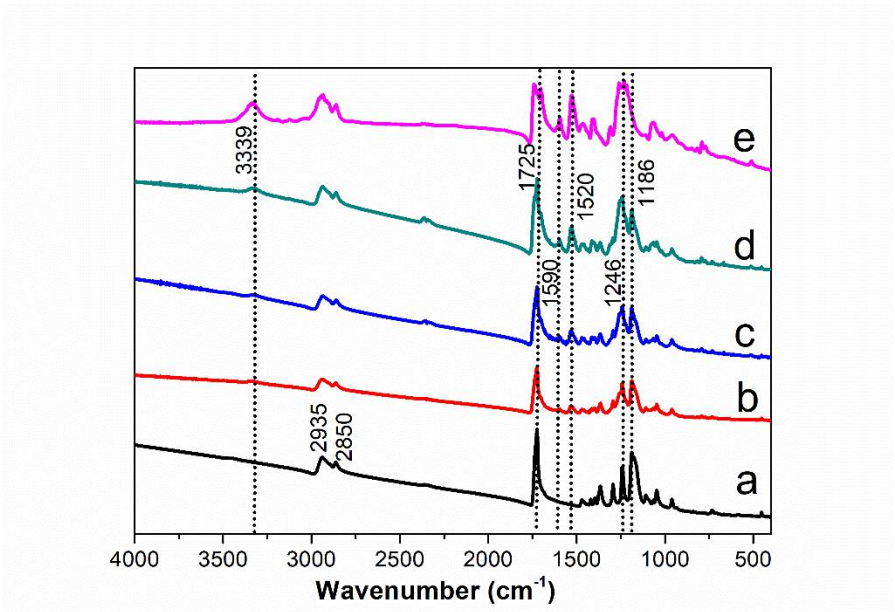

Figure 6-9. Fourier-transform infrared spectra of nanofiber mats fabricated from polycaprolactone (PCL), polyurethane (PU), and their blends (PCL–PU). a, PCL, b, PCL–PU 3:1, c, PCL–PU 2:1, d, PCL–PU 1:1, and e, PU

6.2.4. Mechanical test

Figure 6-10 and 6-11 show representative stress–strain curves of the PCL–PU nanofiber tubes. The elongations of the 60°C treated samples were markedly improved compared with those of the 50°C treated samples. However, the tensile strength and

Young's moduli of the 60°C treated samples did not show obvious improvements compared with those of the 50°C treated samples(Table 6-2). The increase of elongation was attributed to PCL melting and adhering to the PU nanofibers, increasing the fiber interactions and forming a porous film. The mechanical properties (tensile strength and Young's modulus) of PCL–PU nanofibers decreased with decreasing ratio of PU, and the elongation of PCL–PU nanofibers were increased with increasing ratios of PU.

Table 6-2. Mechanical properties of polycaprolactone–polyurethane (PCL–PU) nanofiber tubes

Temp (°C) / PCL : PU	Young's modulus(MPa)		tensile strength (MPa)		elongation (%)	
	50°C	60°C	50°C	60°C	50°C	60°C
① 3:1	61.32	63.19	18.66	17.91	286	313.81
② 2:1	43.15	45.84	11.98	13.37	230.8	341.22
③ 1:1	16.01	10.93	9.22	9.62	289.1	323.81

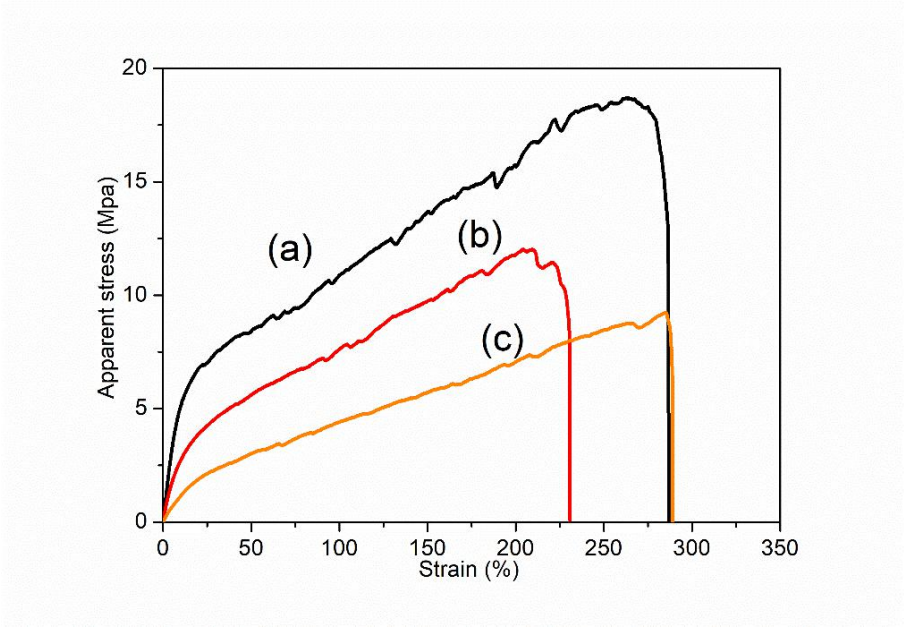

Figure 6-10. Stress–strain curves of polycaprolactone–polyurethane (PCL–PU) nanofiber tubes thermally treated at 50 °C. a, PCL–PU 3:1, b, PCL–PU 2:1, and c, PCL–PU 1:1

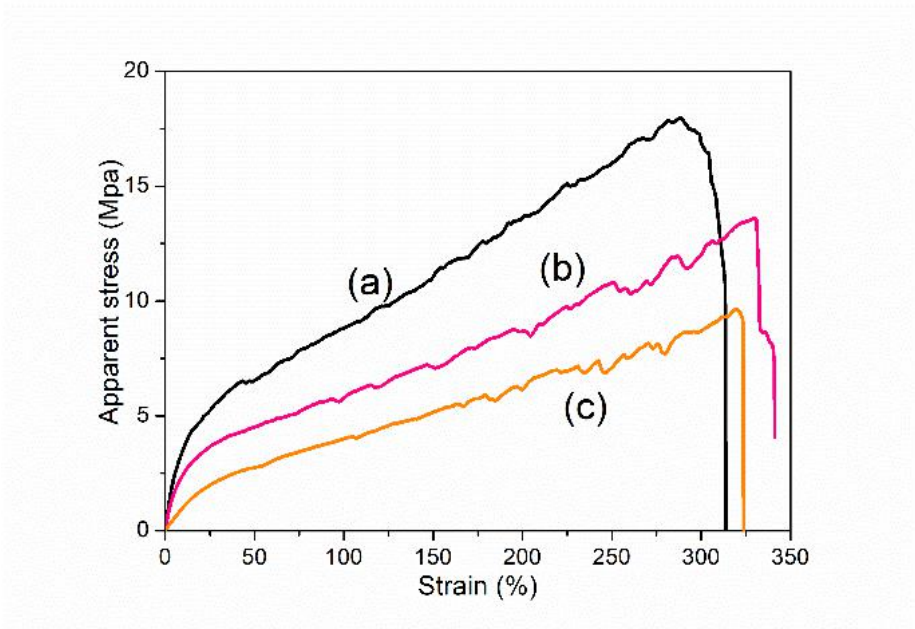

Figure 6-11. Stress–strain curves of polycaprolactone–polyurethane (PCL–PU) nanofiber tubes thermally treated at 60 °C. a, PCL–PU 3:1, b, PCL–PU 2:1, and c, PCL–PU 1:1

6.3. Results and discussion

6.3.1. Discussion on PCL /PU composites nanofiber tube with different content.

In this study, the PCL/PU composite nanofiber tubes were mainly discussed form microscopic morphology, chemical composition and mechanical properties. The chemical composition analysis was proved the ratio of PCL /PU content. The microscopic morphology reflected the mechanical properties to a certain extent. High porous membranes show a lower mechanical strength. It is the reason that 60 °C membranes have stronger tensile strength than 50 °C ones.

6.4. Conclusions

PCL–PU nanofiber tubes with various blending ratios and thermal treatment temperatures were successfully fabricated via electrospinning. The nanofiber tubes prepared by both treatment show a uniform morphology and good structural stability. The fiber diameter and properties such as tensile strength, porosity, and tube wall thickness can be designed to meet the requirements of the application. FTIR shows that the PCL–PU nanofibers exhibit characteristic peaks of PCL and PU, indicating homogeneity in the preparation process. XRD studies demonstrate that the crystallinity of the PCL–PU blends can be improved by increasing the PCL ratio. The PCL–PU nanofiber tubes have a melting temperature (T_m) of about 60 °C as revealed by DSC.

The tensile test shows that the prepared tubes have good mechanical strength and a high elasticity. While not presented here, the mechanical properties and biocompatibility of the prepared tubes still need to be further studied in clinical experiments. It can be expected that the nanofibrous tube is able to apply in artifial graft engineering. This chapter show the thermal method to prepare nanofibrous tube. No drug release property is studied in this chapter. In the next chapter, I report a dual drug release nanofibrous tube through thermal method to solve certain problem such as thrombus.

Reference

1. Lovett M, Cannizzaro C, Daheron L, Messmer B, Vunjak-Novakovic G, Kaplan DL, Silk fibroin microtubes for blood vessel engineering, *Biomaterials,* 2007, 28(35):5271-9

2. Barten, Peter GJ, Contrast sensitivity of the human eye and its effects on image quality, Bellingham, WA: Spie optical engineering press, 1999, Vol. 19.

3. Trovati G, Sanches EA, Neto SC, Mascarenhas YP, Chierice GO, Characterization of polyurethane resins by FTIR, TGA, and XRD, *Journal of Applied Polymer Science,* 2010, 115(1):263-8

4. Ali SA, Editor Mechanical and thermal properties of promising polymer composites for food packaging applications, *IOP Conference Series: Materials Science and Engineering,* 2016, IOP Publishing

5. Ge JC, Choi NJ, Fabrication of Functional Polyurethane/Rare Earth Nanocomposite Membranes by Electrospinning and Its VOCs Absorption Capacity from Air.

Nanomaterials, 2017, 7(3):60

6. Frohlich M, Grayson WL, Wan LQ, Marolt D, Drobnic M, Vunjak-Novakovic G, Tissue engineered bone grafts: biological requirements, tissue culture and clinical relevance, *Current stem cell research & therapy*, 2008, 3(4):254-64

7. Kucinska-Lipka J, Gubanska I, Janik H, Sienkiewicz M (2015) Fabrication of polyurethane and polyurethane based composite fibres by the electrospinning technique for soft tissue engineering of cardiovascular system. Materials Science and Engineering: C. 46:166-76

8. Chiono V, Sartori S, Rechichi A, Tonda-Turo C, Vozzi G, Vozzi F, et al, Poly (ester urethane) guides for peripheral nerve regeneration, *Macromolecular bioscience,* 2011, 11(2):245-56

9. Das B, Chattopadhyay P, Mandal M, Voit B, Karak N, Bio-based biodegradable and biocompatible hyperbranched polyurethane: a scaffold for tissue engineering, *Macromolecular bioscience,* 2013, 13(1):126-39

10. Lligadas G, Ronda JC, Galià M, Cádiz V, Monomers and polymers from plant oils via click chemistry reactions, *Journal of Polymer Science Part A: Polymer Chemistry,* 2013, 51(10):2111-24

11. Bastioli C, Handbook of biodegradable polymers: iSmithers Rapra Publishing, 2005.

12. Pitt CG, Chasalow F, Hibionada Y, Klimas D, Schindler A, Aliphatic polyesters. I. The degradation of poly (ϵ-caprolactone) in vivo, *Journal of Applied Polymer Science,*

1981, 26(11):3779-87.

13. Hutmacher DW, Schantz T, Zein I, Ng KW, Teoh SH, Tan KC, Mechanical properties and cell cultural response of polycaprolactone scaffolds designed and fabricated via fused deposition modeling, *Journal of Biomedical Materials Research Part A*, 2001, 55(2):203-16.

14. Ma K, Qiu Y, Fu Y, Ni Q-Q, Electrospun sandwich configuration nanofibers as transparent membranes for skin care drug delivery systems, *Journal of Materials Science*, 2018, 1-10.

15. Khatri Z, Nakashima R, Mayakrishnan G, Lee K-H, Park Y-H, Ii K, et al, Preparation and characterization of electrospun poly (ε-caprolactone)-poly (l-lactic acid) nanofiber tubes, *Journal of Materials Science,* 2013, 48(10):3659-64.

16. Xie J, MacEwan MR, Schwartz AG, Xia Y, Electrospun nanofibers for neural tissue engineering, *Nanoscale*, 2010, 2(1):35-44.

17. Ramakrishna S, Jose R, Archana P, Nair A, Balamurugan R, Venugopal J, et al, Science and engineering of electrospun nanofibers for advances in clean energy, water filtration, and regenerative medicine, *Journal of materials science,* 2010, 45(23):6283-312.

18. Panseri S, Cunha C, LoIry J, Del Carro U, Taraballi F, Amadio S, et al, Electrospun micro-and nanofiber tubes for functional nervous regeneration in sciatic nerve transections, *BMC biotechnology,* 2008, 8(1):39.

19. Losi P, Lombardi S, Briganti E, Soldani G, Luminal surface microgeometry affects

platelet adhesion in small-diameter synthetic grafts, *Biomaterials,* 2004, 25(18):4447-55.

20. Hench LL, Biomaterials: a forecast for the future, *Biomaterials,* 1998, 19(16):1419-23.

21. Ku SH, Ryu J, Hong SK, Lee H, Park CB, General functionalization route for cell adhesion on non-Itting surfaces, *Biomaterials*, 2010, 31(9):2535-41.

22. Lovett ML, Cannizzaro CM, Vunjak-Novakovic G, Kaplan DL, Gel spinning of silk tubes for tissue engineering, *Biomaterials*, 2008, 29(35):4650-7.

23. Kannan RY, Salacinski HJ, Edirisinghe MJ, Hamilton G, Seifalian AM, Polyhedral oligomeric silsequioxane–polyurethane nanocomposite microvessels for an artificial capillary bed, *Biomaterials,* 2006, 27(26):4618-26.

24. Baguneid M, Seifalian A, Salacinski H, Murray D, Hamilton G, Walker M, Tissue engineering of blood vessels, *British Journal of Surgery,* 2006, 93(3):282-90.

25. Barten PG, Contrast sensitivity of the human eye and its effects on image quality, Spie Optical Engineering Press, *Bellingham*, 1999, vol 19.

Chapter 7

Preparation of PCL drug carried multi-layer nanofibrous tube

Chapter 7: Preparation of drug carried PCL multi-layer nanofibrous tube

7.1. Introduction

In the last chapter, a thermal method is reported to obtain nanofibrous tubes in a more efficiency way. Meanwhile, a dual drug release curves loaded nanofiber tubes are studied and discussed in this chapter through similar thermal method. Currently, more than 450,000 coronary artery bypass graft procedures are performed each year [1]. However, the study of small-caliber artificial blood vessels (inner diameter <6 mm) is currently limited by the issue of thrombus formation [2]. A multi-layer nanofibrous tube with dual drug release profiles may be a way to solve this problem. The rapid drug-release process can prevent short-term thrombosis and the sustained drug-release process can protect against long-term thrombosis. Such tubes require controlled functional parameters and processing methods for reproducible manufacture. Electrospun nanofiber tubes have been deposited continuously over stainless-steel mandrels; However, this process takes a long time (120 – 150 min/per tube), which makes it unsuitable for mass production [3].

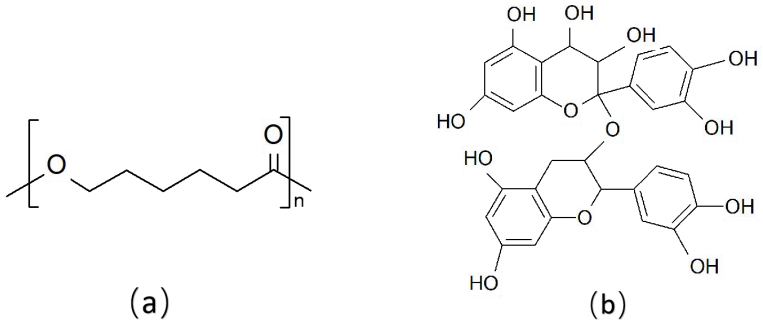

Figure 7-1. Preparation of a polycaprolactone nanofiber tube

Attempts to engineer artificial vessels using natural or synthetic materials have achieved only modest success [4]. For example, tubes carrying an anticoagulant, such as heparin, have been developed [4]. Tissue-engineered vessels seeded with endothelial cells suitable for autologous vein grafts have been subjected to human trials [5,6]. These results, However, were only achieved for artificial grafts with a relatively large inner diameter of 6 to 7 mm [7]. Heparin-carrying tubes with a smaller inner diameter may cause hemolysis [8]. To date, no microvascular grafts (natural, synthetic, or tissue-engineered) have been fully accepted into routine clinical practice, leaving considerable room for improvement in this field [9,10].

Here I propose the use of multi-layer nanofiber tubes composed of polycaprolactone (PCL) and an oligomeric proanthocyanidin (OPC) as small-caliber blood vessel surrogates. PCL is non-toxic [11,12], biocompatible, and degrades slowly in vivo. The chemical structure of PCL is shown in Figure 7-1a [11,13]. These properties, in addition to compliance, variable size, good suture retention, and immunogenicity, represent the qualities of an ideal blood vessel substitute [14].

Meanwhile, OPCs are a class of polyphenols found in a variety of plants; the chemical structure of the OPC used in this work is shown in Figure 7-1b. OPCs are oligomeric flavonoids particularly rich in grape seeds and have been suggested to inhibit the pathogenesis of several systemic diseases because of their antithrombotic, antioxidant, and anti-inflammatory properties [15-17].

In this study, I develop a processing method to manufacture multi-layer PCL tubes with varying inner diameter, mechanical strength, and drug loading. These properties are experimentally verified via scanning electron microscopy (SEM), mechanical testing, and drug-release measurements. The biocompatibility and efficacy of the multi-layer PCL drug-carrying tubes as a vessel surrogate are then evaluated in vitro by monitoring the migration of endothelial cells through a nanofiber mat.

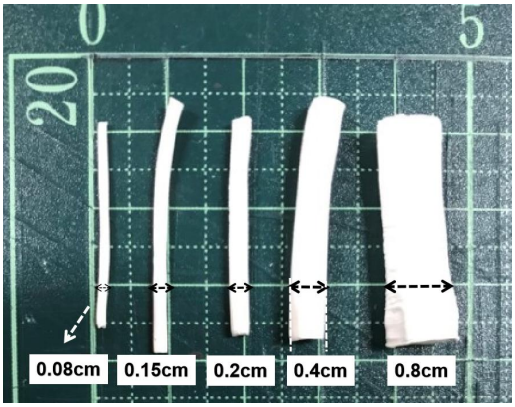

Figure 7-2. Photograph of prepared polycaprolactone nanofiber tubes

Meanwhile, nanofiber tubes with different diameters can be prepared through this thermal method for unequal request. Figure 7-2 shows the prepared PCL nanofiber tubes with unequal standards. It is proved that the thermal method is flexibility and convenient. However, the studied nanofiber tubes in this paper are limited of 4mm diameter.

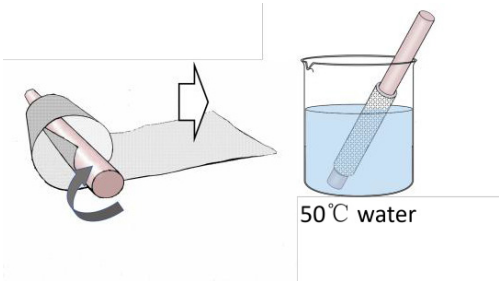

Figure 7-3. Preparation of a polycaprolactone nanofiber tube

7.2. Materials and methods

PCL (Mn: 70 000 – 90 000; melting temperature (Tm): 58 – 60 °C) and wax-free shellac were provided by Kigata, Japan. Phosphate-buffered saline (PBS; 1/15 mol/L, pH 7.4), ethanol, dichloromethane (DCM), dimethylformamide (DMF), and OPC were purchased from Sigma-Aldrich (Japan) or Wako Pure Chemicals (Japan). All chemicals were used without further purification. The cocoons were collected from Aichi, Japan and processed before use. All chemicals were used without further purification. Water was double-distilled just before use. The optimal electrospinning solution contained 10 wt % PCL in DCM/DMF (6:4 w/w), as reported previously [11], which was produced by adding PCL to the stirred solvent mixture to avoid PCL aggregation. An electrospinning apparatus manufactured by Kato Tech Co. Ltd. (Kyoto, Japan) was used. The PCL solution was placed in a 10-mL syringe (Φ 0.8mm, SS-10T; Terumo, Tokyo, Japan) with a stainless-steel needle (NN-2138 N; Terumo) connected to a high-voltage power supply. During electrospinning, the applied voltage was 12 kV and the distance from the needle tip to the substrate was 15 cm. The nanofiber membranes were

produced using 2 mL of PCL solution, a flow rate of 0.3 mm/min, traverse rate of 10 cm/min, and target rate of 2 m/min.

7.2.1. Preparation of PCL drug carried multi-layer nanofiber tube

A smooth stainless-steel mandrel with a diameter of 4 mm was used to roll up the prepared nanofiber membranes to produce tubes with diameters of 2.5 cm (two layers), 3.77 cm (three layers), 6.28 cm (five layers), and 13.5 cm (ten layers). The length of all tubes was 2.5 cm. The diameter and scaffold wall were controllable during this procedure. The prepared nanofiber tubes were then thermally treated in hot water at 50 °C for 5 min. A schematic of PCL nanofiber tube fabrication is illustrated in Figure. 7-3.

7.2.2. Microscopic morphology

All samples were dried at room temperature for 24 h before use. The morphology of the nanofiber tubes was examined by a scanning electron microscope (S-3000 N, Hitachi, Japan). SEM was used to assess the cross section of the prepared tubes as well as to confirm the integration degree between layers achieved by thermal treatment. Macroscopic images of the prepared tubes were acquired using a digital microscope (VHX-2000 N, Keyence, Japan).

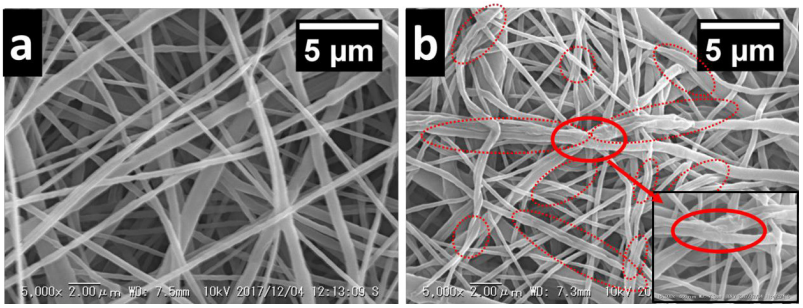

Figure 7-4. Scanning electron microscopy images of polycaprolactone nanofibers (a) before and (b) after thermal treatment at 50 °C.

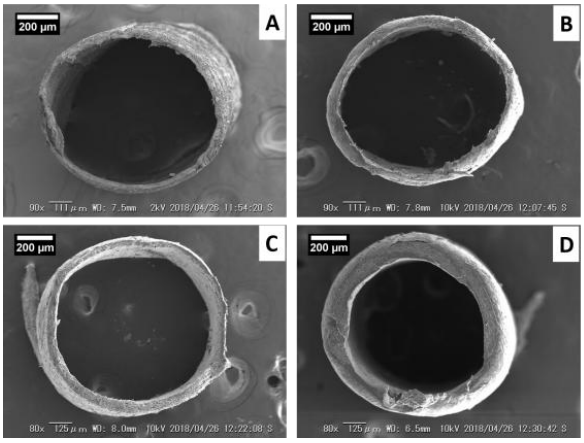

Figure 7-5. Scanning electron microscopy images of polycaprolactone nanofiber tubes with (A) two layers, (B) three layers, (C) five layers, and (D) ten layers prepared by thermal treatment at 50 °C.

The nanofibers produced via continuous electrospinning demonstrated smooth morphologies with no beads (Figure 7-4 A). SEM images of PCL nanofibers that were thermally treated at 50 °C are given in Figure 7-4 B. The thermal treatment temperature of the PCL nanofibers (50 °C) was close to Tm of PCL (60 °C) [19]. Figure 7-4 B reveals bonding between the nanofibers in several places, which are indicated by red circles. This effect was attributed to the PCL nanofibers starting to melt during thermal treatment at 50 °C. Figure 7-5 shows SEM images of the nanofiber tubes with two, three, five, and ten layers and an inner diameter of approximately 800 μm (the tube inner

diameter was controlled at 800 μm for SEM observation). The layers were tightly connected. No interspace was observed in the cross-sectional images of the tubes (Figure 7-6 a-d). In general, the PCL nanofibers had relatively good cohesiveness, which led to the formation of a compact scaffold with a cross section that was close to circular [20]. Table 7-1 lists the diameter distributions of the wall thickness of the PCL multi-layer nanfiber tubes.

Table 7-1. Thickness of the prepared nanofiber tubes

Number of layers	Thickness of diameter(μm)
two	20.11787
three	35.98977
five	56.21288
ten	116.7255

7.2.3. Chemical characters

Fourier transform infrared (FTIR) analysis (IRSpirit, Shimadzu, Japan) was carried out to study the chemical structure of the prepared nanofiber membranes. X-ray diffraction (XRD) was performed on a D/Max-BR diffractometer (Rigaku, Tokyo, Japan) over the 2θ range of 10°~70° using CuKα radiation at 40 mV and 30 mA. Differential scanning calorimetry (DSC) analyses were performed using a Pyris-1 analyzer (Perkin-Elmer). Both the temperature and heat flow were calibrated with an indium standard. All thermal analyses were carried out under air atmosphere.

An FTIR spectrum of the PCL tubes is shown in Figure 7-6 A. FTIR spectroscopy was conducted to analyze the chemical composition of the prepared PCL

nanofibers. Characteristic peaks from PCL were observed at 850–1480 and 1725 cm^{-1}. The PCL nanofibers should bands ascribed to carbonyl stretching ν(C=O) at around 1725 cm^{-1}, asymmetric COC stretching νas(COC) at 1241 cm^{-1}, and O and C–O stretching νs(OC–O) at 1187 cm^{-1} [21]. The two peaks at 2935 and 2850 cm^{-1} corresponded to asymmetric CH_2 stretching νas(CH_2) and symmetric CH_2 stretching νs(CH_2), respectively. The bands at around 1294 and 1187 cm^{-1} were assigned to the backbone C–O and C–C stretching in the crystalline phase (νcr) and amorphous phase (νam), respectively [22].

Figure 7-6 B presents an XRD pattern of the PCL nanofibers. The PCL nanofibers should two main peaks at 2θ = 21.4° and 23.9°, which were attributed to the diffractions of the (110) and (200) lattice planes of semi-crystalline PCL, respectively [23]. DSC thermograms were used to investigate the thermal stability of the prepared PCL nanofibers and are shown in Figure 7-6 C. Tm of the PCL nanofibers was at 60.3 °C, confirming that the PCL nanofibers did indeed start to melt at around 50 °C, as observed in SEM images of the nanofibers.

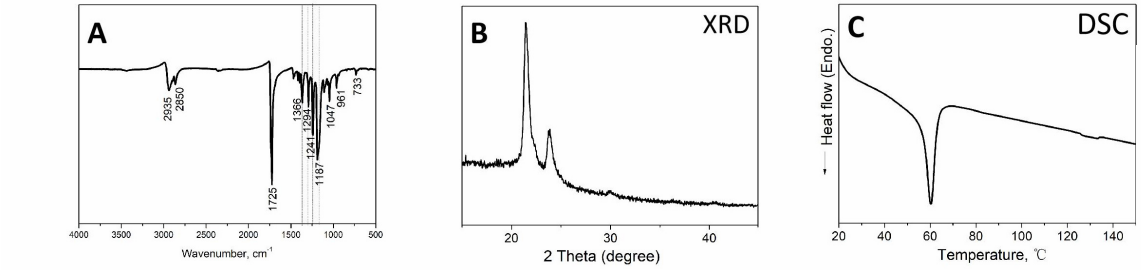

Figure 7-6. (A) Fourier-transform infrared spectrum of a PCL nanofiber mat.(B)X-ray diffraction pattern of a PCL nanofiber mat. (C) Differential scanning calorimetry thermogram of PCL nanofibers.

7.2.4. Tensile test

Tensile tests were performed on the multi-layer PCL nanofiber tubes using a universal testing machine (Tensilon RTC1250A, A&D Company Ltd., Japan) at a crosshead speed of 10 mm/min. The initial length of each tube was obtained using a caliper, and the cross-sectional area was estimated using SEM images of representative tubes and analysis software (ImageJ, National Institutes of Health, USA). The Young's modulus of each tube was determined by offsetting the least-squares line by 1% strain. Ultimate tensile strength was the highest stress value attained during the test and the elongation at break was the last data point before a >10% decrease in the load [7]. The tensile testing of tubes was conducted using the custom specimen configuration shown in Figure 7-7. Plastic junctions were used to connect each PCL nanofiber tube to screws to form each specimen. Photosensitive resin (Bondic, Japan) was used to fix the connections. Figure 7-7 shows that the radian of the plastic junctions can resist unnatural fracture. Consequently, the tubes could be stretched smoothly and their tensile strength was accurately measured.

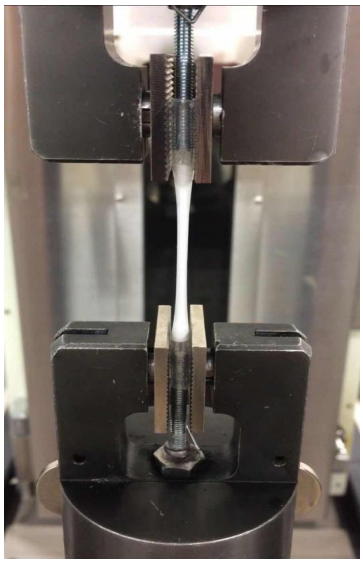

Figure 7-7. Photograph of the template used to prepare tensile specimens of the nanofiber tubes.

Figure 7-8 shows typical stress–strain curves of the prepared PCL multi-layer nanofiber tubes. The tensile strengths, Young's moduli calculated at 1% strain, and elongation percentages of the tubes with two, three, five, and ten layers are listed in Table 7-2. The elongations were not obviously affected by the layer number of the tube. In contrast, the mechanical properties (tensile strength and Young's modulus) of the less-layer nanofiber tubes were a little higher than those of the more-layer tubes. This may because that the connections between layers are weaker than the connections inside nanofiber membranes. However, there isn't a huge difference of each kinds tubes for mechanical properties.

Table 7-2. Mechanical properties of the prepared nanofiber tubes

Number of layers	Young's modulus (MPa)	Tensile strength (MPa)	Elongation (%)
two	16.42±9	5.51±1	105.52±20
three	14.40±4	4.10±0.5	90.73±20
five	13.51±5	4±0.4	90.66±20
ten	10.55±4	3.53±0.2	93.85±10

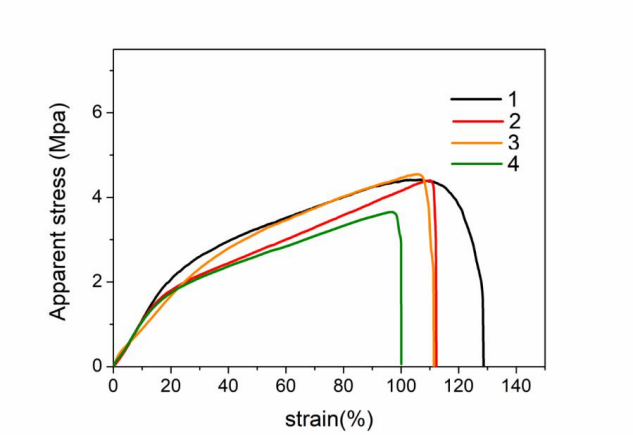

Figure 7-8. Stress–strain curves of polycaprolactone nanofiber tubes with two layers (1), three layers (2), five layers (3), and ten layers (4) prepared by thermal treatment at 50 °C.

7.2.5. The drug release curve form tube and nanofiber membrane

The drug-release characteristics of the prepared samples were investigated by immersing all the nanocomposites in PBS (pH 7.4, 20 mL). To determine the drug concentration of PBS, 4-mL aliquots of the test solution were taken at particular time intervals; 4 mL of fresh PBS solution was then added to maintain the solution volume. An ultraviolet–visible (UV–Vis) spectrophotometer (V530, JASCO, Japan) was used to determine the concentration of OPC present in the collected test solution. To determine

the concentration of OPC, a calibration curve was produced from the UV–Vis absorption spectrum of OPC in advance. The test temperature was maintained at 37 °C and the solution was shaken at 100 rpm using a shaking incubator (PIC-100S, Askul, Japan).

The release of OPC from the interlayers of the prepared tubes is shown in Figure 7-10. The cumulative release reached equilibrium after about 90 min (1.5 h). The cumulative OPC release from the nanofiber membranes reached equilibrium at about 1500 h (more than 60 days) (Figure 7-11). For the PCL nanofibers, obviously slower OPC release was observed over the whole release process compared with that by the interlayer release, during which 80% of the drug was rapidly released within 1.5 h. More drug residues were observed as the layer number of the tube increased. The release of OPC from the PCL nanofibers was very slow. During the electrospinning process, the dissolved OPC concentration of the working solution changed during volatilization and OPC moved to the surface of the nanofibers. Therefore, the rapid release of OPC was observed initially for the PCL nanofibers. The comparatively much higher release rate from the interlayer than from the PCL nanofibers is because OPC only adhered on the surface of the nanofibers during the drug release process in neutral PBS solution. The PCL nanofibers did not appear to be swollen, broken, melted, or unfolded after the drug-release process for 62.5 days, as illustrated in Figure 7-9 Therefore, the PCL nanofibers are biodegraded very slowly, and are considered to be a non-erodible system [24].

Drug release from polymeric systems can be described by the following simple semi-empirical equation:

$$\frac{Mt}{M\infty} = kt^n \quad (1)$$

where Mt and M∞ are the absolute cumulative amount of drug released at time t and infinite time, respectively; k is a constant incorporating structural and geometric characteristic of the device, and n is the release exponent, which is indicative of the mechanism of drug release [25]. When the exponent n is 0.5, the drug delivery process can be considered as a Fickian diffusion release mechanism. When $0.5 < n < 1.0$, the release mechanism is anomalous transport. When n is 1.0, the delivery process be defined as a Case-II transport release mechanism [26]. The calculated n values for the PCL multi-layer nanofiber tubes with two, three, five, and ten layers were 0.1237, 0.1143, 0.1211, and 0.3204, respectively. Therefore, the release mechanism for the PCL multi-layer nanofiber tubes with two to five layers does not fit with any established mechanism of drug release. This means that the mechanism of OPC release is neither a diffusion-controlled drug release ($n = 0.5$) nor a swelling-controlled drug release ($n = 1$). The tubes with two to five layers may swell and deform. Therefore, the reason for the release of OPC must be the large porosity of the multi-layer membrane, which does not restrict the OPC molecules from passing through. The n value for the ten-layer nanofiber tube was closer to 0.5 than that of the other tubes with smaller layer numbers. The reason for this may be that the ten-layer tubes had an inseparable interlayer, which resulted in smaller porosity and thus the release of OPC was restricted to some extent.

The n value for the PCL nanofiber membrane was 0.4133, which is very close to 0.5. This indicates that diffusion is the mechanism controlling the release of OPC from the membrane. Therefore, OPC transport initially occurs through the movement of OPC through the membrane, which is followed by diffusion through the same membrane and desorption to the other side of the membrane. This drug delivery process could be considered as a Fickian diffusion release mechanism [26].

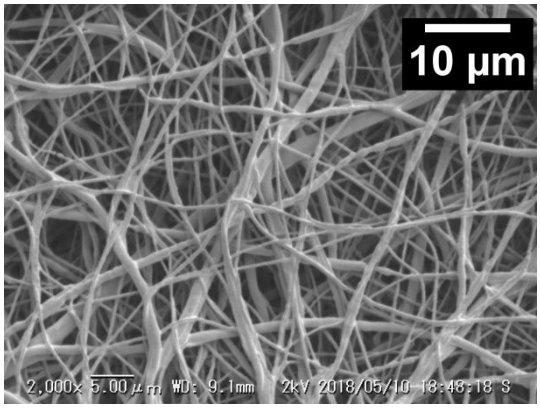

Figure 7-9. SEM image of drug-carrying PCL nanofibers after 62 days drug release process.

An SEM image of the fibers after drug release (Figure 7-9) revealed that they appeared almost unchanged after immersion in the dissolution media. The fiber diameter was also unchanged after drug release.

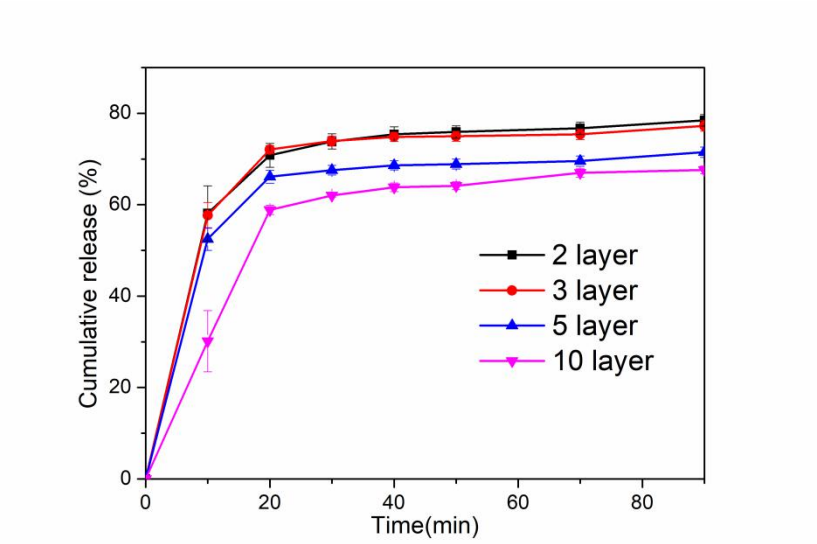

Figure 7-10. In vitro dissolution tests showing oligomeric proanthocyanidin release profiles from interlayers of the prepared tubes with different layer numbers.

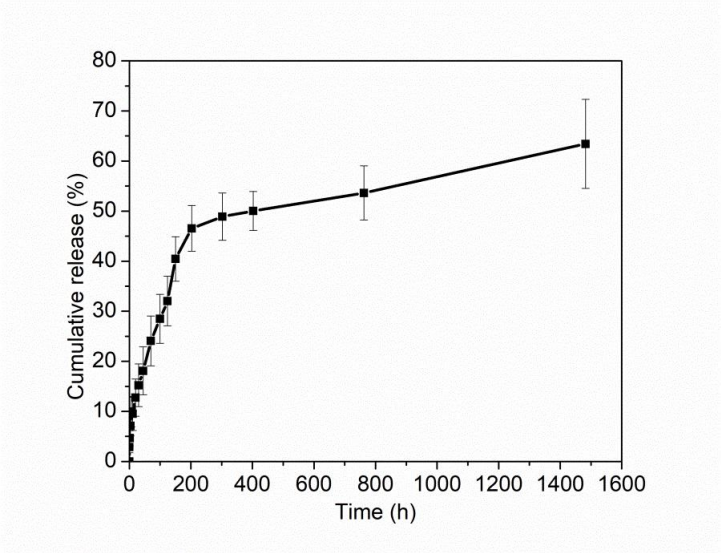

Figure 7-11. In vitro dissolution tests showing the oligomeric proanthocyanidin release profile from polycaprolactone nanofibers.

7.2.6. Biocompatibility test

Human umbilical vein endothelial cells (HUVECs) were cultured according to company protocols [18]. HUVECs (TAKARA, Japan) were grown in M199 liquid

(Sigma-Aldrich) containing bFGF2 (10 μg; 1 vial), 20 v/v% heat-inactivated fetal bovine serum, and 1 v/v% penicillin/streptomycin. Cells were cultured at 37 °C in 5% CO_2/95% air at 95% relative humidity. The cell culture medium was replenished every two days, and cells were passaged at approximately 80% confluence using 0.05% trypsin–EDTA and then centrifuged at 1,500 rpm for 5 min. Tubes with and without OPC were used. Tubes with ten layers were used because they had the best structural stability and formability. The tubes were cut into round sheet shapes with a diameter of 6 mm with three replicates per sample and cultured for 24 h after 5000 cells (1 mL) were poured into the sample wells.

The toxicity of the PCL membranes was verified with the objective of detecting residual DCM from the PCL solution. To detect the residual DCM and DMF in the membranes, the 2-layer PCL nanofibrous tubes and 10-layer PCL nanofibrous tubes were evaluated (No drug loaded). The nanofibrous tubes were cut into round sheet shapes with a diameter of 6 mm with five replicates. The test was conducted by cultivating human umbilical vein endothelial cells (HUVECs) in a 96-well cell culture plate (5,000 cells per well) with 200μl of M199 liquid (contain bFGF2) after 24 h at 37°C under a 5% CO_2 atmosphere. The tests were conducted in quadruplicate with the following samples:

(a) Blank: M199 liquid (contain bFGF2) only;

(b) PCL nanofiber membrane;

(c) PCL-OPC nanofiber membrane;

(d) Control: M199 liquid (contain bFGF2) with cells to represent 100% viability.

After a 24-hour incubation time, 20 μl of WST-1 (Roche No.11644807001) was added to each of the analyzed wells, and a new incubation period was initiated for 3 h at 37°C. After 3 h, 100 μl solution of each well was remove, and the absorbance was measured at 450 nm in the spectrophotometer (Thermo scientificc™ 51119200). The absorbance measured at this wavelength is directly proportional to the number of cells in each well. The cell viability for each treated sample was calculated using the following equation:

$$\frac{Abs_{\text{sample}} - \bar{x}Abs_{blank}}{\bar{x}Abs_{control} - \bar{x}Abs_{blank}} \times 100\%$$

where $\bar{x}Abs_{blank}$ is the average absorbance measured in the wells with no cells but only medium. $\bar{x}Abs_{control}$ is the average absorbance measured in the wells that contained cells but no samples, which was established as 100% cell viability. $\bar{x}Abs_{sample}$ is the absorbance measured for each specific well that contained cells and the nanofiber membrane samples.

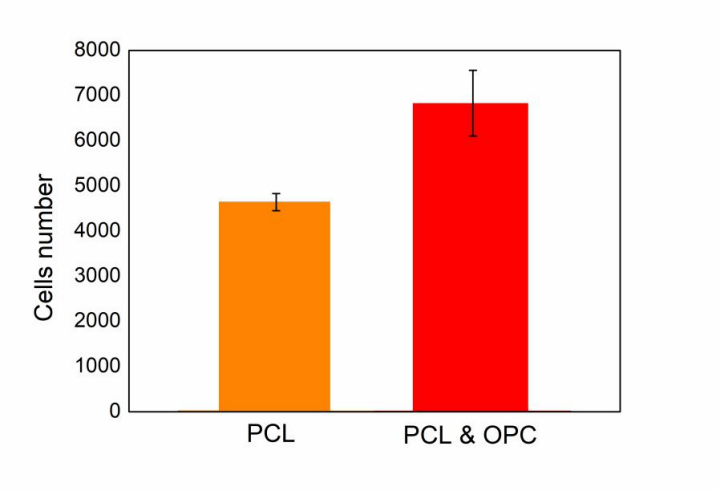

Figure 7-12. Cell adhesion results for nanofiber tubes containing polycaprolactone (PCL) and PCL and OPC nanofiber tube.

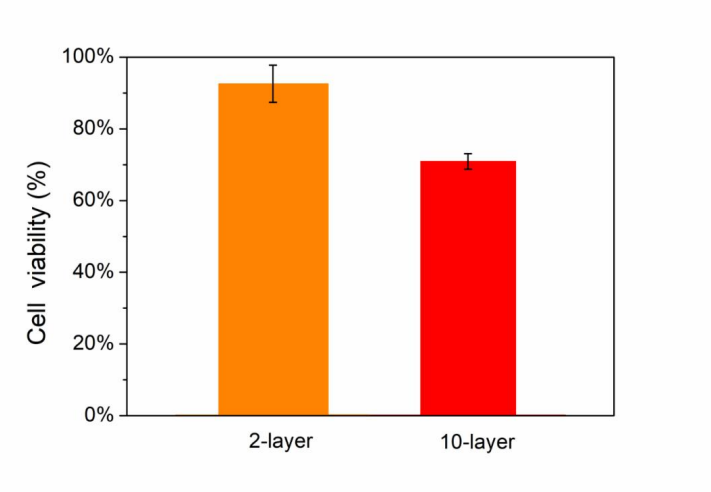

Figure 7-13. Results of cell viability assay.

The adhesion state of the PCL nanofiber tubes was assessed by step-wise seeding of primary HUVEC in vitro. This type of cell attachment suggests the potential to culture functional tissue-engineered artificial vascular grafts in vitro prior to in vivo implantation [7]. The results shown in Figure 7-12 reveal that the experiment went well for both PCL nanofibers and PCL/OPC nanofibers. However, the nanofiber membranes with OPC should a higher adhesion number of cells than that of the PCL nanofiber membrane. The result proved that OPC can support HUVEC cell adhesion [27].

Toxicity of the PCL membranes may be caused by the presence of residual DCM and DMF. The statistical analyses for cell the viability using different amounts of PCL membrane (2 layers and 10 layers), which is shown in Figure 7-13, presented no significant differences.This suggests that there is no toxicity originating from residual DCM and DMF in the PCL membrane and no harmful effect to HVUECs after 24-hour

of incubation. Therefore, the produced PCL nanofibrous tubes can be use drug carriers or internal devices without injuring human cells or tissues.

7.3. Conclusions

The multi-layer PCL nanofiber tubes developed in this work represent a considerable advance over current methods to produce tubular constructs because of their controllability, rapid production, and convenient fabrication. The current reported method to produce nanofiber tubes by rotating a mandrel during an electrospinning process takes at least two hours to produce each tube and the tubes are easily broken when removed from the mandrel [28, 29]. The method presented in this work also allows tubes with different thickness, numbers of layers, diameter, and length to be fabricated, thus offering greater control than past methods. The aimed nanofibrous tubes are made of drug load nanofiber (drug loaded inside of nanofiber) which provide a slow release rate, and then smear drug on the surface of prepared nanofiber membrane, roll up the membrane and mold it through thermal treatment. As a result the multi-layer nanofibrous tubes can carry with dual drug-release profiles. We use the same kind of drug in this application. However, the multi-layer tubes can carry different kinds and amounts of drugs to solve specific problems. When pathologic processes overwhelm the regulatory mechanisms of hemostasis, excessive quantities of thrombin form, initiating thrombosis [30]. Short-term thrombus may form within 5 min of transplant surgery, so the inter-layer drug release by the tubes of 60% -70% within 20 min can treat short-term

thrombus. Meanwhile, the slow release of the remaining drug by the tubes can treat long-term thrombus formation over months. In our study, the drug release from nanofibers lasted for more than two months. The tensile strengths and Young's modulus (calculated at 1%) of the multi-layer tubes reached as high as 5.51 ± 1 and 16.42 ± 9 MPa, respectively. Meanwhile, the elongation percentages of the prepared tubes were as high as about 100%. Meanwhile, the prepared tubes for vascular graft are considered to support HUVECs adhesion and growth. In order to form vascular tissues and then form autologous blood vessel ultimately. PCL has a slow biodegradability and can be supported this process as a scaffold [31]. However, further study still obligatory for clinical applications. The tubes developed in this study are attractive for a variety of applications including vasculature, intervertebral discs, nerve guides, and other complex composite scaffolds.

Reference

1. Mitchell SL, Niklason LE, Requirements for growing tissue-engineered vascular grafts, *Cardiovascular Pathology,* 2003, 12(2):59-64.

2. Hench LL, Biomaterials: a forecast for the future, *Biomaterials,* 1998, 19(16):1419-23.

3. Khatri Z, Nakashima R, Mayakrishnan G, Lee K-H, Park Y-H, Ii K, et al, Preparation and characterization of electrospun poly (ε-caprolactone)-poly (l-lactic acid) nanofiber

tubes, *Journal of Materials Science,* 2013, 48(10):3659-64.

4. Lovett M, Cannizzaro C, Daheron L, Messmer B, Vunjak-Novakovic G, Kaplan DL. Silk fibroin microtubes for blood vessel engineering, *Biomaterials,* 2007, 28(35):5271-9.

5. Fidkowski C, Kaazempur-Mofrad MR, Borenstein J, Vacanti JP, Langer R, Wang Y. Endothelialized microvasculature based on a biodegradable elastomer, *Tissue engineering,* 2005, 11(1-2):302-9.

6. Niklason LE, Abbott W, Gao J, Klagges B, Hirschi KK, Ulubayram K, et al, Morphologic and mechanical characteristics of engineered bovine arteries, *Journal of vascular surgery*, 2001, 33(3):628-38.

7. Lovett ML, Cannizzaro CM, Vunjak-Novakovic G, Kaplan DL. Gel spinning of silk tubes for tissue engineering. Biomaterials. 2008;29(35):4650-7.

8. Tamada Y, Sulfation of silk fibroin by sulfuric acid and anticoagulant activity, *Journal of Applied Polymer Science*, 2003, 87(14):2377-82.

9. Soffer L, Wang X, Zhang X, Kluge J, Dorfmann L, Kaplan DL, et al, Silk-based electrospun tubular scaffolds for tissue-engineered vascular grafts, *Journal of Biomaterials Science, Polymer Edition,* 2008;19(5):653-64.

10. Sanchez C, Arribart H, Guille MMG, Biomimetism and bioinspiration as tools for the design of innovative materials and systems, *Nature materials*, 2005;4(4):277.

11. Ma K, Qiu Y, Fu Y, Ni Q-Q, Electrospun sandwich configuration nanofibers as transparent membranes for skin care drug delivery systems, *Journal of Materials*

Science, 2018, 1-10.

12. Ke M, Wahab JA, Hyunsik B, Song K-H, Lee JS, Gopiraman M, et al, Allantoin-loaded porous silica nanoparticles/polycaprolactone nanofiber composites: fabrication, characterization, and drug release properties, *RSC Advances*, 2016, 6(6):4593-600.

13. Sun H, Mei L, Song C, Cui X, Wang P, The in vivo degradation, absorption and excretion of PCL-based implant, *Biomaterials*, 2006, 27(9):1735-40.

14. Serrano M, Pagani R, Vallet-Regı M, Pena J, Ramila A, Izquierdo I, et al, In vitro biocompatibility assessment of poly (ε-caprolactone) films using L929 mouse fibroblasts, *Biomaterials*, 2004;25(25):5603-11.

15. Fine AM, Oligomeric proanthocyanidin complexes: history, structure, and phytopharmaceutical applications, *Alternative medicine review: a journal of clinical therapeutic*, 2000, 5(2):144-51.

16. Zhang Y, Shi H, Wang W, Ke Z, Xu P, Zhong Z, et al, Antithrombotic effect of grape seed proanthocyanidins extract in a rat model of deep vein thrombosis, *Journal of vascular surgery*, 2011, 53(3):743-53.

17. Arslan R, Bektas N, Bor Z, Sener E, Evaluation of the antithrombotic effects of Crataegus monogyna and Crataegus davisii in the carrageenan-induced tail thrombosis model, *Pharmaceutical biology*, 2015, 53(2):275-9.

18. Bosio, V. E., Brown, J., Rodriguez, M. J., & Kaplan, D. L, Biodegradable porous silk microtubes for tissue vascularization, *Journal of Materials Chemistry B,* 2017, 5(6),

1227-1235.

19. Ali SA, editor Mechanical and thermal properties of promising polymer composites for food packaging applications, *IOP Conference Series: Materials Science and Engineering*, 2016, IOP Publishing.

20. Panseri S, Cunha C, LoIry J, Del Carro U, Taraballi F, Amadio S, et al. Electrospun micro-and nanofiber tubes for functional nervous regeneration in sciatic nerve transections, *BMC biotechnology*, 2008, 8(1):39.

21. Tang F, Li L, Chen D. Mesoporous silica nanoparticles: synthesis, biocompatibility and drug delivery. Advanced materials. 2012;24(12):1504-34.

22. Elzein T, Nasser-Eddine M, Delaite C, Bistac S, Dumas P. FTIR study of polycaprolactone chain organization at interfaces, *Journal of colloid and interface science*, 2004, 273(2):381-7.

23. Meng Z, Zheng W, Li L, Zheng Y, Fabrication and characterization of three-dimensional nanofiber membrance of PCL–MWCNTs by electrospinning. *Materials Science and Engineering: C*, 2010, 30(7):1014-21.

24. Yoshimoto H, Shin Y, Terai H, Vacanti J, A biodegradable nanofiber scaffold by electrospinning and its potential for bone tissue engineering, *Biomaterials*, 2003, 24(12):2077-82.

25. M. Issling, J. Membr. Sci. 308 (2008) J. Siepmann, N.A. Peppas, Adv. Drug Deliv. Rev. 2017, 48,139–1

26. Immich APS, Arias ML, Carreras N, Boemo RL, Tornero JA, Drug delivery

systems using sandwich configurations of electrospun poly (lactic acid) nanofiber membranes and ibuprofen, *Mater Sci Eng C,* 2013, 33(7):4002–4008

27. King M, Chatelain K, Farris D, et al, Oral squamous cell carcinoma proliferative phenotype is modulated by proanthocyanidins: a potential prevention and treatment alternative for oral cancer[J], *Bmc Complementary & Alternative Medicine*, 2007, 7(1):1-12.

28. Khatri Z, Nakashima R, Mayakrishnan G, Lee K-H, Park Y-H, Ii K, et al, Preparation and characterization of electrospun poly (ε-caprolactone)-poly (l-lactic acid) nanofiber tubes, Journal of Materials Science, 2013, 48(10):3659-64.

29. Matsuda A, Kagata G, Kino R, et al, Preparation of chitosan nanofiber tube by electrospinning[J], *Journal of Nanoscience & Nanotechnology*, 2007, 7(3):852.

30. Furie, B., & Furie, B. C, Mechanisms of thrombus formation, *N Engl J Med*, 2008, 359(9), 938-949.

Chapter 8

General conclusions

Chapter 8: General conclusions

Biomedical nanocomposites apllications are proposed with the purpose to combine manifold smart effects (mechanical peperty, physical and chemical properties and biocompetibility effect) which have been widely used in different areas into one kind of composites. The resultant composites (nanofiber composite, nanofiber/nanoparticle composite) exhibit not only decent biocompetibilities but also promising potential in nanopositioning resulting from the combination of the smart effects. This would be helpful to develop nanofabrication at low cost and more efficient way. The main conclusions of our work are given as below.

This study of chapter 2 reported a novel method of shellac nanocomposites. A potential to develop capsule form applications which can remain in the stomach for a long time. The sodium shellac nanocomposites which performed a larger and quicker drug effect in gastric environment. The sodium shellac was mixed in three concentrations with shellac (0%, 50% and 100%) inside of drug carried solution and then electrospinning/electrospray into nanocomposites. Shellac/sodium shellac nanofibers and nanoparticles loaded with ketoprofen were prepared successfully for sustained drug release. The results revealed that the release speed increased with the further addition of sodium shellac and nanoparticles shows quicker drug effect than

nanofiber. However, the application in chapter 2 shows very low mechanical strength. It's to low to put the samples on the testing machine. For increasing the mechanical strength, PCL was added in the next application for making nanofiber membrane. The application will not only be restricted inside of capsule.

The smart behaviors (transparent) of PCL/shellac nanofiber composites are studied in chapter 3. This experimental results should that ethanol vaportreated sandwich-structure PCL/shellac/PCL-salicylic acid membranes possessing good mechanical properties and mensurable transparency. The tensile strength increases with the PCL ratio of the samples. Conversely, PCL ratio had little influence on transparency and the drug release process. The regular transmittance at 555 nm of the membranes is high (about 35%), which is an attractive feature for skin care applications. About 70% cumulative release of salicylic acid by the ethanol vapor-treated membranes was obtained, and the release process was almost finished after about 10 h. The results exhibited that a 8.44 times higher of tensile strength and 37.99 times higher of Young's modulus after treatment.

After the preparation of nanofiber membrane, a kinds of nanofibrous tube was considered to manufacture. Before that, mechanical properties, including PCL nanofiber mat and PCL nanofibrous tube are exhibited in chapter 4, to test the tensile strength between nanofiber mat and nanofibrous tube. Compare the tensile strength cure of nanofibers and nanofirous tube. The nanofiber tube show higher Young's moduli and elongation. It is proved that this smart method prepare solid nanofibrous tubes. The

inter-layer connection makes the tube have higher Young's moduli and the elongations. However, the curve of nanofibrous tube are not smooth. This proves that the wall of the tube sustained uneven forces, because the tube was damaged unevenly.

Firstly, a kind of three layer SF/PU/SF nanofiber drug carried tube were produced by traditional method. Nanofibers were deposited continuously over a stainless-steel mandrel then the nanofibrous tube be removed carefully from the stick. The tube is displayed and the mechanical curves and result of cell culture are proposed in chapter 5. Synthetic materials have poor histocompatibility and tend to cause thrombi. However, the bionic three-layer structure tubes offers favorable biocompatibility, antithrombotic, and mechanical properties. It is designed to simulate natural blood vessels. The PU nanofibers which are used as the middle layer of the tube shows higher tensile strength and better elasticity than SF nanofibers which are used in the inner and outer layers. In contrast, the SF nanofibers show higher biocompatibility than that of the PU nanofibers. This three-layer nanofiber tube may promote the development of graft vessel engineering. However, this method need about every 2 hours for prepare each tube and the tubes are easily to broken when they are removed from the stick. A new thermal method are considered to prepare new kinds of nanofibrous tubes in the next chapter.

The process of thermal method to prepare PCL/PU nanofiber composites tubes are shown in chapter 6. The results show that the PCL/PU nanofibrous tubes with various blending ratios were successfully fabricated via thermal treatment. The treating temperatures are 50°C and 60°C respective. Besides, the nanofibrous tubes prepared by

both treatment show a uniform morphology and good structural stability. The diameters of nanofibers are controllable and the properties such as tensile strength, porosity, and tube wall thickness can be designed to fit the requirements of the applications.

Combine the advantages of the above method, more further advantages of combining mechanical property, controllable drug release rate and biocompatibilty is presented in chapter 7. The prepared drug carried multi-layer PCL nanofiber tubes developed in this chapter represent a considerable advance over current methods to produce tubular constructs because of their controllability, rapid production, and convenient fabrication. The method presented in this work also allows tubes with different thickness, numbers of layers, diameter, and length to be fabricated. Furthermore, the multi-layer tubes can carry two different kinds and amounts of drugs to solve specific problems. When pathologic processes overwhelm the regulatory mechanisms of hemostasis, excessive quantities of thrombin form, initiating thrombosis. Short-term thrombus may form within 5 min of transplant surgery, so the inter-layer drug release by the tubes of 60% – 70% within 20 min can treat short-term thrombus. Meanwhile, the slow release of the remaining drug by the tubes can treat long-term thrombus formation over months. In our study, the drug release from nanofibers lasted for more than two months. The tensile strengths and Young's moduli (calculated at 1%) of the multi-layer tubes reach high to 6.68 MPa and 25.15 MPa, respectively. Meanwhile, the elongation percentages of the prepared tubes is high to 111.23%. The tubes developed in this study are attractive for a variety of applications including

vasculature, intervertebral discs, nerve guides, and other complex composite scaffolds.

In summary, biomedical nanocomposites are a kind of multifunctional composite materials. Based on the complex physical chemical structure of abroad usage of mechanical properties, control drug release and biocompatibilties. PCL, PU or natural polymer such as Silk Fibroin and shellac composites are easy to be applied in various applications. Therefore, I will make efforts to develop more applications of these biomedical nanocomposites in the future. However, more experiments in vivo are needed in the future tests for commercialism.

List of Publications

1. **Ke Ma**, Yiping Qiu, Yaqin Fu and Qing-Qing Ni*, Improved shellac mediated nanoscale application drug release effect in a gastric-site drug delivery system *RSC Advances* 7, 53401-53406. (21 Nov 2017 published)

2. **Ke Ma**, Yiping Qiu, Yaqin Fu and Qing-Qing Ni*, Electrospun sandwich-configuration nanofibers as transparent membranes for skin-care drug delivery systems, *Journal of Materials Science* 15, 10617-10626. (25 Apr 2018 published)

3. **Ke Ma**, Hong Xia & Qing-Qing Ni*, Drug carrier three-layer nanofibrous tube for vascular graft engineering, *Journal of Biomaterials Science, Polymer Edition* (ID: 1493670 DOI:10.1080/09205063.2018.1493670). (24 Jun 2018 accepted)

4. **Ke Ma**, Hong Xia, Yiping Qiu, Yaqin Fu & Qing-Qing Ni*, Controllable polycaprolactone‐polyurethane nanofiber tubes using thermal treatment of electrospun nanofibers, *Journal of materials science materials in medicine* (under review).

5. **Ke MA**, Sélène Rozet, Yasushi Tamada, Juming Yao & Qing-Qing Ni*, Multi-layer nanofibrous tubes with dual drug-release profiles for vascular graft engineering, *Journal of Drug Delivery Science and Technology.* (10 January 2019 accepted).

6. **Ke Ma**, J. A. Wahab, B. Hyunsik, K. H. Song, J. S. Lee, M. Gopiraman*, I. S. Kim*,

Allantoin-loaded porous silica nanoparticles/polycaprolacton nanofiber composites: fabrication, characterization, and drug release properties, *RSC Advances* 6, 4593-4600. (08 Dec 2015 published)

7. F. Hamano, S. Hiromichi, **K. Ma**, M. Gopiraman*, C. T. Lim, I. S. Kim*, Cellulose acetate nanofiber mat with honeycomb-like surface structure, *Materials Letters* 169, 33 – 36. (1 Dec 2015 published)

8. H. S. Bang, **K. Ma**, K. Ii, C. Y. Kang, B. S. Kim, M. Gopiraman, J. S. Lee*, I. S. Kim*, A simple method for the fabrication of metallic copper nanospheres-decorated cellulose nanofiber composite, *Journal of Materials Science and Technology* 6, 4593-4600. (27 Apr 2016 published)

9. Kyohei Yamaguchi, Jatoi Abdul Wahab, **Ke Ma**, Xu Gang, Hyunsik Bang, Mayakrishnan Gopiraman*, Ick Soo Kim*, Highly dispersed nanoscale hydroxyapatite on cellulose nanofibers for bone regeneration, *Materials Letter* 168, 56 – 61. (4 January 2016 published)

Scientific Presentation

◆ **International conference**

1. **Ma Ke,** Mayakrishnan Gopiraman and Ick Soo Kim, Allantoin-loaded porous silica nanoparticles/polycaprolactone nanofiber composites:fabrication, characterization, and drug release properties,13th Asian Textiles Conference (Deakin University, Geelong, Victoria, Australia) 3-6 Nov 2015, Australia.

◆ **Domestic conference**

1. **Ma Ke,** Mayakrishnan Gopiraman and Ick Soo Kim, 薬物徐放への応用に向けたイネ由来多孔質シリカ粒子複合ナノファイバーの作製, The 68th Annual Meeting of The Textile Machinery Society of Japan, 5 Jul 2015, Osaka, Japan.

Acknowledgements

I would like to express my sincere gratitude to my supervisor, Professor Qing-Qing Ni, for his instructive advice on my work. His advice helps me to overcome several key problems in my work and teaches me how to write a scientific paper in a strict manner. Thanks to his guidance, I can complete my PhD.

Then special thanks extend to my sweet Lubin Qu, who helped me correct my paper amidst his busy schedule and encouraged me. I am also deeply indebted to all the staffs in Shinshu University Global Leader Program for Fiber Renaissance for their long-lasting support and encouragement.

I also want to express my thanks to Prof. Tamada for his help for my research. He help me with my cell culture experiment and provided place and condition for my experiment. I always have good discussion related to my work and his advice is pretty helpful.

The researcher in our group, Hong Xia, gives me a lot of help and assistance in experiments and living. She helps me to make progress in my research quickly.

I want to express my gratitude to Shinshu University Advanced Leading Graduate Program by the Ministry of Education, Culture, Sports, Science and Technology (MEXT), Japan that supported me by a Grant-in-Aid of my research. Thank you for the technicians in our campus, for their kindness and help.

The same to my kind friends in Japan: Hairong Chen, Xiaoyu Guan, Wanwan Liu,

Bing Liu, Piw Piw, Yongjie Yan, Jun Hong, Yinan Jing, Yajun Liu, Xiaojuan Li and Linang Cui. Thanks to their help for my living and PhD.

Finally, I need to thanks my parents. They always encourage me so that I have the opportunity to go all out for what I desired without any hesitation.